Second Series *November 15, 1931* *Vol. 38, No. 10*

THE
PHYSICAL REVIEW

THE STRUCTURE OF SOFT X-RAY LINES

By William V. Houston
California Institute of Technology

(Received October 1, 1931)

Abstract

The experimental work on soft x-rays has shown that the lines produced by the bombardment of a solid target are much broader than those emitted by a vapor. This is due to the fact that the upper level is not sharp. The breadth and the shape can be calculated from the various models which have been used for describing the behavior of electrons in metals. The free electron model gives a line which has a sharp edge on the short wave-length side. This is not observed in Be. The calculated width, however, agrees well with the observed. The bound electron model gives a more satisfactory shape for Be, but the width cannot be exactly determined. The comparison of the line shapes calculated on the basis of these two models with that observed in Be shows that, although the free electron model gives a good approximation to the zero point energy, the distribution of energy levels is strongly affected by the periodic potential in the crystal.

THE experimental work on very soft x-rays and on far ultraviolet spectra has shown that although there is a correlation between the lines of these two types, there are also outstanding differences. The lines emitted by an excited vapor, such as is produced by a hot spark discharge, are sharp lines of the type ordinarily found in optical spectra. On the other hand, lines in the same region, when produced by bombardment of a solid target, are found to have a very considerable width, and to be displaced from their position as observed in the hot spark.[1] To give an explanation of this fact one must remember that the x-radiation is emitted during a transition between stationary states of the solid body, while with the source in the vapor state, the transition is between states of a single atom. That this can be neglected in the treatment of the ordinary x-ray spectra is due to the fact that the very low levels of an atom are practically undisturbed when the atom becomes part of a crystal.

In terms of the model in which the interaction between electrons is not explicitly considered, and in which each electron moves in a potential field due to the nuclei and all the other electrons, the process of excitation and emission of a soft x-ray line may be described as follows. The excitation con-

[1] Ericson and Edlen, Zeits. f. Physik **59**, 656 (1930); M. Soderman, Zeits. f. Physik **65**, 656 (1930).

sists in the removal, by the bombarding electron, of another electron from one of the low levels of the target. In the case of low levels it may equally well be said that the electron is removed from one of the low levels of a particular atom in the target. This electron may be put into one of the unoccupied upper states of the crystal, or it may be entirely ejected. The emission of the x-ray then takes place when an electron from an upper state falls into the vacant lower state. If this electron comes from one of the highest group of ordinarily occupied states, that is from the group of states occupied by the valence electrons, it may have had any one of a large number of energies in this initial state. On this account the observed line will consist of a large number of superposed lines which blend together to give a wide band. The width and the shape of this band are determined by the distribution in energy of the upper levels as well as the distribution of transition probabilities. In case the lower state is one of a group of levels whose energies differ somewhat among themselves, this too must be taken into account. In most cases accessible to observation this is probably negligible. These observations, then, furnish a convenient means of checking experimentally the energy level distribution required by the various models for the behavior of electrons in metals.

The work of Söderman on Be furnishes a good example of what may be done in this direction.

The Free Electron Model

The model used by Pauli, Sommerfeld,[2] and others assumes that the outstanding characteristic of the valence electrons is their ability to move more or less freely through the crystal. The wave functions given by this model, as well as the distribution of energy values are given by Sommerfeld. The total number of stationary states whose energies lie between E and $E+dE$ is proportional to $E^{1/2}dE$. For ordinary temperatures, the temperature energy is so small compared with the zero point energy that it may be neglected. In this case, all of the energy levels up to those having the critical energy $\overline{E} = (h^2/2m)(3n/8\pi)^{2/3}$ will be occupied, and all those states having higher energy will be empty. In this expression for the critical energy, h is Planck's constant, m is the mass of an electron, and n is the number of free electrons per cubic centimeter.

In Be the electrons which occupy the L levels in the atoms will form the group of free electrons in the metal. It is then necessary to find the transition probability between one of these "free" states and an unoccupied K state. This can be found in the usual way from the knowledge of the functions. When averaged over all possible relative positions of the K function and the "free" function, the square of the amplitude of the electric moment turns out to be

$$M^2 = DE/(h^2Z^2/8\pi^2ma_0^2 + E)^6 \qquad (1)$$

D is a constant whose value is not essential, since only the dependence on E

[2] W. Pauli, Zeits. f. Physik **41**, 81 (1927); A. Sommerfeld, Zeits. f. Physik **47**, 1 (1928).

affects the shape of the x-ray line. The fact that the transition probability depends only on E and not on the direction of motion of the free electron is due to the spherical symmetry of the K function. In Eq. (1) Z is the effective nuclear charge which determines the extent of the K function, a_0 is the radius of the first Bohr orbit, while the other symbols have their usual significance. The combination of the transition probabilities with the distribution of energy levels gives for the shape of the emitted line

$$I \sim E^{3/2}/(h^2Z^2/8\pi^2ma_0^2 + E)^6 \tag{2}$$

from $E=0$ to $E=\overline{E}$. In this expression the ν^4 factor is neglected since the width of the line is only a small part of its total frequency.

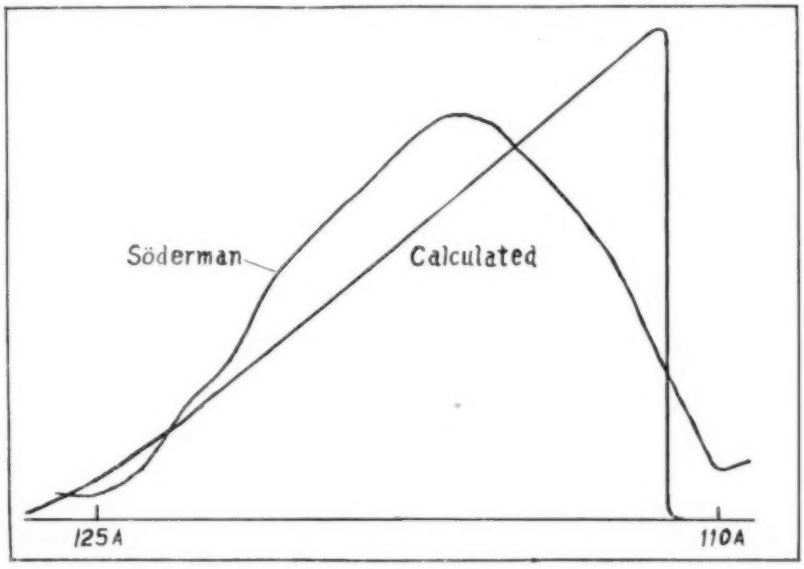

Fig. 1. Comparison of line observed in Be with that calculated from the free electron model.

Fig. 1 shows the agreement of this calculated curve with the observations of Söderman for Be. The width is calculated on the basis of two free electrons per atom. The height of both curves is of course arbitrary. The distinctive feature of the free electron model is the sharp edge on the short wave-length side. This does not appear in the observations, although there is a certain amount of asymmetry to be seen. The calculated width agrees very well, however, with that observed.

The Bound Electron Model

The other model for which calculations can readily be made is that introduced by Bloch.[3] From this point of view each electron is initially attached to a particular atom, but can easily jump to an adjacent atom under the influence of an external field. In this case the spread of the energy levels is pro-

[3] F. Bloch, Zeits. f. Physik **52**, 555 (1928).

duced by the perturbation of the electron by the surrounding atoms. The energy of a stationary state is given by Bloch to be

$$E_{lmn} = E_0 + \alpha - 2\beta\{\cos(2\pi l/G_1) + \cos(2\pi m/G_2) + \cos(2\pi n/G_3)\} \quad (3)$$

E_0 is the energy of the electron in the field of its own nucleus only. α is the electrostatic perturbation of the adjacent nuclei and electrons, while β is the exchange integral. l, m, and n are integers which designate the state and may have values such that the arguments of the cosines range between $-\pi$ and $+\pi$.

The number of energy levels lying between E and $E+dE$ is very difficult to evaluate analytically, but a rough graphical integration gives the form indicated in Fig. 2. The width of the group of levels depends upon the value of the integral β. For the curve shown in Fig. 2 the functions suggested by Slater[4] were used in evaluating this integral. Each atom was assumed to have six effective neighbors, and their distance was determined from the density as if the crystal had a simple cubic lattice. In this model the transition probability is about the same for all states since it is essentially the transition probability from an L state to a K state. Although the theoretical determination of the width is subject to a number of uncertainties, the figure shows that it is of the right order of magnitude. The shape of the curve agrees roughly with the observations.

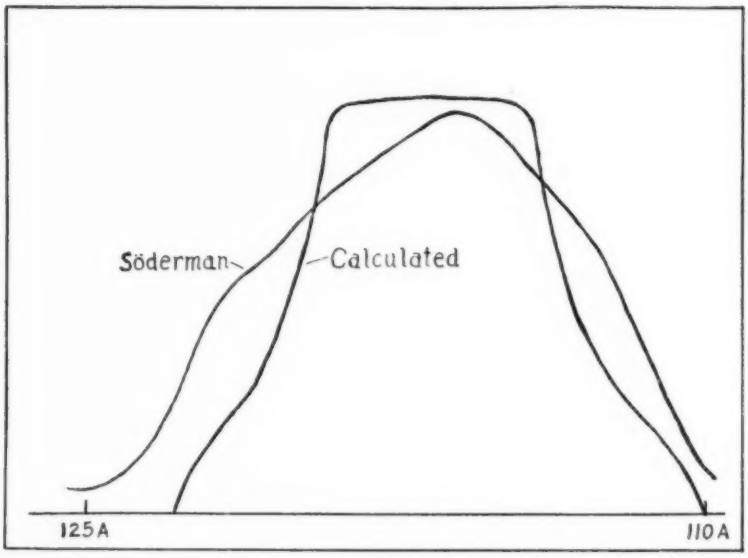

Fig. 2. Comparison of line observed in Be with that calculated from the bound electron model of Bloch.

[4] J. C. Slater, Phys. Rev. **36**, 57 (1930).

Discussion

The distinctive difference between the two theoretical curves lies in the sharpness at the short wave-length edge. In each case the Pauli exclusion principle, or the Fermi statistics, causes all of the states whose energy is less than a certain critical amount to be occupied, and all others to be empty. In the free electron model the density of states increases continually with the energy, so that there is a sharp edge. The other model, which takes some account of the periodic variations of potential within the crystal, indicates that the density of the states is not a monotonic function of the energy, but consists of a series of maxima which roughly correspond to the various types of state in the free atom. In case the outer shell of the atom is closed, as is the case with Be, the end of the occupied states falls at a minimum and does not produce a sharp break. On the other hand, an element such as Li should have a sharp edge on its lines, since there are only enough electrons to fill up half of the states in the first group. The observed shape of the curve indicates that in Be the potential variations do produce a considerable effect on the distribution of the energy levels.

In all of these calculations the lower level has been treated as single since a rough calculation shows that it will be much narrower than the upper level.

The operation of the Pauli exclusion principle is clearly seen in the fact that the lines have any width at all. If the classical statistics were applicable all of the electrons would be in states at or near the lowest value of the energy.

UPPER ATOMIC-NUMBER LIMITS FOR SATELLITES OF THE X-RAY LINE $L\beta_2$*

By R. D. Richtmyer**
Department of Physics, Cornell University

(Received October 5, 1931)

Abstract

The region of the x-ray spectrum in the immediate neighborhood of the line $L\beta_2$ has been photographically studied for the elements of atomic number 50, 51, 52, 53, 56, 58, and 60, with a view to determining more precisely the atomic number ranges of the satellites (five in number) of $L\beta_2$. It appears that these ranges have clearly defined upper limits in the cases of all but one of the satellites of $L\beta_2$, and that the previously supposed presence of these satellites beyond these limits, approximately atomic number 53, can be traced in some cases to certain diagram lines which had not heretofore been thoroughly investigated, and that the presence of the satellites beyond these limits is in general to be doubted, at least as far as present accuracy and sensitivity of observation are concerned. The existence and sharpness of these limits seems to be in conflict with the Wentzel-Druyvesteyn double-ionization theory of the origin of the satellites. A table of new wave-lengths is included.

THE purpose of this investigation of the satellites of the x-ray line $L\beta_2$ was to determine with greater certainty, if possible, the range (apparently restricted at both ends) of atomic numbers of the elements for which these satellites can be observed.

$L\beta_2$ has five satellites, which appear as shown in Fig. 1. The two more prominent ones, numbered 4 and 6 in the figure, were early observed by Siegbahn, and are recorded in his *Spectroscopy of X-rays*. Siegbahn calls these $L\beta_{11}$ and $L\beta_{12}$, but they are perhaps most frequently called $L\beta_2'$ and $L\beta_2''$. They are clearly resolved for the elements of atomic number from 40 to 50, inclusive, and are listed unresolved by Siegbahn for several additional scattered elements. When unresolved he sometimes also calls them $L\beta_8$. Three more satellites were reported in 1929 by F. K. and R. D. Richtmyer[1] for the atomic number range 40 to 50, inclusive, and are called by them $L\beta_2$(a), $L\beta_2$(b), and $L\beta_2$(c).

A Siegbahn vacuum spectrometer was used, with a calcite crystal, and was found to be very satisfactory. The usual photographic method of procedure was followed, the crystal being oscillated slowly through a small angle during the exposure, to eliminate false lines due to crystal imperfections. The voltage used in the case of each element was five times the excitation voltage of the parent line $L\beta_2$, for reasons to be discussed later, and the high-voltage, direct-current generating outfit used made it possible to measure and control the voltage with considerable assurance. The copper anode of the tube con-

* Presented at the December, 1930 meeting of the American Physical Society in Cleveland.

** The author wishes to make grateful acknowledgment for the privilege of using certain pieces of apparatus purchased for the use of F. K. Richtmyer by the Heckscher Research Council of Cornell University.

[1] F. K. and R. D. Richtmyer, Phys. Rev. **34**, 574 (1929).

tained a bevelled slot into which a copper wedge would fit. The element in question, in the most convenient, sufficiently stable form or compound was placed on this wedge.

The angle of diffraction of the various satellites was determined by measuring, by means of a comparator, their positions on the photographic plate relative to the position of the parent line, whose wave-length is accurately known. The wave-length of the satellites could then be determined by means of the expression

$$\Delta\lambda = 2d\left\{\cos\left(\theta - \frac{\Delta\theta}{2}\right)\right\}\Delta\theta$$

where θ is the Bragg angle for $L\beta_2$. The error in the wave-length difference brought about by the approximations involved in this expression was determined as of the order of magnitude of one part in 100,000 in the narrow region

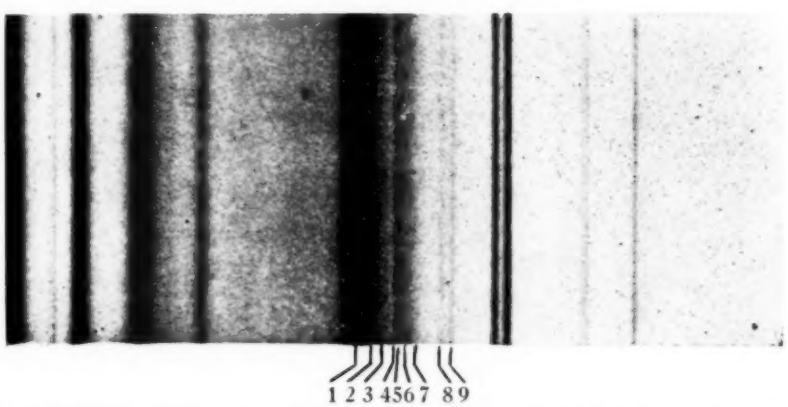

Fig. 1. A portion of the x-ray spectrum for Sn. The numbered lines are: 1, $L\beta_2$; 2, $L\beta_2$(a); 3, $L\beta_7$; 4, $L\beta_2'$; 5, $L\beta_2$(b); 6, $L\beta_2''$; 7, $L\beta_2$(c); 8, $L\beta_{10}$; 9, $L\beta_9$. On the original plate, which has more depth of contrast than the reproduction, all these lines are clearly visible.

of the plate at the center where the satellites are found. The lighting conditions and magnification of the comparator had to be carefully controlled to render the very faint lines visible. The exposure of the plates in the spectrometer was so regulated by trial and error to give maximum visibility of the satellites, and ranged from two to eight hours, depending upon the element.

TABLE I. *Wave-lengths (x-units).*

	Sn (50)	Sb (51)	Te (52)	I (53)	Ba(56)	Ce (58)	Nd (60)
$L\beta_2$	3167.9*	3016.6*	2876.1*	2746.08*	2399.3*	2204.1*	2031.4*
$L\beta_2$(a)	3162.2	3010.9†	2870.9†	2740.45†	2395.8†	2200.1†	2028.4†
$L\beta_2'$	3142.3	2992.9	2852.7†	2724.35†			
$L\beta_2$(b)	3138.9						
$L\beta_2''$	3134.6	2985.4	2845.2†	2718.5†			
$L\beta_2$(c)	3129.9						
$L\beta_7$	3149.4	2998.5†	2857.4†	2724.35†	2375.4	2176.4	2004.9
$L\beta_9$	3106.6	2964.7	2832.35†	2709.05†	2371.5	2183.7	2012.2
$L\beta_{10}$	3113.1	2971.7	2839.0†	2715.1†	2382.0	2190.66	2019.1
?				2731.8†			

* Values taken from M. Siegbahn, *The Spectroscopy of X-Rays.*
† Lines not previously reported.

TABLE II. *Difference in frequency between $L\beta_2$ and satellites (in ν/R units).*

	Sn (50)	Sb (51)	Te (52)	I (53)
$L\beta_2$ (a)	0.521	0.592	0.566	0.684
$L\beta_2'$	2.33	2.34	2.595	2.63
$L\beta_2$ (b)	2.66			
$L\beta_2''$	3.06	3.08	3.432	3.365
$L\beta_2$ (c)	3.49			
	Ba(56)	Ce (58)	Nd (60)	
$L\beta_2$ (a)	0.552	0.746	0.664	

The results of the experiments are shown in Tables I and II and Figs. 2 and 3. Many lines, other than those given in Table II, were found on the plates, and a rough check up of their wave-lengths showed them to be lines previously reported, other than satellites of $L\beta_2$. Fig. 2 is the "differential Moseley graph" introduced by F. K. Richtmyer for dealing with satellites,

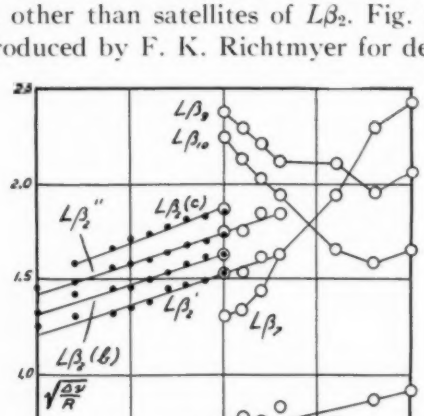

Fig. 2. For the ordinates, $\Delta\nu$ is the frequency difference between the line in question and $L\beta_2$. R is Rydberg's constant. Note that for the satellites the square root of this frequency difference is a linear function of the atomic number of the emitter. Black dots, F. K. Richtmyer and R. D. Richtmyer, Phys. Rev. **34**, 574 (1929); circles, R. D. Richtmyer, present work.

and it is seen that the straight-line law is still followed by the new points of this work. Fig. 3 is essentially an ordinary Moseley graph which has undergone a certain linear transformation. A Moseley graph is of course obtained by plotting the values of $(\nu/R)^{1/2}$ for a given x-ray line, as a function of atomic number, where ν is the frequency of the line, and R is Rydberg's constant. The points so plotted lie so nearly on a straight line that an ordinary drawing of them does not show any deviations. But if one subtracts from the ordinates of these points the corresponding ordinates of a straight line passing roughly through the points, and then plots these differences, on a magnified ordinate scale, as a function of atomic number, slight deviations can be made to show up. In other words, the ordinates of Fig. 3 are $(\nu/R)^{1/2}-f(Z)$, where $f(Z)$ is a particular linear function of atomic number. The straight line which was chosen for that purpose in this case was the straight line passing through the values of $(\nu/R)^{1/2}$ of the parent line, $L\beta_2$, for elements of atomic number 50 and 60.

All the lines shown are satellites of $L\beta_2$ except $L\beta_7$, $L\beta_9$, $L\beta_{10}$, and the single, unidentified line for iodine. As is shown by the graphs, one of the lines for iodine may be interpreted as either $L\beta_7$, $L\beta_2'$, or both. Those of Siegbahn's points for Cs(55) and Ba(56) which have been interpreted on the graphs as $L\beta_{10}$ (the lines which are marked by an asterisk in Fig. 3) are listed by him as the unresolved doublet $L\beta_2'$ and $L\beta_2''$, or, in his notation, $L\beta_{11}$ and $L\beta_{12}$. The present interpretation of them as $L\beta_{10}$ seems preferable for three reasons: in the first place, the satellites $L\beta_2'$ and $L\beta_2''$ decrease very rapidly in intensity in the atomic number range 50 to 53, and are barely visible at all for iodine. The line in question as observed for Ba(56) was rather intense. Secondly, Siegbahn's points fit in admirably with the previously unreported values for $L\beta_{10}$ for the intervening elements Te(52) and I(53). Thirdly, the lines in question, as also all other diagram lines, are slightly narrower and more

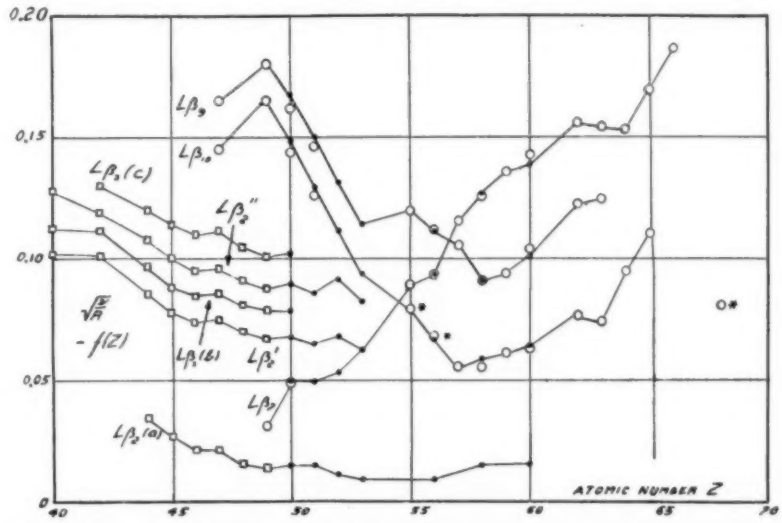

Fig. 3. The lines marked with an asterisk are listed by Siegbahn as $L\beta_{11}$ and $L\beta_{12}$ ($L\beta_2'$ and $L\beta_2''$ in the notation used in this article). Circles, M. Siegbahn; squares, F. K. and R. D. Richtmyer, Phys. Rev. **34**, 574 (1929); black dots, present work. See text.

distinct than any of the satellites, and are not overlaid with a faint continuous background, as are the satellites. The point for atomic number 68, and a similar one for 71, Siegbahn calls also the unresolved doublet $L\beta_2'$ and $L\beta_2''$. In view of the behaviour of the satellites in the region studied, it seems probable that Siegbahn's interpretation is open to question.

In the case of lines which have been measured before (see Fig. 3), the present values for their wave-lengths check, for the most part, to within one or two tenths of an x-unit with previous values.

The abruptness with which the satellites[2] disappear with increasing atomic number at their upper limit merits some attention. In 1927 Druyvesteyn,[3]

[2] Throughout this paragraph, discussion is restricted to the satellites $L\beta_2'$, $L\beta_2$(b), $L\beta_2''$, and $L\beta_2$(c).

[3] Druyvesteyn, Zeits. f. Physik **43**, 707 (1927).

following classical quantum mechanics, derived a relation for the ratio of the number of KL ionizations to the number of K ionizations which should take place under given circumstances. With Druyvesteyn's relation we can predict how the intensity of the satellites should vary with atomic number if we expose our plates in such a way that the parent line has always the same intensity. Druyvesteyn's formula is

$$\frac{\text{No. } KL}{\text{No. } K} = A\left(\frac{Z-\alpha_L}{Z-\gamma_L}\right)^2 \frac{\alpha_L}{(Z-\gamma_L)^2}$$

where α_L and γ_L are the partial and total screening constants of the L shell, q_L is the number of electrons in the L shell, and A is a factor which is constant for a given ratio of the initial energy of the cathode electrons to the binding energy of the K shell. This ratio remains constant, if, as in the case of the present experiments, the ratio of the voltage used to the K excitation voltage is maintained at a constant value. In applying Druyvesteyn's relations to the present case, the question is raised whether a similar formula holds for the ratio of the number of LM ionizations to the number of L ionizations. It seems that this is the case under the experimental conditions used. There are, following Druyvesteyn in part, six methods of importance by which LM ionization can be brought about: (1). The cathode particle expells first an L electron and then an M electron. (2). The cathode particle expells first an M electron and then an L electron. (3). The cathode particle expells an L electron with sufficient energy that it can ionize the M shell. (4). The K shell is initially ionized, and LM comes as a result of a radiationless rearrangement. (5). From the transition KL to LM. (6). From the transition KM to LM. The distinctions between the first three methods may not be sharp, depending upon our pictures of subatomic processes, but at least these three methods are the exact analogues of the ones Druyvesteyn considered for his case of KL ionization, while the last three methods above are excluded in the present case, because the voltage used was less than half the K excitation voltage. Therefore the above formula should apply to the present case by writing everywhere L for K and M for L. This formula may be trusted to give us a rough idea of the intensity relations we should expect. It predicts a gradual falling off of intensity with increasing atomic number; a falling off which would be barely perceptible within a small range of atomic numbers. For instance, assuming α_M and γ_M to be of the order of 10, the intensity of the satellites for 56(Ba) should be only about fifty percent less than the intensity of the satellites for 47(Ag), and only about twenty-five percent less than for 50(Sn). For 53(I) it should be about ten or twelve percent less than for 50(Sn). Quantitative determination of the intensities of these satellites as they appear on the photographic plates close to the strong parent line is very difficult and uncertain, and was therefore not attempted. But judging from comparison with the familiar example of the $K\alpha$ doublet, where the intensity ratio is 2:1, the rate at which the intensity of the satellites falls off is of a much larger order of magnitude than would be expected from Druyvesteyn's

relation. For both 47(Ag) and 50(Sn) the satellites are really quite intense lines, though of course very much less intense than the parent line. For 53(I) the satellites are extremely faint; only two of them show at all. For 56(Ba) they could not be made to show under any conditions or length of exposure, provided that the aforementioned reinterpretation of Siegbahn's previously reported lines is correct.

No alteration of the intensity of the line $L\beta_2$(a) from 50(Sn) to 60(Nd) was noticed. This line apparently differs fundamentally from the other satellites.

Possibly contemporary quantum mechanics will predict new intensity relations for the satellites.

The results of the experiments may be summed up as follows. There are definite upper limits for the atomic-number ranges of four of the five satellites of $L\beta_2$. At its upper limit, each of these satellites disappears abruptly with increasing atomic number, in a way which cannot be accounted for on the double-ionization theory of the origin of satellites. These limits are, respectively; $L\beta_2'$, 53(I); $L\beta_2$(b), 50(Sn); $L\beta_2''$, 53(I); and $L\beta_2$(c), 50(Sn). I feel that not without much more sensitive methods can they be observed for elements beyond the limits here set. The first and third of these satellites had not previously been reported for elements beyond 51(Sb). For a fifth satellite, $L\beta_2$(a), which is very close to the parent line, no such upper limit was found. This satellite was found for all the elements investigated.

For some of the elements investigated there are several faint diagram lines in the frequency range where the satellites occur, and considerable confusion has been caused by them, because they are of the same order of intensity as the satellites, and because information about them is incomplete. It was possible to observe them and measure their wave-lengths for the elements studied, and therefore to clear up this confusion to some extent. In many cases previous wave-lengths and interpretations are corroborated, but in one or two cases new interpretations are made necessary.

The author wishes to express thanks to Professor F. K. Richtmyer for valuable aid in conducting this research and in preparing this manuscript.

DISPERSION OF X-RAYS IN CALCITE

By Louis A. Pardue
Yale University

(Received September 23, 1931)

Abstract

The dispersion of x-rays in calcite has been investigated. The total radiation and the $K\alpha_1$ line from a molybdenum target tube operated at about 44,000 volts were used in different experiments. The decrement of unity in the index of refraction for the $K\alpha_1$ wave-length was found to be $(2.001 \pm 0.009) \times 10^{-6}$. This does not agree with the value computed on the Drude-Lorentz theory. The specimen was a right prism with the optic axis parallel to the 90° refracting edge. No evidence was found for double refraction. The intensities of Mo$K\alpha_1$ radiation reflected from calcite mirrors were measured for angles in the neighborhood of the critical angle. These experimental values were compared with the values computed on the basis of Thibaud's modification of Fresnel's equation and found to be in fair agreement.

OPTICAL terminology and theory may be applied to x-rays if due account is taken of their higher frequency. Since the different theories of the dispersion of x-rays agree in the limiting case where the frequency of the radiation is much greater than the natural frequency of the electrons in the dispersing medium, the results (Table I) for the refractive index of calcite for Mo$K\alpha_1$ are suggestive. The values reported for δ are considerably larger than the value resulting from all theories in the limiting case for higher frequencies. The theoretical value is

$$\delta \equiv 1 - \mu = ne^2/2\pi m\nu^2$$

where μ is the index of refraction, n the number of electrons per cm^3 in the dispersing medium, e the charge on an electron, m the electronic mass, and ν the frequency of the radiation. Table I gives the results of the various investigators and their methods.

Table I.

	$(1-\mu)\ (10)^6$ Theor.	Exper.	Method
Davis and Hatley[1]	1.84	2.0	Crystal wedge
Hatley[2]	1.84	2.03 ± 0.09	Crystal wedge
Compton[3]	1.84	2.10 ± 0.15	Deviation

[1] C. C. Hatley, B. Davis, Phys. Rev. [2] **23,** 290 (1924).
[2] C. C. Hatley, Phys. Rev. [2] **24,** 486 (1924).
[3] A. H. Compton, Phys. Rev. [2] **37,** 1694 (1931).

While the probable errors are large there is a definite lack of correspondence between theory and experiment. It was deemed desirable to make a very careful study of dispersion of Mo$K\alpha_1$ x-rays in calcite, having in mind the possibility of double refraction, about the only phenomenon in optics

whose counterpart in x-rays has escaped detection. The specimen of calcite chosen was a right prism with the optic axis parallel to the 90° refracting edge. To have the optic axis so directed is a logical choice in seeking double refraction in x-rays but one without strong support. An investigation was made of the energy reflected from polished and cleaved faces of calcite at angles in the neighborhood of the critical angle.

Arrangement and Adjustment of Apparatus

In these experiments the Société[3] Genevoise spectrometer was used. The various adaptations of it to the different needs will be pointed out with reference to Fig. 1. X is the x-ray tube (a water-cooled molybdenum target tube of the Coolidge type), S_1, S_2, S_3 and S_4 are slits. C_1 and C_2 are calcite crystals, and P is the 90° calcite prism with the optic axis parallel to the 90° edge. P was mounted on a specially designed holder which permitted the

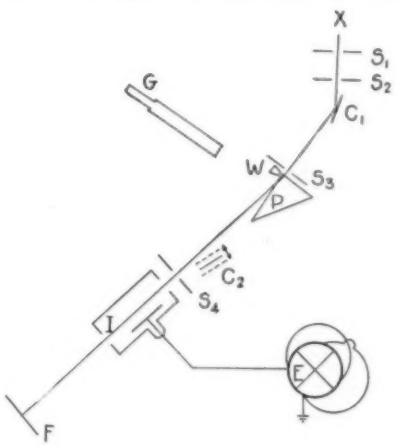

Fig.. 1

prism to be rotated about both horizontal and vertical axes in steps so small that any desired angular setting could be made easily. The holder also permitted the prism to be moved into and out of the beam laterally, keeping the faces of the prism accurately parallel to themselves. The 90° edge was in the axis of rotation of the prism mounting. The beam passed through this axis and nearly normal to one face of the prism. I is an ionization chamber and F is a photographic plate. The ionization currents were compared with a quadrant electrometer or a pliotron tube mounted over C_2. Methyl bromide (CH_3Br) vapor was used in the chamber to increase the absorption and ionization. The gain is due to the greater density of methyl bromide vapor as compared with air and to the higher K absorption of bromine for molybdenum rays. The angular positions of the prism were determined by means of an autocollimating telescope G, while the angular positions of C_1 and C_2 were determined by means of divided circles attached to the instrument. The divided circle attached to C_2 is presumably very good, being marked by the makers in 10 minute intervals which could be subdivided to 1 second by means of reading microscopes.

The slits, crystals and prisms were made parallel to the axis which supported C_2. This was accomplished by setting the axis of the autocollimating telescope perpendicular to the axis carrying C_2. To attain this a mirror with accurately parallel sides was placed on the table supporting C_2 and the autocollimating telescope and table were adjusted until the elevation of the beam reflected into the telescope did not change when the mirror was turned through 180°. The axis had previously been made vertical by means of a level. Since the telescope carried an accurate cathetometer level, the crystals on the mountings could be made parallel to the axis. Also by means of a steel mirror with accurately parallel sides placed between the jaws of the slits, the slits were made parallel to the axis. In the refraction experiments a lead wedge, W, was placed very close to the edge of the prism to stop as much as possible of the beam from getting by. The photographic plate was screened with lead from the direct beam practically all of the time during which a refraction photograph was being taken. This screen was removed during the last few minutes in order to obtain the direct beam from which to measure for the displacement of the refracted line.

To fix the angular position of the prism with respect to the beam, total reflection was used. P was rotated to different angular positions and the changes in intensity were noted by means of the electrometer readings. Having found the critical angle in this manner, the prism was turned into such a position that it would give total reflection. A photograph of the reflected line and the direct line on a plate at a known distance gave reliable data from which to compute the angle which the reflecting surface made with the beam. With this knowledge P could be turned to any desired angular position for refraction. The angles through which P was turned were measured by the autocollimating telescope, G, which had been calibrated previously against the circle attached to C_2. This telescope consisted of an object lens of 43 cm focal length and an eye combination which was the microscope of the Gaertner comparator used to measure the plates taken in this work. The microscope had a magnification of 28. When the reflector was turned through 1 second, the reflected image moved through 5.37 microscope divisions. The image reflected from the prism was such that the angles through which the prism was turned could easily be measured to 1 second.

Reflection and refraction were obtained for the heterogeneous radiation direct from the tube and for monochromatic radiation. When direct radiation was used, the arm carrying S_1, S_2 and C_1 was removed and the two slits were placed between P and the tube X. The double crystal arrangement permitted the determination of rocking curves and reflecting power of the crystals.

The measurement of the deviation of the refracted beam can be found in terms of the distance of the photographic plate from the refracting edge and the displacement on the plate of the refracted line from the undeviated line. Fig. 2 shows the rays and suggests how the measurements were taken.

The distance from F to A' was measured by pressing the end of a brass rod which had been squared in a lathe against the plate F and marking the point opposite A' with a sharp knife blade. This length was then measured

by comparison with a standard meter bar. The length AA' was measured with a traveling microscope. In the total reflection experiments the distance FA' was needed, while in the refraction experiments FA was needed. The edges of the lines measured to are clearly indicated in the diagram. Distances on the photographic plates were measured with a Gaertner traveling microscope reading to 0.001 mm. The calibration of the screw on the microscope was checked against a Zeiss scale and found to have no error larger than the errors of reading. That the plate (19 cm long) was satisfactorily perpendicular to the beam was checked by sighting along the arm of chamber I which was parallel to the beam.

The fact that the optic axis was parallel to the 90° edge of the prism was confirmed by a measurement of the indices of refraction of the ordinary and extraordinary rays on an optical spectrometer.

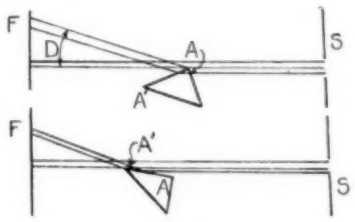

Fig. 2.

Experimental Results and Conclusions

As already mentioned, the specimen used in these experiments on total reflection and refraction was a 90° calcite prism having the optic axis parallel to the 90° edge. At first the two faces forming the 90° angle were highly polished. Later the polish on one face was removed by grinding in order to obtain a sharper edge, since the one left by the makers was a few hundredths of a millimeter thick. With the blunt edge it was impossible to obtain refraction at small angles of incidence on the emergent face. Total reflection from this edge was a disturbing feature. The dimensions of the faces forming the 90° angle were 10 mm×8 mm. A measurement of the ordinary and extraordinary indices of refraction for the Hg 5461 line gave 1.66169 and 1.4880 respectively as compared with the values 1.661647 and 1.487890 given by Baly[4] showing that the optic axis was very closely parallel to the 90° edge.

The experiments on total reflection, besides being useful in setting the prism for refraction, give some very interesting results. They give a determination of the index of refraction of calcite for the $K\alpha_1$ line of molybdenum as accurate at least as that obtained by the deviation method used by Davis-Hatley[1] and Hatley[2], who have determined the now accepted value. The broken curve, Fig. 3, shows the variation of the intensity of the reflected radiation in passing through the critical angle and the lack of any definite break shows there is no appreciable double refraction.

The prism was turned back to a point corresponding to a point on the

[4] E. C. C. Baly, Spectroscopy, Third Ed., Vol. 1, p. 83.

curve of maximum reflected intensity. A total reflection photograph gave 1.66×10^{-3} radians for the angle between the prism and the beam. Taking the mid-point of descent of the curve for the critical angle, we obtain for the critical angle 1.95×10^{-3} radians. The accuracy of this determination is limited in part by the choice of the critical angle from Fig. 3. Since the steep portion of the descent has an angular width of about 0.2×10^{-3} radians, the method has necessarily a possible error of 5 percent. Fig. 3 shows also in full line the theoretical curve for calcite. This was computed from the expression

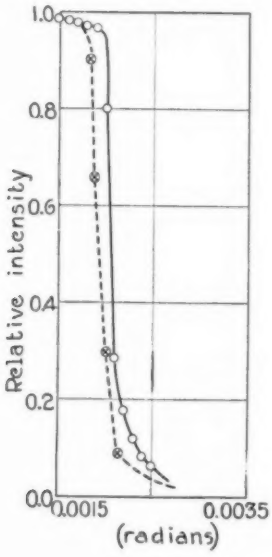

Fig. 3.

derived by Thibaud[5] for the ratio of the intensity of the reflected beam to that of the incident beam:

$$A = \frac{(1+m)^2 + 2(m^2+a^2)^{1/2} + 2(1+m)\left[2(m^2+a^2)^{1/2}\right]^{1/2}\cos\phi/2}{(1+m)^2 + 2(m^2+a^2)^{1/2} - 2(1+m)\left[2(m^2+a^2)^{1/2}\right]^{1/2}\cos\phi/2}$$

in which $\pi<\phi<2\pi$ and m is defined by the equation $\theta=(1+m)\theta_c$ where θ is the glancing angle of incidence and θ_c is the critical angle. The remaining quantities are defined in terms of the following relations:

$$K = k\lambda/4\pi;\quad a = K/2\delta;\quad \theta_c^2 = 2\delta;\quad \tan\phi = \left[-a(1-\delta)\right]/(m-a^2\delta);$$

$k\equiv$absorption coefficient; and $1-\delta\equiv$index of refraction. Table II gives the values of the constants used.

TABLE II.

k	20.6
a	2.91×10^{-3}
θ_c (radians)	2.00×10^{-3}
$\delta\times10^6$	2.00
$\lambda\times10^8$	0.709

[5] J. Thibaud, Jour. de Physique [7] 1, 37 (1930).

k and δ were measured in these experiments, k being determined by the absorption in a plate of calcite 1 mm thick. The faces of the plate were parallel to cleavage planes. The curve shown is typical of several that were taken for monochromatic radiation. Curves were also taken for the direct radiation from the molybdenum tube. These had a descent somewhat broader than those obtained with monochromatic radiation. The tube, however, was operated at a voltage somewhat higher than the excitation voltage of the K-series of molybdenum. The voltage varied slightly in different experiments but was always approximately 40,000 peak. Total reflection was also obtained from a cleavage face of a calcite crystal at C_2. Here the descent of the intensity curve was very broad. A total reflection photograph from this cleavage face, which was a very good one as evidenced by its x-ray reflection of the Bragg type, gave a very broad and diffuse line. In fact it had several components. This crystal reflected 18.7 percent of the incident monochromatic radiation when crystals were in the antiparallel position. The tolerance angle was also measured for this position and was found to be 12 seconds in the first order.

The first experiments on refraction were performed with the direct radiation from the molybdenum target tube. The prism was set in the reflecting position by the process mentioned above. The prism was then turned to such a position that the angle ρ between the beam and the emerging face had the desired value, 9 minutes in the first experiment. A 5 hour exposure gave the refracted lines on a plate 166.6 cm from the refracting edge. The target of the tube was about 40 cm from this edge. ρ was made less in succeeding experiments until it was impossible to get refraction at 2 minutes. The edge was found not to be sharp. The edge was made sharp by grinding the entering face which had been highly polished. After the grinding it was not polished again. The refraction experiments were repeated, and it was found that good refracted lines could be obtained at values of ρ less than one minute. The lines were as sharp as they were before the entering face was ground, showing that the condition of the entering face has little part in refraction. The photographs showed a line due to the $K\alpha$ doublet and one due to the $K\beta$ doublet. Also there was radiation due to shorter wave-lengths. The fact that this refracted band of shorter wave-lengths came to a fairly sharp edge and did not reach the lines suggests that the short wave-lengths coming from the general radiation from the tube included considerable radiation from tungsten which had been deposited on the target. A study of the intensity curves,[6] due to A. W. Hull, for a molybdenum tube operating at the voltage used here (around 44,000 but not held constant) would not lead one to expect this edge if molybdenum radiation alone were present. On the other hand a comparison with the energy curve for a tungsten target[6] would lead one to expect this edge. A rough calculation (this could not be made precise because of the overexposure of the central line) confirmed the view that the band was due to general radiation.

[6] B. Davis, Phys. Rev. [2] **9**, 64 (1917).

Refraction was also obtained for an edge formed by two good cleavage faces from one of which total reflection was obtained as mentioned above. The refracted lines were very diffuse. Since the entering face does not effect refraction, then the emerging cleavage face is not suitable for refraction experiments. The fault could not be with the edge since the cleavage edge was much better than the edge on the 90° prism even after the grinding of the latter. These experiments on refraction with the direct radiation were not made very quantitative since the object was to get refraction with monochromatic radiation.

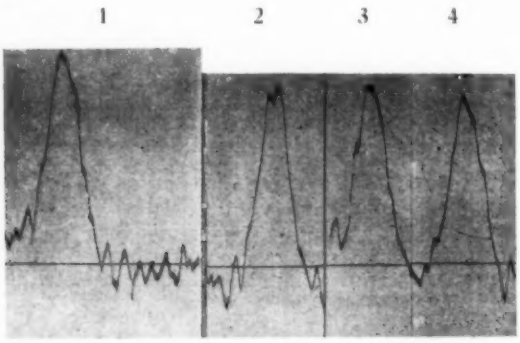

Fig. 4.

To obtain refraction with the $K\alpha_1$ line of molybdenum, C_1 was set to reflect $K\alpha_1$ at the best intensity. A good reflected line was obtained from C_1 in 2 seconds when the peak voltage was 45,000 volts and the current through the tube was 25 m.a. The angle ρ was made 7 minutes in the usual way. A good $K\alpha_1$ refracted line was obtained in 24 hours but on too dark a background to permit a close examination to be made of it. The wedge, W, was readjusted and ρ was made 1.45 minutes. The refracted line was good on a clear background. It was 0.077 mm broad and was free from a regular struc-

Fig. 5.

ture when examined under a microscope and by means of densitometer photographs (Fig. 4). Curves 1, 2, 3, and 4 were taken across different positions of this refracted line with a magnification of 40. Other refracted lines, less broad, obtained for smaller values of ρ and at longer exposures (up to 36 hours) also failed to show any fine structure which could be attributed to double refraction.

Fig. 5 shows the refracted line on the right and at the left the undeviated line from another of the good plates.

An attempt was made to find a possible fine structure by reflecting the refracted beam from C_2, but the beam was too weak to give an ionization cur-

rent measurable with an electrometer sensitivity such that the normal ionization did not mask the increase due to the refracted beam.

The refraction photographs permit a determination of the index of refraction of calcite for the $K\alpha_1$ line which has a smaller probable error than the now accepted value which was determined by the deviation from Bragg's formula. From the theory worked out by Stauss[7]

$$D + \rho = (\rho^2 + 2\delta)^{1/2}$$

in which D is the deviation due to refraction and δ is the dimensionless decrement of unity in the index of refraction. ρ has already been defined. In this equation the angles are to be expressed in radians.

Table III gives the data and results on the 11 plates taken. The distance FA' was 169.7 cm, AA' was 0.8 cm.

From the critical angle (1.95×10^{-3} radians) we get $\delta=1.90\times10^{-6}$. This value is subject to greater uncertainty than the others and is not averaged with them.

TABLE III.

Plate	d (mm)	ρ (radians)$\times10^3$	$\delta K\alpha_1\times10^6$
1.	3.096	0.192	1.993
2.	2.900	0.298	1.950
3.	2.743	0.432	1.941
4.	2.845	0.380	2.021
5.	2.838	0.380	2.012
6.	2.988	0.316	2.084
7.	2.227	0.920	2.050
8.	2.805	0.389	1.989
9.	2.313	0.791	1.989
10.	2.514	0.615	1.989
11.	2.840	0.360	1.995
		Mean	2.001 ± 0.009

It is the author's pleasure to acknowledge his indebtedness to Professor C. D. Cooksey for initiating this work, and to him, Professor L. W. McKeehan, and Mr. Donald Cooksey for much helpful advice throughout the course of the investigation. Also to Professor L. W. McKeehan the writer wishes to express his thanks for placing at his disposal the necessary facilities for doing the work.

[7] H. E. Stauss, J.O.S.A. **19**, 167 (1929).

FAINT BRANCHES IN THE OH BANDS

By G. M. Almy and G. D. Rahrer
University of Illinois

(Received October 3, 1931)

Abstract

Intense photographs of the OH bands in the near ultraviolet reveal a number of weak branches of the ${}^{0}P$ and ${}^{s}R$ types. The identification of these branches is made by a comparison of the observed wave numbers of the faint lines with their calculated wave numbers. No lines due to the molecule $O^{18}H$ were found, although under the conditions of the experiment they were to be expected.

INTENSE photographs of the group of OH bands in the near ultraviolet have been made primarily for the purpose of obtaining, in emission, bands due to $O^{18}H$. This object has not been realized but a study of the plates has disclosed a number of faint branches due to weak transitions (for which $\Delta K = \pm 2$) which have not been previously reported.

The spectrum of a heavy uncondensed discharge through water vapor was photographed with an E-1 Hilger quartz spectrograph. The water vapor was pumped rapidly through the 2 mm capillary (about 15 cm in length) of the discharge tube, which was viewed end-on. The continous spectrum of hydrogen was troublesome but its intensity was greatly reduced by increasing the rate of flow through the discharge tube with the use of a liquid air condenser placed between the tube and the pump.

The weak branches which have been identified are those of the type designated by the symbols ${}^{0}P_{12}$ ($\Delta K = +2$) and ${}^{S}R_{21}$($\Delta K = -2$). ${}^{S}R_{21}$ branches have been reported for the (0, 0) band at λ3064 by Watson,[1] for the (1, 0) band at λ2811 by Jack,[2] and the ${}^{0}P_{12}$ branch of the (0, 0) band has been identified by Almy.[3] The positions of the lines of these branches can be calculated by the following formulas, based on combination principles:[4]

$$ {}^{0}R_{21}(J) = Q_1(J) + \Delta_2F_2'(J) - 0.216(J - \tfrac{1}{2}) $$

$$ {}^{S}P_{12}(J) = Q_2(J) - \Delta_2F_2'(J - 1) + 0.216(J - \tfrac{1}{2}). $$

The comparison of the measured and the calculated wave numbers of five unreported branches in three different bands is given in the following tables. The agreement in wave numbers, together with the intensities, leaves little doubt as to the correct assignment of these lines.

As to the isotope effect, no lines due to $O^{18}H$ have been found. The relative abundance of O^{16} to O^{18} has been variously estimated at 630 to 1,[5] 1075

[1] W. W. Watson, Astrophys. J. **60,** 145 (1924).
[2] D. Jack, Proc. Roy. Soc. **A115,** 375 (1927).
[3] G. M. Almy, Phys. Rev. **35,** 1495 (1930).
[4] Cf. R. S. Mulliken, Phys. Rev. **32,** 388 (1928) and Almy, reference 3.
[5] R. Mecke and W. H. J. Childs, Zeits. f. Physik **68,** 362 (1931).

to 1,[6] and 1250 to 1.[7] The strongest $O^{16}H$ band (0, 0) was photographed in a region favorable for observation of the isotope effect in about five seconds. Thus the corresponding lines due to $O^{18}H$ should have appeared in one or two hours. Exposures up to four hours showed no lines which could have been properly assigned to $O^{18}H$. It is possible that they were masked by the hydrogen continuum.

TABLE I. $^{S}R_{21}$ *branch of the* $\lambda 2608$ *(2, 0) band.*

$J+1/2$	Intensity	Calculated wave number	Observed wave number
2	0	38404.35	38404.50
3	1	38442.07	38442.90
4	0	38475.83	38476.61
5	0	38504.76	38504.72
6	0	38526.18	38526.74
7	0	38542.23	38542.85
8	0	38551.61	38552.18
9	0	38553.32	38552.18
10	0	38550.94	38552.18

TABLE II. $^{S}R_{21}$ *branch of the* $\lambda 3428$ *(0, 1) band.*

$J+1/2$	Intensity	Calculated wave number	Observed wave number
2	3	29073.9	R_1(6-1/2)
3	5	29128.4	R_2(13-1/2)
4		29182.7	Not observed
5	1	29237.7	29236.9
6	1	29286.7	29285.8
7	1	29340.3	29341.2
8	0	29390.4	29390.6
9	0	29437.7	29437.4
10	0	29482.8	29493.8

TABLE III. $^{O}P_{12}$ *branch of the* $\lambda 2608$ *(2, 0) band.*

$J+1/2$	Intensity	Calculated wave number	Observed wave number
2	5	38036.77	Q_2(5-1/2)
3	1	37965.07	37964.73
4	5	37885.61	Q_2(8-1/2)
5	1	37798.02	37797.73
6	3	37702.41	P_2(7-1/2)
7	0	37601.62	37601.35
8	2	37492.88	Q_2(13-1/2)
9	0	37377.95	37378.08

TABLE IV. $^{O}P_{12}$ *branch of the* $\lambda 2811$ *(1, 0) band.*

$J+1/2$	Intensity	Calculated wave number	Observed wave number
2	1	35241.92	35240.94
3	1	35173.07	35172.65
4	2	35097.45	35097.03
5	2	35015.10	35014.69
6	2	34926.73	34927.13
7	10	34833.29	Q_2(14-1/2)
8	2	34735.64	34735.21
9	1	34632.21	34632.51
10	5	34524.74	P_2(1-1/2) of (2, 1) band
11	1	34412.25	34411.85
12	1	34296.05	34295.58
13	1	34175.53	34176.52
14	1	34050.94	34050.77
15	1	33926.50	33927.18
16	0	33787.97	33787.86
17	6	33652.27	P_2(21-1/2)
18	0	33511.00	33510.91
19	0	33366.05	33365.51

TABLE V. $^{O}P_{12}$ *branch of the* $\lambda 3428$ *(0, 1) band.*

$J+1/2$	Intensity	Calculated wave number	Observed wave number
2	4	28691.5	P_2(3-1/2)
3	3	28624.2	P_2(5-1/2)
4	1	28556.1	28555.8
5	1	28485.8	28487.5
6	1	28412.0	28413.1
7	2	28339.8	P_1(13-1/2)
8	0	28260.3	28261.3
9	0	28182.0	28182.4
10		28102.0	Not observed
11	0	28018.2	28018.3

[6] S. M. Naudé, Phys. Rev. **36,** 333 (1930).
[7] H. D. Babcock, Proc. Nat. Acad. Sci. **15,** 471 (1929).

INVESTIGATIONS IN THE FAR INFRARED

By John Strong*
California Institute of Technology

(Received September 22, 1931)

Abstract

An instrument is described for investigations of the reflectivity, transmissivity and emission of various materials over the spectral range 20 to 150μ. The following measurements are reported: Reflectivities of rough surfaces, galena, β-magnesia, zincite, stibinite, corundum, sphalerite, molybdenite and cuprite. Transmissivities of KBr, KI a layer of KCl evaporated on a lacquer film, a thin film of amorphous quartz, liquid CCl_4, and powdered Al and Cu. Emission of liquid and solid NaCl near the melting temperature.

Introduction

IN THE near infrared a prism spectrometer is useful for preliminary investigations when high resolving power is not required. It is the purpose of this paper to describe an instrument to play a similar role in the far infrared and to present the results of investigations carried out with this instrument.

This new instrument employs the reststrahlen method of obtaining monchromatic bands of radiation. The instrument is so designed that investigations on the reflectivity, transmissivity and emission of various materials may be expeditiously carried on over the spectral range 20 to 150μ. In order to see that the results obtained by the reststrahlen method may be equivalent to those obtained in the near infrared with a prism spectrometer it is necessary to bear in mind that the practice of representing position in the infrared spectrum by wave-length is less natural than representation by frequency. This is because the width of absorption lines, the distance between lines and the extension of an absorption band, are, when plotted against frequency, approximately the same in all regions of the spectrum, that is to say, they do not depend on wave-length. For filters the sharpness of transition from opacity to transparency will be the same. In order to get an equally accurate picture of a spectrum in any region of the infrared the number of observations per unit spectral range, on a frequency scale, is the same. The so-called far infrared, i.e. wave-lengths greater than 20μ, is not very wide when frequencies are considered. The importance of this region is due to the character of its spectra rather than their quantity. In fact the far infrared from 20–150μ corresponds, in frequency range, to approximately $\frac{1}{2}\mu$ at 3μ. This means that the twelve rather uniformly distributed wave-lengths which were employed for the present investigation correspond to about 24 points per μ at 3μ. This is about five times the frequency of points taken by Coblentz[1] in his classical studies with a prism spectrometer.

* National Research Fellow.

[1] W. W. Coblentz, Investigations of Infrared Spectra, 1908.

The Restrahlen

Table I, taken in part from "Das Ultrarote Spektrum" by Schaefer and Matossi, describes the twelve reststrahlen bands used in the present investigation.

Table I.

Number of reflections	Crystal mirrors	Filter (3 mm paraffin in each case)	Wave-length in μ	Frequency in $\sim$/cm	Energy in cm of deflection (scale at 3 meters)
4	Quartz	1 cm KCl	20.7	483	44
3 1	Fluorite Metal	5 mm KCl	23	435	18
2 2	Fluorite Calcite	3 mm KBr	27.3	366	42
4	Calcite	none	29.4	340	95
3 1	Fluorite Metal	0.4 mm quartz 1.2 mm KBr	32.8	305	2.6
3 1	Aragonite Metal	0.4 mm quartz	41	244	1.6
4	NaCl	2 mm quartz	52	192	5.2
4	KCl	"	63	159	2.0
4	KBr	"	83	120	1.6
4	KI	"	94	106	1.0
4	TlBr	"	117	85	1.7
4	TlI	"	152	66	1.0

The use of a paraffin window for the thermocouple (about 3 mm in thickness) has the advantage that it does not transmit the short wave-length reststrahlen of quartz at 8.7μ and calcite at 6.7μ to the receiver. With this filter the use of the 20.7 and 29.4μ reststrahlen is exactly the same as the other reststrahlen.

The substitution of a 1 cm KCl filter for the 2.5 mm AgCl filter recommended by Rubens and Nichols[2] for the 20.7μ reststrahlen is justified by transmission curves given by Rubens and Trowbridge[3] for AgCl and KCl.

Regarding the 41μ reststrahlen, Rubens[4] states, "Die Reststrahlen von Arrogonit waren, wie ihre Zerlegung im Gitterspektrum erkennen liess, ziemlich inhomogen und zeigten zwei Maxima, ein schwächeres bei 35, ein stärkeres bei 41μ."

In the present experiments, the 27.3μ rays were not polarized as specified by Liebisch and Rubens.[5]

Four calcite mirrors gave radiations which were transmitted by quartz. These were the 94μ radiations observed by Rubens. The fraction of the cal-

[2] H. Rubens and E. F. Nichols, Wied. Ann. **60**, 418 (1897).
[3] H. Rubens and A. Trowbridge, Wied. Ann. **60**, 724 (1897).
[4] H. Rubens, Berliner Berichte, p. 199, (1919).
[5] H. Liebisch and H. Rubens, Berliner Berichte 1919, p. 876.

cite reststrahlen transmitted by 2 mm quartz was 0.0136. In the data which follow in this paper this lack of homogeneity in the 29.4μ reststrahlen was disregarded.

The Apparatus

The apparatus has been described in an earlier paper.[6] However, there have been several alterations of the earlier form of the apparatus. These are shown in Fig. 1 and are described below;—The Welschbach mantle, used previously, was replaced by a Globar heater. The use of a Kahlbaum paraffin window with a Globar heater gives the advantages of the Welschbach mantle, namely a scarcity of near infrared radiations without the disadvantages of its fluctuations. The Globar heater (3/8″×8″) was mounted in a cooled brass cylinder—the radiations emerging through a circular hole in the center of the

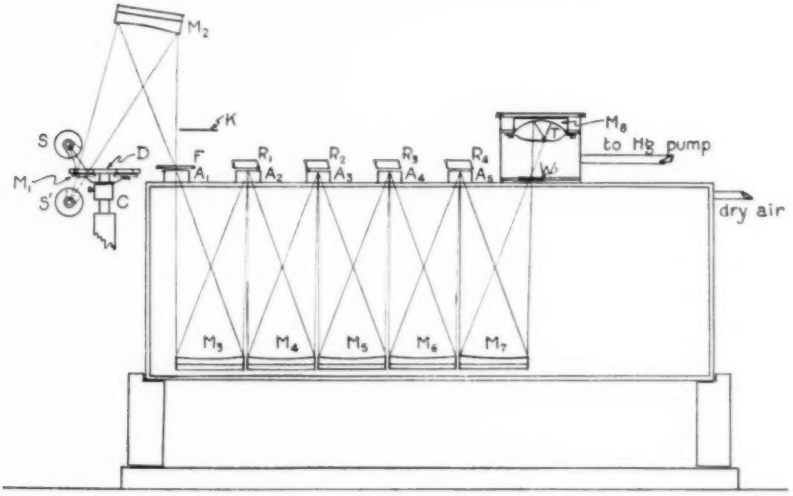

Fig. 1. Diagram of apparatus.

cylinder. For reflectivitives this source was placed in the position S (see Fig. 1) the emitted radiations being reflected to M_2 by means of the mirror M_1. By revolving the disk D the mirror M_1 may be either of the three samples being investigated or a silver mirror. These are clamped under the four symmetrical holes in the disk by the collar and spring washer C. For measuring transmissions the Globar heater takes the position S'. One of the holes in the disk is open in this case and the other three are covered with samples.

When the silver mirror reflects the energy from the heater to M_2 the reststrahlen energy may be determined by observing the galvanometer deflection as the metal shutter, K, is successively placed in and out of the radiation path. For transmission, the reststrahlen energy is determined with the radiation passing through the empty hole. The ratio of the reflected or transmitted energy to the reststrahlen energy gives respectively the reflectivity or transmissivity of the sample. In practice, the reflection or the transmission of three samples was determined each time the reststrahlen energy was determined.

[6] John Strong, Phys. Rev. **37**, 1565 (1931).

The radiations collected by M_2 are passed through the filter F and then through the aperture A_1. M_3 collects this energy to reflect it to the first reststrahlen mirror R_1. After four successive reflections R_1 to R_4 the mirrors M_7 and M_8 focus the radiation onto the thermocouple receiver. The thermocouple window, W, is 3 mm paraffin (Kahlbaum M.P. 68–70°C). The advantage of using the auxiliary mirror, M_8, to give a small focus on the thermocouple receiver is represented by a factor of 4.

The air in the apparatus was dried by passing it over $CaCl_2$ and P_2O_5. A continuous stream of dry air made diffusion of moisture into the apparatus through the holes A_1 to A_5 impossible. These holes were each covered with a lacquer membrane. The reststrahlen crystals and filters were painted with very thin colorless lacquer to protect them from attack by atmospheric moisture.

The apparatus was protected from thermal fluctuation by a felt jacket. The restrahlen crystals R_3 and R_4 were covered with a metal housing so the thermocouple could not "see out." This practice adds to the steadiness of the galvanometer.

The galvanometer used with the thermocouple was a L. and N. type H.S. and was mounted on a vibrationless support. The scale, placed at 6 meters from the galvanometer, was read with a 24 power telescope to 1/10 mm.

The galvanometer was given 15 seconds to come to equilibrium between readings. This time was accurately measured with a metronome to facilitate the cancellation of drift. The reflectivities or transmissivities of three samples may be determined four times at each of the twelve wave-lengths in an afternoon if the apparatus is kept working constantly.

The advantages of this apparatus for making preliminary spectral investigations by the reststrahlen method may be summarized as follows; (1) The reststrahlen crystals required are small, making them more easily obtainable. (2) The change from one set of crystals to another may be made quickly without disturbing the dry air in the radiation path. (3) The use of a paraffin filter facilitates measurement at 20.7 and 29.4μ.

The following measurements illustrate the applicability of this instrument for preliminary investigations in the far infrared.

Reflectivities

Rough surfaces

Lord Rayleigh[7] showed, by qualitative experiments, that rough surfaces reflect long infrared waves almost as well as polished surfaces. The practice of using a rough mirror to isolate the near infrared from the far infrared makes the quantitative investigation of the reflectivity of rough surfaces desirable. In order to study this, three rough mirrors were prepared by grinding brass on brass with 400, 200 and 60 carborundum. The reflectivities of these mirrors in the far infrared are shown in Fig. 2. The large variations of the observed points from the curves are probably due to some interference effects rather than to experimental error.

[7] Lord Rayleigh, Proc. of the Royal Inst. XVI, p. 563, 1901.

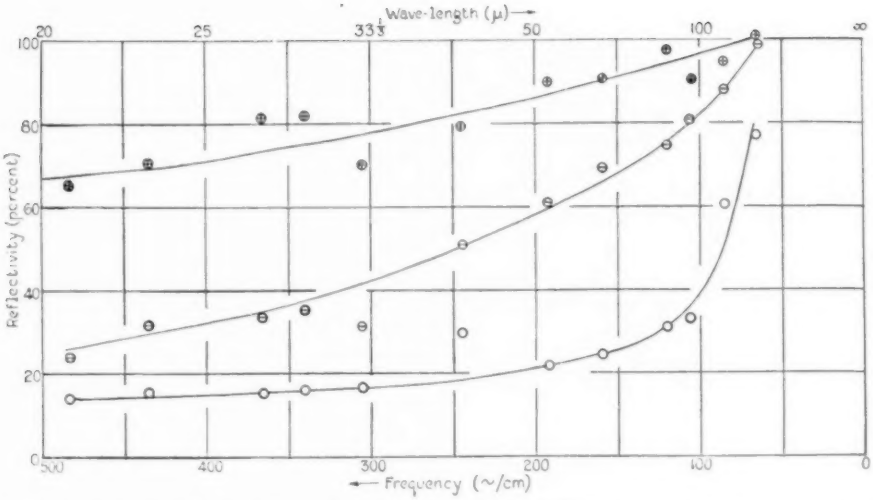

Fig. 2. Reflectivities of brass ground with 400 carborundum, crosses; 220 carborundum, thetas; and 60 carborundum, circles.

Galena

The measurements of the reflectivity of galena are shown in Fig. 3. It will be observed there are two maxima, one near 80μ and the other near 120μ. The sample was polished to a high luster except at places where small pieces of the crystal chipped out. The surface used was parallel to a cleavage plane.

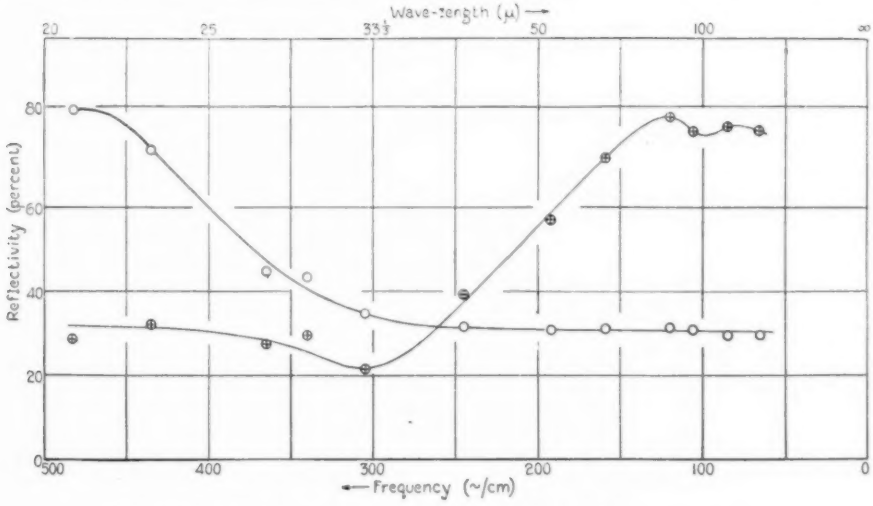

Fig. 3. Reflectivity of beta-magnesia, circles, and galena, crosses.

Four galena reflectors gave a reststrahlen whose intensity when filtered by 2 mm of quartz was 1.3 times that of the rocksalt reststrahlen. The reflection of galena for these radiations was 72 percent. The transmissivity of 0.1 mm black paper was 22 percent. For 152μ the transmissivity of the paper was 38 percent.

Magnesia

The reflectivities of magnesia for the far infrared are shown in Fig. 3. The sample was from a dense polycrystalline mass fused in an electric furnace. The exact position of the reflection maximum can only be determined with higher resolving power than was here obtainable.

Zincite

The reflection of a natural zincite crystal is shown in Fig. 4. The reflectivity is not to be considered as accurate in absolute value because the zincite was not sufficiently uniform to take a good polish. The surface was, however, much less rough than the 440 brass shown in Fig. 2. The curve is drawn with maxima at 22 and 28μ to agree with the predictions of S. Tolksdorf.[8]

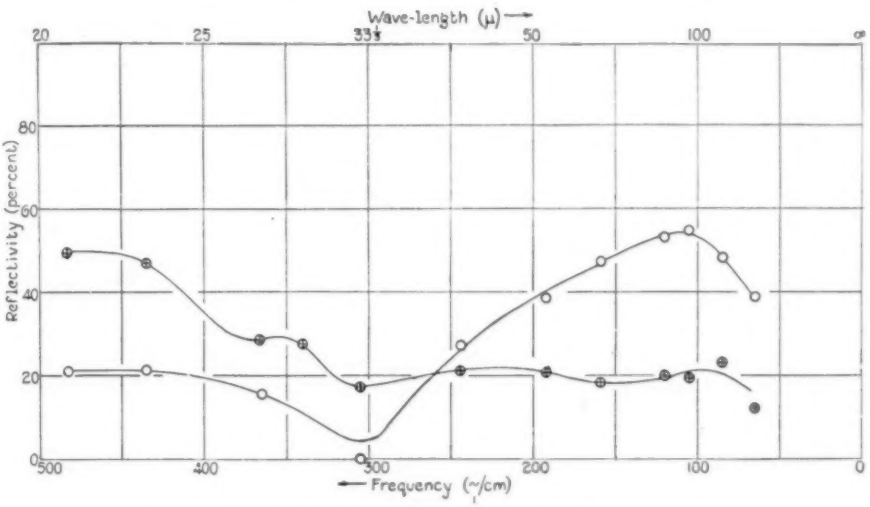

Fig. 4. Reflectivities of zincite, crosses and stibinite, circles.

Stibinite

The sample of stibinite was cleaved from a small crystal. It was neither flat nor large enough for the hole in the plate *D* (see Fig. 1). Nevertheless the results plotted in Fig. 4 indicate a maximum of reflectivity at 94μ.

Sphalerite

Because of nonuniformity this crystal did not take a good polish. As a consequence of this, the reflectivities are not to be considered quantitatively correct. The results (Fig. 5) agree with those of Rubens for (ZnFe)S in having a maximum at 30.9μ.

Corundum

The sample was not large enough to afford quantitative investigations. The results (Fig. 5) show maxima at 23μ and 27μ which may possibly be the fundamental bands whose overtones were observed by Coblentz[9] at 11.8 and

[8] S. Tolksdorf, Zeits. f. phys. Chem. **132,** 161 (1928).

[9] W. W. Coblentz, Investigations, part V, p. 18, 1908.

13.5μ. It will be observed there is a third and weaker maximum at 52μ. In Fig. 6 the reflectivities of cuprite and molybdenite are shown. Neither of these substances showed very remarkable spectra in the infrared. The samples were not perfect, so a quantitative interpretation of the results is not justified.

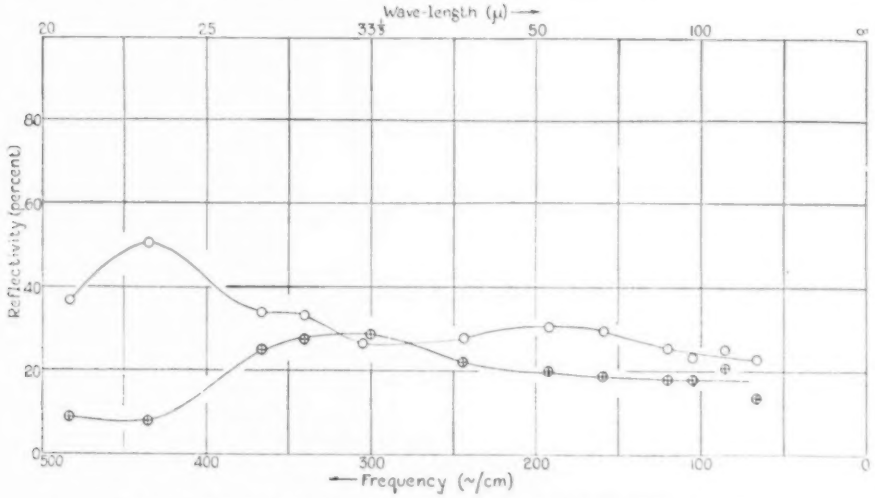

Fig. 5. Reflectivities of corundum, circles, and sphalerite, crosses.

Transmissivities

KBr and KI

The transmission of 3.19 mm of KBr and 0.83 mm of KI is plotted in Fig. 7. It is well to keep in mind the result reported in an earlier paper,[6] namely that 2 cm of KI transmits 50 percent of the 32.8μ reststrahlen. These results do not distinguish between loss of light due to surface reflection and that due to body absorption.

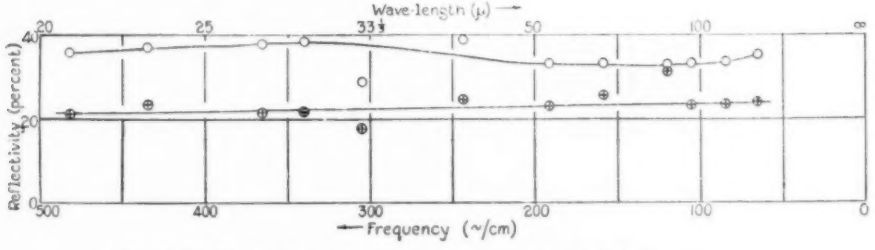

Fig. 6. Reflectivities of cuprite, circles; and molybdenite, crosses.

KCl evaporated on a lacquer film

This experiment was made to see if an evaporated film would not be free of the anomaly reported by Hirsekorn[10] for the lacquer films on which KCl smoke was deposited. The evaporated film gave only a single absorption at the expected position. The sample was prepared by evaporation of KCl onto a lacquer film in vacuum. Hirsekorn evaporated at atmospheric pressure and

[10] H. G. Hirsekorn, Ann. d. Physik **6**, 985 (1930).

observed two maxima of absorption on either side of the region of metallic reflection for KCl.

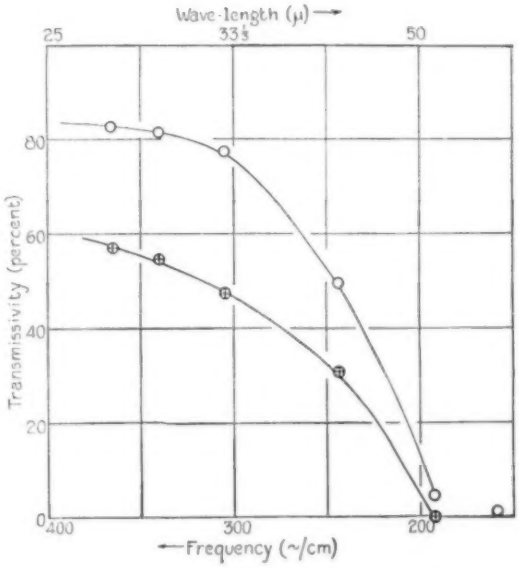

Fig. 7. Transmissivities of 3.19 mm KBr, crosses; and 0.83 mm of KI, circles.

Quartz film

Thin films of amorphous quartz have been used as absorption cell windows in the far infrared by Czerny.[11] For such purposes it is useful to know their transmission. This is shown in Fig. 8 for a film, about 10μ thickness, of

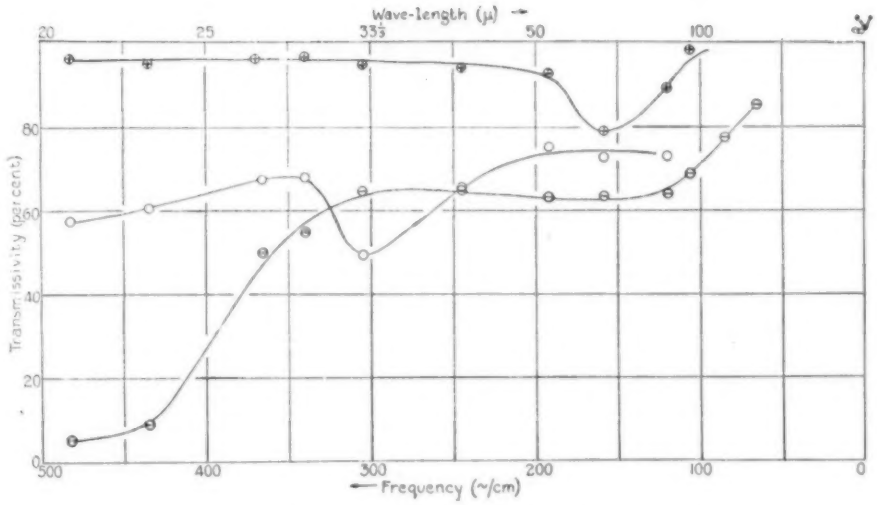

Fig. 8. Transmissivities of 10μ film of amorphous quartz, thetas; liquid CCl_4, circles; KCl evaporated on lacquer film, crosses.

[11] M. Czerny, Zeits. f. Physik **44**, 235 (1927).

amorphous quartz. The increase in transmission beyond 83μ may be ascribed to the destructive interference between the light reflected from the front and back surfaces of the quartz film.

CCl_4

CCl_4 has a band system analogous to CH_4. Trumpy[12] has predicted for CCl_4 an active frequency at 311$\sim$/cm. This is the only active frequency in the far infrared. In order to test for the presence of this band a solution of CCl_4 in paraffin was placed between two thin paraffin sheets. This was chosen in preference to the gas method because of the low vapor pressure of CCl_4. The transmission of this sample showed a minimum at the predicted position in the spectrum (see Fig. 8).

I believe this method of studying the transmission of liquids in the far infrared to be superior to the use of a thin cell bounded by windows because it is free from objectionable interference effects. These effects may be particularly annoying in the far infrared where (if the windows are quartz) the reflectivities are high and the Bragg reflection consequently more troublesome.

Copper and aluminum powders

These powders were suspended in Kahlbaum paraffin and sheets as thin as 0.15 mm proved to be opaque although this was not to be expected since the particles were small as compared with the wave-length of the radiation.[13]

Emission

NaCl

The emission of NaCl on a platinum ribbon was investigated just below and just above the melting temperature. The results are given in Table II.

Table II. *Ratio of emission of NaCl on Pt ribbon above melting temperature to emission below melting temperature.*

63μ	52μ	41μ
1.24	1.01	1.20

The results are unfortunately not decisive because at the lower temperature very little NaCl volitalized whereas the molten salt sent up a little curl of smoke which may have absorbed some of the radiations as it was partially in the radiation path. However, it is probable that the characteristic frequency of NaCl at 52μ disappears on melting.

[12] B. Trumpy, Zeits. f. Physik **66**, 790 (1930).

[13] In this connection the result of another experiment is of interest. The fluorite reststrahlen was not transmitted through a tube 10 feet long filled with the smoke from burning phosphorus.

THE INFRARED SPECTRUM AND THE MOLECULAR CONFIGURATION OF N_2O

By E. K. Plyler and E. F. Barker
University of Michigan

(Received October 8, 1931)

Abstract

Vibration spectrum. The three normal vibrations of N_2O are all active. The fundamental bands at 17.0μ, 7.78μ and 4.50μ, and the three harmonics have all been observed; also six combination bands at wave-lengths greater than 2μ. The 17.0μ fundamental and two combination bands involving this fundamental have strong zero branches, while the harmonic and two combination bands involving the harmonic transition have no zero branches. All other bands are doublets.

Rotational analysis. Three bands at 17.0μ, 7.78μ and 8.60μ have been resolved under high dispersion. All show rotation lines with continuously varying intensities (no alternation) and almost uniform spacing, the same for each band, viz. 0.84 cm^{-1}. The corresponding value of the moment of inertia, 59.4×10^{-40}, is practically equivalent to that computed from the doublet separations of the various bands.

Form of the molecule. The molecule is apparently linear but not symmetrical. The observations are not consistent with a triangular configuration, nor with the symmetrical linear configuration N−O−N, but they may be correlated precisely by means of the model N≡N=O.

THE infrared vibration spectrum of the N_2O molecule has been studied by Warburg and Leithauser[1], by E. v. Bahr[2], and more recently by Snow[3] but none of these observations were extended to wave-lengths sufficiently great to include all of the bands, nor was the available resolution adequate to reveal the rotational structure. Snow presented arguments based upon the physical properties of the gas which suggest that the molecule is linear in form, and believed that his results indicated the symmetrical arrangement N-O-N. Since the total number of electrons is the same as for CO_2 which is certainly linear and symmetrical[4] this would require that both in properties and spectrum the two gases should be very much alike. The observations indicate, however, a much richer spectrum for N_2O, with many more bands of appreciable intensity and without the restrictions as to combination frequencies which apply to CO_2.

The observations to be described below extend to about 20μ and include a number of bands not previously reported. The rotational structure is clearly resolved in several typical cases, and suggests at once a linear model, but certainly not a symmetrical one. The three fundamental frequencies are all active, as would have been expected for a triangular configuration of the atoms; they are however numerically inconsistent with the mechanical solu-

[1] Warburg and Leithauser, Ber. D. phys. Ges. **1**, 148 (1908).
[2] E. v. Bahr, Verh. D. phys. Ges. **15**, 710 (1913).
[3] Snow, Proc. Roy. Soc. **A128**, 294 (1930).
[4] Martin and Barker, Phys. Rev. **37**, 1708 (1931).

tion for this case,[5] on the assumption of central force fields, yielding for the apex angle an imaginary value. It is quite apparent that the asymmetry must involve a difference in the distances from the oxygen atom to the two nitrogen atoms, rather than a departure from linearity. Such a situation seems probable only if the oxygen atom occurs at one end rather than at the middle of the group, the molecular form being $N \equiv N = O$.* In this case the vibration corresponding to ν_1, the inactive frequency for symmetrical molecules, would be represented in the absorption spectrum by fundamental and harmonic bands of the doublet type. The same would be true of ν_3, while ν_2 should exhibit zero branches in the fundamental and odd numbered harmonic bands, but none in even numbered harmonics. This follows immediately from the correspondence principle, and has been derived rigorously by Dennison.[6]

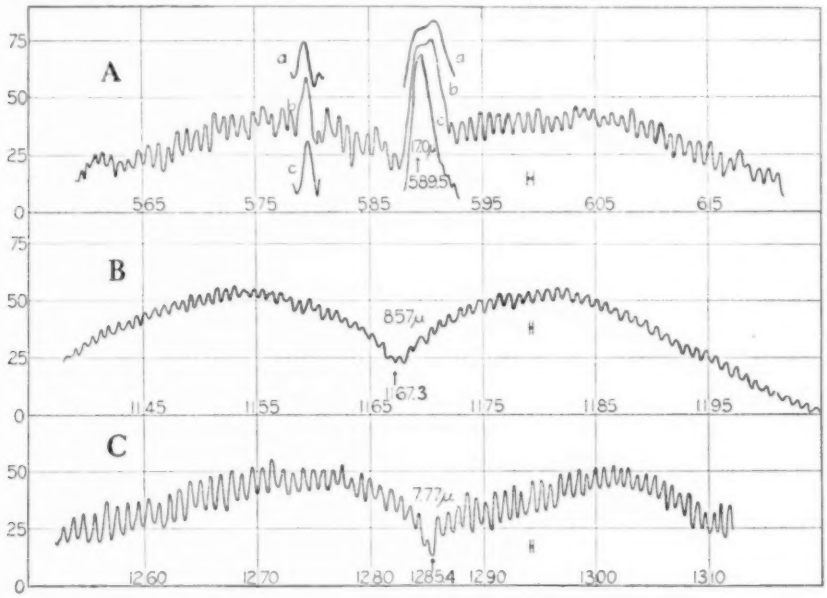

Fig. 1. Bands of N_2O showing rotational structure.
A. The fundamental ν_2, 26 cm cell, pressures 4, 16 and 30 cm.
B. The harmonic $2\nu_2$, 6 cm cell, 24 cm pressure.
C. The fundamental ν_1, 6 cm cell, 10 cm pressure.

The Observed Fundamental Bands

The lowest frequency fundamental band occurs at 17.0μ and arises from a change in electric moment perpendicular to the linear axis of the molecule, i.e. from the vibration ν_2. It has been resolved by means of a grating with a $7'' \times 9''$ surface ruled 1200 lines per inch, which was so effective that slits 0.6

[5] Dennison, Phil. Mag. **1**, 203 (1926).

* During the course of the investigation our observations were submitted to Professor Dennison, and he first suggested this interpretation, which is apparently the only completely consistent one. We understand that the idea originated in a discussion between Dennison and Snow on the subject of the N_2O spectrum.

[6] Dennison, Rev. Mod. Phys. **3**, 280 (1931).

mm wide (including a frequency range of about 0.4 cm^{-1}) were adequate. The outline of this band is shown in Fig. 1A, upon a scale too small to indicate the individual readings which were taken at intervals of about 0.2 cm^{-1}. There is a strong zero branch at about 590 cm^{-1} with positive and negative branches consisting of lines appearing single at this resolution, which are

TABLE I. *Observed frequencies for the fundamental ν_2 at 17.0μ, and residuals from the computed values.*

Positive branch			*Negative branch*	
wave numbers	residuals	m	wave numbers	residuals
		2	587.3	+.03
		3	6.4	+.10
592.4	−.04	4	5.6	+.06
3.3	−.10	5	4.9	−.08
4.0	+.05	6	3.9	+.07
4.9	−.01	7	3.1	+.03
5.7	+.04	8	2.4	−.09
6.5	+.07	9	1.4	+.07
7.4	+.01	10	0.6	+.03
8.3	−.05	11		
9.1	−.01	12		
600.0	−.07	13	78.1	+.03
0.8	−.03	14	7.4	−.11
1.6	+.01	15	6.5	−.05
2.4	+.07	16	5.7	−.09
3.3	+.01	17	4.8	−.03
4.1	+.04	18	3.9	+.04
4.9	+.09	19	3.0	+.11
5.7	+.13	20	2.2	+.07
6.5	+.17	21	1.4	+.03
7.4	+.12	22	0.6	.00
8.3	+.05	23	69.9	−.11
9.1	+.10	24	9.0	−.06
10.0	+.04	25	8.1	.00
0.8	+.10	26	7.3	−.04
1.7	+.04	27	6.5	−.08
2.5	+.08	28	5.6	.00
3.4	+.02	29	4.7	+.06
4.2	+.07	30	3.8	+.13
5.2	−.09	31	3.0	+.10
6.1	−.14	32	2.3	−.04
7.0	−.20	33	1.5	−.16
7.8	−.16	34		
8.6	−.11	35		
9.5	−.15	36		
20.4	−.20	37		
1.2	−.17	38		

spaced about 0.84 cm^{-1} apart. There is practically no convergence, as indicated in Table I, and the positions of the lines are well represented by the equation

$$\nu_2 = 589.01 \pm 0.839m + 0.0001m^2 \qquad (1)$$

m being merely an ordinal number, not equal to the quantum number J. The residuals in the table are differences between values from this equation and the observed frequencies; in only a few cases are they greater than 0.10 cm^{-1}, which is about the limit of accuracy in measurement. The maximum of the curve observed with 4 cm pressure in the cell, lies at 589.5 cm^{-1}, but this frequency would certainly be reduced somewhat if still less absorbing material were used.

In addition to the rotation lines there also appear secondary maxima at 590.6 and 579.6 which must be zero branches for the absorption due to molecules already possessing one or more quanta of vibrational energy. The former results in a curious broadening of the zero branch on its high frequency side as the amount of absorbing gas is increased, finally developing a double peak. Clearly this is not the result of a parabolic displacement of successive lines in the zero branch, since the convergence is so small. The proportion of molecules in the first excited state at ordinary temperatures is fairly large, in fact about 13.6 percent due to the low frequency and also to the fact that this state has a weight of two. For the first excited state the motion is isotropic in a plane normal to the molecular axis, and hence involves one quantum of rotational energy about this axis.[7] It may be represented by $1_{\pm 1}$, the normal state being 0_0, where the principal quantum number designates the vibrational state, and the subscript indicates angular momentum about the figure axis. From this state two transitions are possible, one to the double

TABLE II. *Observed frequencies for the fundamental ν_1 at 7.78μ, and residuals from the computed values.*

Positive branch			*Negative branch*	
wave numbers	residuals	*m*	wave numbers	residuals
1286.1	+.11	1	1284.5	+.03
7.0	+.03	2	3.8	−.11
7.9	−.03	3	2.9	−.05
8.7	−.02	4	2.0	+.00
9.5	+.01	5	1.1	+.05
90.3	+.04	6	2.0	+.09
1.2	−.06	7	79.4	+.02
2.0	−.04	8	8.6	−.04
2.8	−.04	9	7.7	.00
3.6	−.03	10	6.8	+.03
4.4	−.02	11	6.0	−.04
5.2	−.03	12	5.1	−.01
6.0	−.04	13	4.2	.00
6.9	−.15	14	3.4	−.07
7.6	−.06	15	2.5	−.06
8.4	−.07	16	1.5	+.03
9.2	−.09	17	0.6	+.05
1300.0	−.11	18	69.7	+.05
0.7	−.04	19	8.8	+.04
1.5	−.07	20	8.0	−.05
2.2	+.00	21	7.0	+.06
2.9	+.06	22	6.1	+.04
3.7	+.02	23	5.2	+.02
4.5	−.06	24	4.3	−.02
5.2	+.03	25	3.3	+.09
6.0	+.01	26	2.4	+.05
6.7	+.03	27	1.5	+.03
7.4	+.08	28	0.6	.00
8.2	+.01	29	59.7	−.03
8.9	+.05	30	8.7	+.03
9.7	−.02	31	7.8	−.02
10.4	+.02	32	6.9	−.04
1.0	+.14	33	5.8	+.10
1.8	+.07	34	4.9	+.04
		35	4.0	.00
		36	3.1	−.03

[7] Dennison, Rev. Mod. Phys. **3**, 296 (1931), particularly Fig. 6.

level $2_{\pm 2}$, and one to the single level 2_0. These may be assigned the frequencies 590.6 and 579.6 respectively, corresponding to the two subsidiary zero branches. The rotation lines of these bands cannot be seen, of course, but they doubtless are responsible for slight displacements of observed maxima, making the residuals larger than they would otherwise be.

The band at 7.78μ, Fig. 1C was analysed with a 7″×9″ grating having 2400 lines per inch. The slit widths were 0.20 mm equivalent to about 0.27 cm^{-1}, and observations were made at intervals of 0.20 cm^{-1}. There is no zero branch, although a very weak line appears at the center, probably belonging to one of the bands originating in molecules already excited to the first vibration state of ν_2. The positive and negative branches have almost exactly the same spacing as in the lower frequency band, but there is some convergence toward smaller wave-lengths. The positions of the lines are given in Table II,

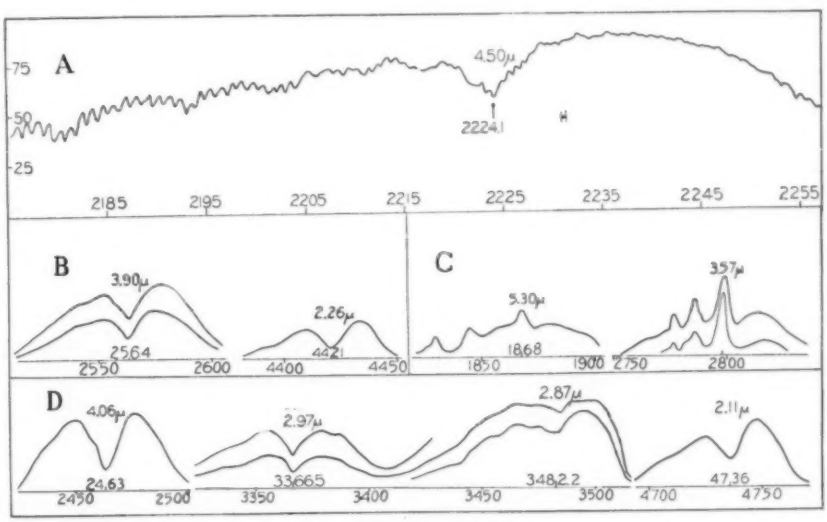

Fig. 2. Band envelopes.

A. The fundamental ν_3, partially resolved.

B. The harmonics $2\nu_1$ at 3.90μ and $2\nu_3$ at 2.26μ.

C. Combination bands $\nu_1+\nu_2$ at 5.30μ and $\nu_2+\nu_3$ at 3.57μ.

D. Combination bands $\nu_1+2\nu_2$ at 4.06μ, $2\nu_2+\nu_3$ at 2.97μ, $\nu_1+\nu_3$ at 2.87μ and $2\nu_1+\nu_3$ at 2.11μ.

together with the residuals (computed values minus observed values) obtained from the equation

$$\nu_1 = 1285.37 \pm 0.837m - 0.0017m^2. \qquad (2)$$

Although ν_1 and ν_2 are vibrations of essentially different character, the coefficients of the linear terms in both Eqs. (1) and (2) are practically equal, the corresponding difference in moment of inertia being no greater than would be expected as a result of deformations involved in the vibrations themselves. If the molecule had been in the form of a triangle with one atom at each vertex, thus constituting an asymmetrical rotator, the rotation lines would have been very irregular both in spacing and intensity: or, as a special case, the

rotator might have been symmetrical, with moments of inertia $A = B = C/2$, but none of the bands would then exhibit a single strong zero branch as ν_2 does here, for no change in electric moment parallel to the symmetry axis could occur.

The third fundamental band lies at 4.50μ. It has been mapped with a grating having 7200 lines per inch and is shown in Fig 2A. The slit included 0.33 cm^{-1}. Although many trials were made to determine the optimum conditions for resolution, no clear cut rotation series could be obtained. From certain sections of the band it is evident that the line spacing is the same as in the other fundamentals, but the envelope shows a scalloped appearance for all gas pressures, indicating superposed bands of appreciable intensity. As before, these are probably due to absorption by molecules already vibrating in the lowest frequency mode. The interaction between ν_2 and ν_3 is apparently large, so that the maximum of the positive branch for the first upper stage band falls very near the center of the primary band, which is so obscured that an accurate determination os its position is impossible. The fact that the 7.8μ band is not so distorted indicates relatively less interaction between ν_1 and ν_2. The frequency indicated as the center, 2224.1 cm^{-1}, is that of the lowest point of this portion of the curve.

The relative intensities of the fundamentals ν_2 (17.0μ), ν_1 (7.8μ), and ν_3 (4.5μ) may be estimated as approximately 4:7:10.

The Harmonic and Combination Bands

The harmonic of the 17.0μ band, located at 8.6μ, is shown in Fig. 1B, as mapped with the 2400 line grating. If the molecule were linear and symmetrical this transition would yield zero intensity of absorption;[6] if linear but unsymmetrical the component of the electric moment normal to the axis would still remain constant, but there would be a varying component along the axis, giving rise to a band with positive and negative branches but no zero branch. This is exactly as observed. The line spacing is about 0.84 cm^{-1} as before, and the intensity is about one fifth as great as that of the fundamental. The observed wave numbers shown in Table III are fairly well represented by the equation

$$\nu = 1167.31 \pm 0.835m + 0.0009m^2. \qquad (3)$$

Beginning from the first excited state only one absorption band occurs in this region, instead of two as in the fundamental. It corresponds to the double transition $1_{\pm 1} \rightarrow 3_{\pm 1}$, but the suppression of the zero branch makes its position difficult to determine. The fact that the depressions between the lines are not nearly so marked as in the neighboring band at 7.8μ, indicates the disturbing effect of this superposition, which probably also explains the large residuals for small values of m.

Harmonics of the other two fundamentals are shown in Fig. 2B without high resolution. These are doublets, as would be expected. Six combination bands have been observed in the same manner. Of these two involve the fundamental transition in ν_2, and exhibit zero branches (λ5.3 and λ3.57, Fig. 2C)

TABLE III. *Observed frequencies for the harmonic $2\nu_2$ at 8.60μ, and residuals from the computed values.*

Positive branch wave numbers	residuals	m	*Negative branch* wave numbers	residuals
1167.8	+.34	1	1166.4	+.08
8.8	+.18	2	5.5	+.14
9.7	+.12	3	4.6	+.22
70.7	−.03	4	4.0	−.01
1.4	+.11	5	3.1	+.07
2.2	+.15	6	2.3	+.03
3.2	.00	7	1.6	−.06
4.0	+.05	8	0.7	−.01
4.9	−.01	9	59.9	−.03
5.8	−.05	10	9.1	−.05
6.7	−.05	11	8.3	−.05
7.5	−.04	12	7.4	+.02
8.4	−.09	13	6.6	+.01
9.2	−.03	14	5.8	−.01
80.0	+.04	15	5.0	.00
0.9	.00	16	4.2	−.02
1.8	−.04	17	3.3	+.08
2.7	−.06	18	2.6	−.04
3.6	−.11	19	1.8	−.03
4.4	−.03	20	1.0	−.03
5.3	−.13	21	0.2	−.02
6.1	−.04	22	49.5	−.05
7.0	−.06	23	8.7	−.11
7.9	−.03	24	8.0	−.18
8.7	+.03	25	7.1	−.09
9.6	+.03	26	6.3	−.09
90.5	+.02	27	5.4	+.02
1.4	+.03	28	4.7	−.09
2.3	+.03	29	4.0	+.02
3.2	+.04	30	3.1	−.03
4.1	−.05	31	2.2	+.09
4.9	+.05	32	1.5	+.01
5.8	+.04	33	0.7	+.04
6.7	+.04	34	0.0	−.04
7.6	+.04	35	39.2	.00
8.5	+.03	36		
9.3	+.13	37		
1200.3	+.06	38		
1.1	+.14	39		
2.1	+.05	40		
3.0	+.06	41		

while two others involve the first harmonic of ν_2 and are doublets (λ4.05 and λ2.97, Fig. 2D). The zero branch bands each show three maxima corresponding to transitions $0_0 \rightarrow 1_1$, $1_1 \rightarrow 2_0$, and $1_1 \rightarrow 2_2$ for the ν_2 component.

The positions and approximate intensities for all of the observed bands are assembled in Table IV, with the assigned interpretations indicated. From the equation given by Dennison* for the positions of the various vibration levels it is possible to determine in first approximation the anharmonic correction terms. Aside from a common constant the levels are given in frequency units by the expression

$$V_1\nu_1 + V_2\nu_2 + V_3\nu_3 + x_{11}V_1^2 + x_{22}(V_2^2 - \tfrac{1}{3}l^2) + x_{33}V_3^2 + x_{12}V_1V_2 + x_{13}V_1V_3 + x_{23}V_2V_3$$

* Reference 6, p. 296. Although written for the linear symmetrical molecule, this equation is equally applicable to the unsymmetrical group of three colinear atoms, as may easily be seen.

TABLE IV. *Positions and relative intensities of observed bands.*

	λ	ν (obs.)	int.	ν^0	transition in V_2
		579.5	4		$1_1 \rightarrow 2_2$
ν_2	17.0	589.0	40	593.0	$0_0 \rightarrow 1_1$
		590.5	4		$1_1 \rightarrow 2_0$
ν_1	7.78	1285.4	70	1288.7	
ν_3	4.50	2224.1	100	2237.9	
$2\nu_2$	8.60	1167.3	20		
$2\nu_1$	3.90	2564.2	16		
$2\nu_3$	2.26	4420.7	2		
		1868.0	0.5		$0_0 \rightarrow 1_1$
$\nu_1+\nu_2$	5.30	1845	0.1		$1_1 \rightarrow 2_2$
		1829	0.1		$1_1 \rightarrow 2_0$
$\nu_1+2\nu_2$	4.06	2462.2	6		
		2799.1	1.2		$0_0 \rightarrow 1_1$
$\nu_2+\nu_3$	3.57	2786	0.3		1_1+2_2
		2777	0.3		1_1+2_0
$2\nu_2+\nu_3$	2.97	3366.5	1.6		
$\nu_1+\nu_3$	2.87	3482.2	10		
$2\nu_1+\nu_3$	2.11	4736.0	0.8		

where l measures angular momentum about the axis, in units of $h/2\pi$. By taking differences between the appropriate expressions of this sort for different observed bands, sets of equations are obtained from which the values of the x's may be determined, and hence the frequencies ν^0 corresponding to infinitesimal amplitudes. Table V shows the values of these coefficients, with the transitions from which they are obtained. The values of ν^0 appear in

TABLE V. *Anharmonic correction coefficients.*

coefficient	value	transitions employed
x_{11}	−3.3	$(0\rightarrow 2)V_1-(0\rightarrow 1)V_1$
	−4.0	$(0_2\rightarrow 2_0)V_2-(0_0\rightarrow 1_1)V_2$
x_{22}	−4.0	$(1_1\rightarrow 2_0)V_2$
	−1.25	$(1_1\rightarrow 2_2)V_2$
x_{33}	−13.8	$(0\rightarrow 2)V_3-(0\rightarrow 1)V_3$
	−7.7	$(0\rightarrow 1)V_1+(0_0\rightarrow 1_1)V_2$
x_{12}	−6.3	$(0\rightarrow 1)V_1+(0_0\rightarrow 2_0)V_2$
	−15.4	$(0\rightarrow 1)V_1+(1_1\rightarrow 2_2)V_2$
	−10.0	$(0\rightarrow 1)V_1+(1_1\rightarrow 2_0)V_2$
x_{13}	−27.3	$(0\rightarrow 1)V_1+(0\rightarrow 1)V_3$
	−26.1	$(0\rightarrow 2)V_1+(0\rightarrow 1)V_3$
	−14.0	$(0_0\rightarrow 1_1)V_2+(0\rightarrow 1)V_3$
x_{23}	−14.3	$(1_1\rightarrow 2_2)V_2+(0\rightarrow 1)V_3$
	−13.3	$(1_1\rightarrow 2_0)V_2+(0\rightarrow 1)V_3$
	−12.5	$(0_0\rightarrow 2_0)V_2+(0\rightarrow 1)V_3$

Table IV, column 5. The above expression is, of course, a first approximation only: with our interpretation of the bands it gives consistent values whenever l is not greater than unity. It does not, however, fit very well the assignments $(2_2\rightarrow 1_1)V_2=590.5$ and $(1\rightarrow 0)V_1+(2_2\rightarrow 1_1)V_2=1845$.

Form of the Molecule

The considerations bearing upon the question of geometric arrangement of the atoms in the molecule of N_2O may be summarized as follows: (1) The observed bands are of two types, one with an intense zero branch and one without, but in each case the rotation lines of the positive and negative branches form simple series with the same spacing. This excludes the possibility of a triangular configuration, which would result either in an asymmetrical rotator with very irregular lines, or in a symmetrical rotator with two different line spacings. (2) The moment of inertia as computed from the fine structure using the formula $B=h/4\pi^2 I$, is 59.4×10^{-40}, which is of the same order of magnitude as the value obtained from the doublet differences of the band envelopes. This doublet difference is practically the same in all bands and averages 29 cm^{-1}, corresponding to $I=55\times10^{-40}$, a value somewhat smaller than the previous one because of slight broadening of the bands due to the large proportion of the molecules already excited vibrationally at room temperature. This numerical agreement also indicates the linear arrangement of atoms in the molecule. (3). The uniformly varying intensities in fine structure lines indicates that the molecule is not of the form N–O–N, since nuclear spin in the N atoms would then lead to alternating intensities, as in the bands of N_2. (4) The absence of any restriction upon vibrational transitions also excludes the possibility of the symmetrical arrangement. All combinations of ΔV_1, ΔV_2 and ΔV_3 appear, with zero branches only when ΔV_2 is odd. (5) The variation of specific heat with temperature is a further indication that the molecule is linear. Snow has kindly informed us that his computations using our three fundamental frequencies reproduce the specific heat curve very accurately.

A very rough comparison of the relative strengths of the two chemical bonds may be obtained by assuming infinitesimal harmonic vibrations as of mass points fastened together by two weightless springs, and vibrating along the line of centers. Let the force constants be K_1 and K_2 for the N–N and the N–O linkages respectively, the interaction between the two extreme atoms being neglected. From the character and the frequencies (ν_1 and ν_3) of the two normal vibrations, and the known masses of the atoms, it follows at once that $K_1=2.4\times10^6$ and $K_2=2.2\times10^6$ dynes/cm.

Raman Lines

The observed Raman spectrum of N_2O consists of a single line[8] at 1281 cm^{-1}, in fairly good agreement with our value for ν_1. For linear molecules ν_2 would not appear in the Raman scattering, due to the symmetry of the vibration.[9] Neither would ν_3 appear if the configuration were symmetrical. However, it should be observed, though possibly with low intensity, for the unsymmetrical arrangement indicated above.

[8] Dickinson, Dillon and Rasetti, Phys. Rev. **34,** 582 (1929).

[9] Placzek, Zeits. f. Physik **70,** 84 (1931).

Permanent Electric Moment

The electric moment of N_2O is apparently very small[10] which at first glance seems to favor the hypothesis of a symmetrical molecule. It is probably not zero, however. In the absence of definite information concerning the electron distribution and the interatomic distances, it is impossible to estimate precisely what value would be expected for an unsymmetrical linear configuration. It is clear, however, that the position of the electrical center for the positive nuclei is very sensitive to changes in the relative distances from central to extreme atoms, and it might happen to fall very close to the corresponding center for the electron shell. Hence our model is not necessarily inconsistent with the observed dipole value.

[10] Braunmuhl, Phys. Zeits. **28**, 141 (1927).

THE RAMAN EFFECT IN CERTAIN ORGANIC COMPOUNDS

By M. E. High
Mendenhall Laboratory of Physics, Ohio State University

(Received August 31, 1931)

Abstract

The Raman spectra of the normal and iso forms of propyl ether, amyl ether, propyl propionate, butyl propionate, amyl propionate, and also methyl propionate have been measured. Certain characteristic frequencies remain unchanged throughout the series but other frequencies which appear singly in the normal forms are split into several frequencies in the iso forms, due to the rearrangement of the atomic groups. The Raman spectra have also been observed in the ortho, meta and para forms of chlorotoluene, cresyl methyl ether, nitrochlorobenzene and nitrotoluene. In addition to the characteristic frequencies which remain unchanged there are certain frequencies which consistently increase from the ortho to meta to para forms. Similar increases are noted in the infrared absorption spectra of the xylenes.

Introduction

DATA on the incoherent scattering of light, as first observed by Raman,[1] should give important information about the different modes of vibration and rotation of molecules and the energies associated with each of these modes of vibration and rotation. Hence a study of the Raman effect in organic molecules gives a means of advancing our knowledge of these molecules. Dadieu and Kohlrausch[2] and others have already shown that certain atomic groupings in organic molecules are definitely associated with frequency shifts observed in the Raman effect.

It is the purpose of this investigation to compare the Raman effect in certain normal forms of organic compounds with the Raman effect in the iso forms of these same compounds and to investigate the influence on the Raman effe·t of shifting the substituents from the ortho to the meta and to the para position in organic compounds.

Experimental

The design of the apparatus used follows that suggested by Wood[3] and modified by Morris,[4] except that four mercury arcs were used instead of one. The arcs were vertical, as was also the tube which contained the substance to be examined. The scattered light, after passing through a totally reflecting prism was focused on the slit of the spectrograph. The tube containing the liquid was about 25 mm in diameter and 12 cm long. A blast of air kept the liquid and the arcs cool. The spectrograph was a specially constructed, high-speed instrument, with lenses of 6 inch focal length and 2.5 inch aperture. There were two 60 degree glass prisms with faces 2.5 by 4 inches.

[1] Raman, Ind. J. Phys. **2,** 387 (1928).
[2] Dadieu and Kohlrausch, Ber. **63,** 251 (1930); J. O. S. A. **21,** 286 (1931).
[3] Wood, Phil. Mag. **6,** 729 (1928).
[4] Morris, Phys. Rev. **38,** 141 (1931).

TABLE I.

Substance Formula	$\Delta\nu$	$\Delta\nu$	$\Delta\nu$	$\Delta\nu$	$\Delta\nu$	$\Delta\nu$	$\Delta\nu$
n-propyl ether $C_3H_7-O-C_3H_7$	874(2) (ea)	1091(2) (ade)	1282(3) (ae)	1446(4) (ae)	2864(3) (adeg)	2931(3) (egh)	
iso-propyl ether $(CH_3)_2CH-O-CH(CH_3)_2$	791(6) (ade)	848(2) (ae)	903(5) (ae)	930(1) (de)	1453(8) (ae)	2872(3) (ef)	2916(2) (afh)
n-amyl ether $CH_{11}-O-C_5H_{11}$	764(2) (ae)	1292(4) (ae)	1447(7) (ae)	2853(5) (ae)	2904(5) (aeh)	2957(5) (aegh)	
iso-amyl ether $(CH_3)_2(CH)_2(CH_2)_4O$	765(4) (ae)	815(1) (ade)	908(1) (ae)	950(3) (ade)	1144(4) (ade)	1449(9) (ae)	2862(7) (ae)
n-propyl n-propionate $C_2H_5-COO-C_3H_7$	490(1) (ae)	889(1) (ade)	1033(2) (de)	1076(1) (de)	1450(9) (ae)	1735(4) (a)	2874(6) (defg)
iso-propyl propionate $C_2H_5-COO-CH(CH_3)_2$	431(5) (ade)	482(2) (ae)	597(5) (ae)	825(8) (ade)	875(3) (ade)	926(8) (ae)	1109(2) (ae)
n-butyl propionate $C_2H_5-COO-C_4H_9$	281(5) (ae)	1288(3) (ae)	1450(8) (ae)	1737(5) (a)	2917(band) (aeh)		
iso-butyl propionate $C_2H_5-COO-CH_2CH(CH_3)_2$	282(5) (ae)	821(3) (ae)	889(2) (ae)	1456(7) (ae)	1737(4) (a)	2920(band) (aeh)	
n-amyl propionate $C_2H_5-COO-C_5H_{11}$	956(4) (ae)	1080(2) (ae)	1292(3) (ae)	1446(8) (ae)	1732(4) (a)	2918(band) (aeh)	
iso-amyl propionate $C_2H_5-COO-(CH_2)_2CH(CH_3)_2$	770(2) (ae)	822(3) (ae)	1449(7) (ae)	1731(3) (a)	2910(band) (aeh)		
methyl propionate $C_2H_5-COO-CH_3$	435(4) (ae)	593(2) (ae)	838(7) (ade)	1072(3) (ae)	1442(4) (ae)	1735(4) (a)	2941(5) (aegh)
o-chlorotoluene $C_6H_4-Cl-CH_3$	160(8) (a)	*246*(7) (a)	356(4) (a)	442(6) (a)	543(9) (a)	673(9) (a)	797(7) (ab)
m-chlorotoluene $C_6H_4-Cl-CH_3$	*186*(3) (ae)	*233*(3) (ae)	414(5) (ae)	515(6) (ae)	682(7) (ade)	995(10) (ae)	1081(4) (ae)
p-chlorotoluene $C_6H_4-Cl-CH_3$	*304*(3) (ae)	*373*(4) (ad)	631(5) (ade)	794(10) (ade)	1085(8) (ade)	1205(5) (ae)	1378(2) (ae)
o-cresyl methyl ether $C_6H_4-CH_3-OCH_3$	*174*(4) (ae)	*235*(2) (ae)	491(6) (ae)	580(4) (ae)	743(9) (ade)	982(0) (ae)	1044(7) (ae)
m-cresyl methyl ether $C_6H_4-CH_3-OCH_3$	209(2) (a)	284(1) (a)	457(2) (a)	721(4) (ae)	784(4) (ae)	995(6) (a)	1271(4) (a)
p-cresyl methyl ether $C_6H_4-CH_3-OCH_3$	233(2) (ae)	334(4) (ae)	415(5) (ae)	515(5) (ade)	637(5) (de)	814(10) (ade)	1175(4) (de)
For the remaining compounds all Raman lines were excited by Hg 4358							
o-nitrochlorobenzene $C_6H_4-NO_2-Cl$	147(3)	470(2)	665(3)	749(3)	874(3)	1057(7)	1160(8)
m-nitrochlorobenzene $C_6H_4NO_2-Cl$	178(2)	670(3)	896(1)	1014(5)	1143(5)	1369(10)	1604(5)
p-nitrochlorobenzene $C_6H_4-NO_2-Cl$	217(1)	366(0)	401(1)	635(3)	859(3)	1122(8)	1360(10)
o-nitrotoluene $C_6H_4-NO_2-CH_3$	150(3)	555(4)	673(1)	1062(4)	1098(1)	1167(2)	1214(3)
m-nitrotoluene $C_6H_4-NO_2-CH_3$	1011(2)	1103(2)	1231(2)	1364(10)	1602(3)	2920(0)	3057(2)
p-nitrotoluene $C_6H_4-NO_2-CH_3$	281(2)	643(3)	682(1)	806(2)	869(5)	1117(8)	1217(3)

TABLE I. (*Cont.*)

Substance Formula	$\Delta\nu$	$\Delta\nu$	$\Delta\nu$	$\Delta\nu$	$\Delta\nu$	$\Delta\nu$	$\Delta\nu$
n-propyl ether C_3H_7–O–C_3H_7							
iso-propyl ether $(CH_3)_2CH$–O–$CH(CH_3)_2$	2929(9) (deh)	2975(9) (adefh)	3073(1) (fh)				
n-amyl ether C_5H_{11}–O–C_5H_{11}							
iso-amyl ether $(CH_3)_2(CH)_2(CH_2)_2O$	2906(7) (aeh)	2958(7) (aegh)	3145($\frac{1}{2}$) (ef)				
n-propyl n-propionate C_2H_5–COO–C_3H_7	2933(9) (aeh)	2975(4) (eh)					
iso-propyl propionate C_2H_5–COO–$CH(CH_3)_2$	1138(1) (de)	1172(2) (ae)	1456(9) (ae)	1737(7) (a)	2933(7) (aeh)	2980(7) (afh)	3115(1) (ah)
n-butyl propionate C_2H_5–COO–C_4H_9							
iso-butyl propionate C_2H_5–COO–$CH_2CH(CH_3)_2$							
n-amyl propionate C_2H_5–COO–C_5H_{11}							
iso-amyl propionate C_2H_5–COO–$(CH_3)_2CH(CH_2)_2$							
methyl propionate C_2H_5–COO–CH_3							
o-chlorotoluene C_6H_4–Cl–CH_3	1041(10) (abe)	1201(4) (ae)	1379(3) (ae)	1592(8) (ae)	2914(6) (ae)	3056(8) (ae)	
m-chlorotoluene C_6H_4–Cl–CH_3	1208(4) (ae)	1369(2) (ae)	1581(3) (ae)	2920(4) (ae)	3057(7) (aegh)		
p-chlorotoluene C_6H_4–Cl–CH_3	1596(6) (ae)	2921(2) (aeh)	3059(5) (adefg)				
o-cresyl methyl ether C_6H_4–CH_2–OCH_3	1156(4) (ae)	1185(2) (de)	1236(7) (ade)	1296(5) (ae)	1441(2) (ae)	1595(7) (ae)	2909(2) (af)
m-cresyl methyl ether C_6H_4–CH_2–OCH_3	1445(4) (a)	1613(5) (a)	2920(5) (a)				
p-cresyl methyl ether C_6H_4–CH_2–OCH_3	1207(3) (ae)	1287(5) (ae)	1370(1) (ae)	1448(4) (ae)	1605(4) (ae)	2917(2) (aefgh)	
For the remaining compounds all Raman lines were excited by Hg 4358							
o-nitrochlorobenzene C_6H_4–NO_2–Cl	1374(10)	1604(5)	3052(2)				
m-nitrochlorobenzene C_6H_4–NO_2–Cl	3055(2)						
p-nitrochlorobenzene C_6H_4–NO_2–Cl	1604(6)	3054(3)					
o-nitrotoluene C_6H_4–NO_2–CH_3	1360(10)	1592(4)	2918(1)	3051(2)			
m-nitrotoluene C_6H_4–NO_2–CH_3							
p-nitrotoluene C_6H_4–NO_2–CH_3	1360(10)	1613(7)	2915(1)	3053(3)			

Results

In Table I data are given for the compounds studied. The frequency shifts are given in wave numbers. If a frequency is *underscored* it means that that frequency appeared as an anti-Stokes line as well as a Stokes line. The number in parenthesis after each frequency is the intensity, estimated visually from the plates. The letters in parenthesis following the intensity indicate the mercury lines which gave rise to a Raman line corresponding to the particular frequency. The letters signify mercury lines as follows:

	Wave-length in A.U.	Wave number in cm^{-1}		Wave-length in A.U.	Wave number in cm^{-1}
a	4358	22938	e	4047	24705
b	4348	22994	f	3663	27290
c	4339	23038	g	3654	27354
d	4078	24516	h	3650	27388

Discussion of Results

There are certain frequencies which remain unchanged throughout each of the series. These are the frequencies which are defined by Dadieu and Kohlrausch[2] as "inner" frequencies, and are due to molecular configurations which are present in each molecule. The vibration, which occurs in this configuration, is, therefore, very little affected by the remaining part of the molecule.

In the ethers and propionates under consideration, one of these constant frequencies is about 1450 cm^{-1}. This frequency has been assigned by Dadieu and Kohlrausch[2] and by Trumpy to the vibration of the group.

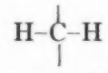

which occurs in each of the compounds. The C–H bond ordinarily gives frequencies in the neighborhood of 3000 cm^{-1}. That the CH_2 group can produce such a low frequency as 1450 cm^{-1} is explained by Dadieu and Kohlrausch by assuming that the hydrogen atoms vibrate at right angles to the direction of the linkage.

Another frequency, common to all the propionates, is 1735 cm^{-1}, approximately. Dadieu and Kohlrausch[2] have assigned this frequency to the C=O bond. The frequencies 2865 and 2929 cm^{-1} have been assigned by Dadieu and Kohlrausch to vibration of the group

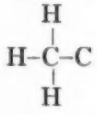

and the frequency 2967 cm^{-1} to the linkage type

In the amyl and butyl propionates these three frequencies are not resolved but appear as a band.

TABLE II.

Substance	H –C– H	C=O	H H C–C H		H X–C–X H	NO_2	C=C	C–H aliphatic	C–H aromatic
n-propyl ether	1446	—	2864	2931	—	—	—	—	—
iso-propyl ether	1453	—	2872	2929	2975	—	—	—	—
n-amyl ether	1447	—	2853	—	2957	—	—	—	—
iso-amyl ether	1449	—	2862	—	2958	—	—	—	—
n-propyl propionate	1450	1737	2874	2933	2975	—	—	—	—
iso-propyl propionate	1456	1737	—	2937	2980	—	—	—	—
n-amyl propionate	1446	1732	—	—	—	—	—	—	—
iso-amyl propionate	1449	1731	—	—	—	—	—	—	—
n-butyl propionate	1450	1737	—	—	—	—	—	—	—
iso-butyl propionate	1456	1737	—	—	—	—	—	—	—
methyl propionate	1442	1735	—	2941	—	—	—	—	—
o-chlorotoluene	—	—	—	—	—	—	1592	2914	3056
m-chlorotoluene	—	—	—	—	—	—	1581	2920	3057
p-chlorotoluene	—	—	—	—	—	—	1596	2921	3059
o-dichlorobenzene*	—	—	—	—	—	—	1569	—	3066
m-dichlorobenzene*	—	—	—	—	—	—	1575	—	3072
p-dichlorobenzene*	—	—	—	—	—	—	1572	—	3061
o-xylene*	—	—	—	—	—	—	1594	2916	3043
m-xylene*	—	—	—	—	—	—	1597	2917	3042
p-xylene*	—	—	—	—	—	—	1618	2917	3040
o-cresyl methyl ether	—	—	—	—	—	—	1595	2909	—
m-cresyl methyl ether	—	—	—	—	—	—	1613	2920	—
p-cresyl methyl ether	—	—	—	—	—	—	1605	2917	—
o-nitrochlorobenzene	—	—	—	—	—	1374	1604	—	3052
m-nitrochlorobenzene	—	—	—	—	—	1369	1604	—	3055
p-nitrochlorobenzene	—	—	—	—	—	1360	1604	—	3054
o-nitrotoluene	—	—	—	—	—	1360	1592	2918	3051
m-nitrotoluene	—	—	—	—	—	1364	1602	2920	3057
p-nitrotoluene	—	—	—	—	—	1360	1613	2915	3053
Average Values	1450	1735	2865	2932	2969	1364	1590	2918	3054

* From Dadieu and Kohlrausch, J.O.S.A. **21,** 286 (1931).

In the ortho, meta and para group there is a frequency 3050 cm^{-1} which is present in each substance except cresyl methyl ether and which has been assigned by Dadieu and Kohlrausch[2] to the aromatic C–H bond. They have assigned the frequency 2918 cm^{-1} to the aliphatic C–H bond and the frequency 1600 cm^{-1} to the C=C bond. Ganesan and Venkateswaran,[6] as well as Dadieu and Kohlrausch, have assigned the frequency 1364 cm^{-1} to the nitro group, NO_2.

Comparison of normal and iso forms

The molecules of the normal forms of ethers and propionates are supposed to consist of chains and in the iso forms these chains are split at one or both ends. Any difference in the Raman spectra ought to be explained, therefore, in terms of this rearrangement of the parts of the molecules.

In n-propyl ether there is a frequency 874 cm^{-1} which may be due to vibration of the group CH_3-CH_2. In the iso form this frequency is split into four frequencies: 791, 848, 903 and 930 cm^{-1}. This splitting must come from

[5] Trumpy, Zeits. f. Physik **62,** 806 (1930).

[6] Ganesan and Venkateswaran, Ind. J. Phys. **4,** 195 (1929).

the rearrangement of the groups in the split chain. A possible source of these frequencies is the group

$$\begin{matrix} CH_3 \\ CH_3 \end{matrix} > CH$$

This more complex arrangement would be expected to have a greater number of possible vibration frequencies than the simpler group CH_3-CH_2. There is also a corresponding increase in the number of frequencies in the iso form as compared to the normal form in amyl ether and propyl propionate. (Fig. 1.) The results for amyl and butyl propionate are not satisfactory because of the large amount of continuous spectrum and the weakness of the lines.

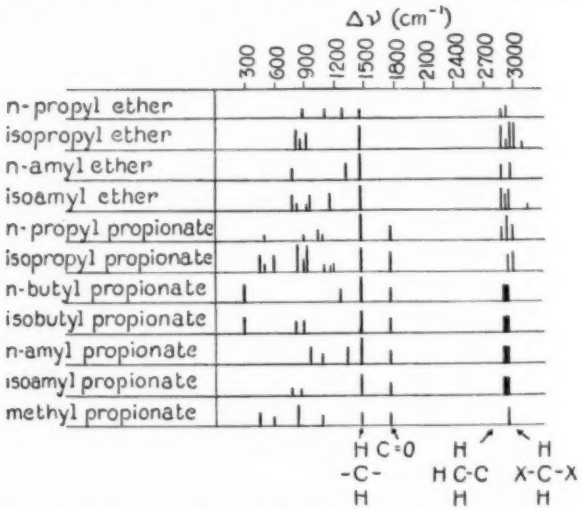

Fig. 1. Raman frequencies of normal and iso forms, showing the more complex spectra of the iso forms.

Comparison of ortho, meta and para forms

In these compounds there is a large number of frequencies, between approximately 150 and 1300 cm^{-1}, which have not been assigned to a particular vibrator. While these frequencies do not remain constant from one compound to another, yet there is a regularity in the shifts of some of them. (Fig. 2). In each case the smallest, and usually the two smallest frequencies increase progressively from the ortho to the para forms of the compound. But in addition to these smallest frequencies there are larger frequencies which have this same regular increase. Fig. 3 shows the frequencies which thus shift.

It is important to notice that these same shifts occur in the infrared spectra of ortho, meta and para-xylene. Coblentz[7] calls attention to the regular shifting of two infrared bands in o, m and p-xylene. These two bands, at about 9.7 and 13.4 μ are shown in Fig. 3 under *infrared*. It will be seen from Fig. 3 that there is a Raman frequency which corresponds to each of these particular infrared frequencies. (The dotted Raman frequencies were not observed by Dadieu and Kohlrausch). There are also two additional Raman frequencies

[7] Coblentz, "Investigations of Infrared Spectra," Carnegie Institution of Washington Publication 35 (1905).

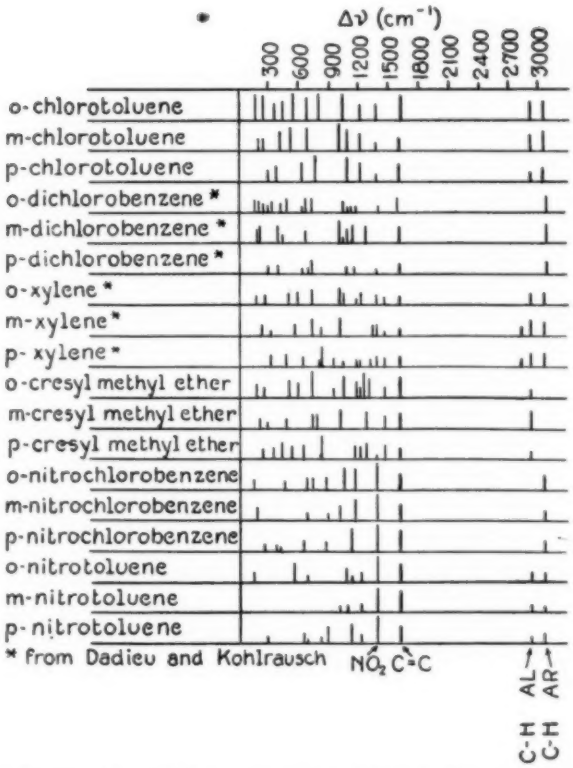

Fig. 2. Raman frequencies of ortho, meta and para forms, showing characteristic frequencies and shifting of certain other frequencies.

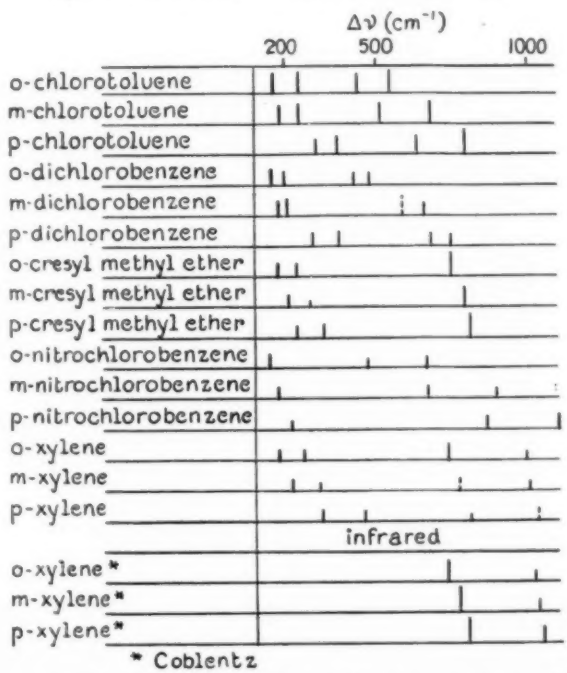

Fig. 3. Increase in frequencies from ortho to meta to para forms.

which show the same sort of shift but which lie outside the region studied by Coblentz. For xylene, then, the Raman spectra show the same shifts which occur in the infrared spectra, but in addition the Raman spectra show this same sort of shift in other frequencies which have not yet been observed by infrared methods.

In Fig. 3 the frequencies which show shifts similar to those of the xylene frequencies are plotted. Nitrotoluene is not included because of the failure to observe the smaller frequencies in m-nitrotoluene.

Comparison with infrared data

A comparison between the Raman spectrum and infrared spectrum of a substance shows in general that there are certain frequencies common to both spectra and other frequencies which appear only in the Raman spectrum or only in the infrared spectrum. In Table III the wave-lengths common to both

TABLE III.

	Wave-length in μ			Wave-length in μ	
Substance	Raman	Infrared*	Substance	Raman	Infrared**
o-nitrotoluene	3.43	3.42	methyl propionate	3.40	3.4
	6.26	6.25		5.76	5.8
	7.35	7.5		6.94	6.9
	8.56	8.4		9.3	9.2
	9.4	9.36		12.0	11.9
p-nitrotoluene	3.28	3.23	iso-amyl propionate	5.76	5.9
	3.43	3.43		6.94	7.0
	7.35	7.5		12.2	12.5
	8.88	8.65		13.0	13.1

* Coblentz, "Investigations of Infrared Spectra," Carnegie Institution of Washington Publication 35 (1905).

** Weniger, Phys. Rev. **31**, 388 (1910).

spectra are given for the four compounds for which infrared data were available. There are other frequencies in each spectrum which are found only in that spectrum. These results are in accord with the theoretical treatment of Ganesan and Venkateswaran.[6] They have pointed out that an infrared absorption band involves only two energy levels and a transition must be permissible between these two levels, while a Raman frequency involves three levels, the initial and final and a third level. Hence the presence of an infrared band depends on the possibility of a transition between two given levels, while the occurrence of a Raman frequency depends on the presence of a suitable third level, and these two conditions may be quite independent.

Continuous spectrum

Every Raman spectrum contains a certain amount of continuous background. One method for removing most of this continuous background in certain cases has been reported in the Physical Review **38,** 374 (1931).

In conclusion the author wishes to express his appreciation to Professor Alpheus W. Smith for suggesting the problem and for his advice and assistance in the work. He is also indebted to Dr. M. L. Pool for valuable suggestions and criticism throughout the course of the work.

THE RAMAN EFFECT AND THE CARBON-HALOGEN BOND

By William D. Harkins and Harold E. Bowers
George Herbert Jones Chemical Laboratory,
University of Chicago

(Received September 14, 1931)

Abstract

By far the most intense line in the Raman spectra of (organic) aliphatic bromides exhibits a Raman wave number ($\Delta\bar{\nu}$) of about 600 cm^{-1} in the methyl derivative, of 564 cm^{-1} if from two to five carbon atoms are present in the normal chain, and of about 539 cm^{-1} if the chain is branched sufficiently close to the bromine atom. These frequencies are the most characteristic of the carbon-bromine bond. It is assumed that these Raman lines, and the corresponding most intense lines in the spectra of the chlorides and of the iodides, are produced by a decrease (or increase in anti-stokes lines) by unity in the vibrational quantum number. On the basis of this assumption the use in the calculations of this paper of only the first term in the brackets of the more general equation

$$\epsilon^v = hc[\bar{w}_e(v+\tfrac{1}{2}) - x_2(v+\tfrac{1}{2})^2 + \cdots]$$

may be considered to give only a small error, possibly of the order of one percent. Here w is the wave number, but the w used elsewhere in this paper gives the frequency, since for simplicity it includes the hc term. Although the fundamental frequency associated with the carbon-halogen bond in normal aliphatic compounds decreases by about 8 percent if the number of carbon atoms in the molecule is increased from one to two, a further increase in the length of the molecule up to 5 carbon atoms does not give any further decrease; that is, the frequency is independent of the length of the molecule. The fundamental frequencies which for the methyl halides are associated with this bond are 2.13×10^{13} for the chloride, 1.81×10^{13} for the bromide, and 1.60×10^{13} per second for the iodide. The value 1.81×10^{13} for the bromide with one carbon atom, is reduced to 1.69×10^{13} if three, four or five carbon atoms are present in the molecule. If it is assumed that the mechanical frequency (w_0) is, for a value of $\Delta v = \pm 1$, related approximately by the equation

$$\Delta\nu = w_0(v'-v'') = \frac{1}{2\pi}\left(\frac{f}{\mu}\right)^{1/2}(v'-v'')$$

to the Raman frequency ($\Delta\epsilon$) which is associated with this bond, then the vibration of the bromine atom with respect to the adjacent part of the hydrocarbon chain, has a frequency which is independent of the length of the molecule, provided more than one carbon atom is present. The conclusion from these results is that the force constant which corresponds to the carbon-bromine bond, and therefore, presumably, the strength of the bond, either remains constant, or else increases only slightly as the length of the molecule increases. However, the force constant for methyl halides may be appreciably higher than those for the longer chain compounds. This indicates that the characteristic frequency of this bond corresponds to an inner vibration: that is, in general only a part of the rest of the organic molecule vibrates with respect to the halogen atom to give this frequency. The force constant characteristic of the carbon-halogen bond is found to have, for the methyl halides, values of about 3.0 for the chloride, 2.6 for the bromide, and 2.2×10^{-5} dynes per cm for the iodide. Thus the values decrease in the same order as the corresponding heats of dissociation. The values are much less than that (5×10^{-5} dynes per cm) previously found for single bonds (C·C, C·O, and C·N) in organic compounds. Another frequency, about 53

percent of that more distinctly characteristic, and with a value of about 300 cm^{-1} for the wave number, seems to be also associated with carbon-bromine bond, possibly with some type of transverse vibration. A not too distant branching of the chain of the aliphatic hydrocarbon causes a decrease of about 5 percent in the characteristic frequency associated with the carbon-bromine bond, and probably indicates a decrease in the strength of the bond. The value 1638 cm^{-1} is obtained for the wave number which is associated with the double bond of allyl bromide, while Dadieu and Kahlausch obtain 1639 cm^{-1} for the chloride and 1645 cm^{-1} for the alcohol. This illustrates the smallness of the effect of the change of mass of the substituted group upon the frequency at the double bond, which seems to indicate an inner and not an outer vibration. Experimental data are presented for the Raman spectra of nine (organic) aliphatic bromides. The spectra were taken by a large three prism Steinheil G. H. glass spectrograph, by the use of two constricted quartz mercury arcs. The ultraviolet light from these arcs was filtered out by special glass filters in order to prevent the appearance of a brown color in the liquid, and the resultant continuous fluorescence spectrum.

1. Introduction

WHILE very extensive researches have been carried out to determine the Raman frequencies most closely associated with various substituted radicals in organic compounds, there have been no investigations which show in a satisfactory way the effect of a change of length of the organic molecule upon any such frequency.[1] The work reported here was begun in 1929 to remedy this deficiency. In order to prevent the extra complication which arises when several atoms are present in the radical, it was decided to study the frequencies associated with a single halogen atom in the molecule.

2. Experimental Method

The Raman spectra were taken by the use of a large Steinheil three prism glass spectrograph. The Pyrex tube used to hold the liquid is similar in shape to that designed by Wood. The liquid, after purification by distillation, is put into a glass bulb (Fig. 1) which is kept sealed to the Raman tube. After evacuation of the tube, the liquid is distilled over into the Raman tube. This liquid is then poured back into the tube, and this process repeated several times to give an "optically empty" liquid.

The source of light was a set of vertical constricted 220 volt quartz mercury arcs. It was found that these arcs work smoothly if started on a 220 volt D.C. circuit, but the quartz of the capillary deteriorates rapidly when the arc is in operation. Thus the best Raman spectra are obtained if the capillary is replaced by a new one after each day of operation.

Organic bromides are changed chemically and colored brown by the action of ultraviolet light. The colored liquid thus produced gives rise in such work to a continuous fluorescence spectrum which obscures the Raman lines to some extent. To prevent this photochemical action various Corning glass filters were used to absorb wave-lengths below λ3650A.

When two 220 volt constricted arcs were used it was found that in the presence of the filters it was necessary to give an exposure of 10 to 12 hours

[1] A. Dadieu and K. W. F. Kohlrausch, however, have (J. Opt. Soc. Am. **21**, 298 (1931)) published values for molecules up to 4 carbon atoms in length.

to obtain an entirely satisfactory Raman spectra. Without the filters the time is greatly reduced, but many lines are partly obscured by the continuous spectrum. With chlorides or hydrocarbons, the filters are not in general necessary.

3. Wave-Lengths and Shift of Frequency

The approximate wave-length of each line was obtained by direct comparison with the spectrum of an iron arc, but the final values were calculated by the use of the Hartmann formula, from the wave-lengths of adjacent well-known lines in the mercury spectrum.

Many of the Raman lines are broad and diffuse. This seems to be due in some cases to the overlapping of Raman lines, excited by two or more lines of the incident spectrum. The shift of frequency ($\Delta\nu$) was obtained by calcu-

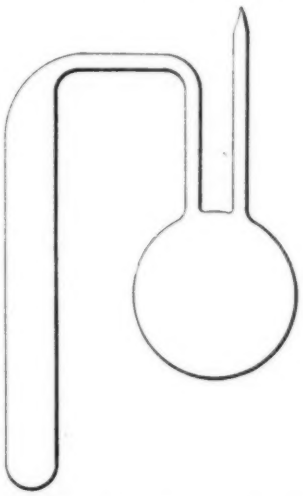

Fig. 1. Raman tube of the Wood type as modified by Langer and Meggers.

lating all of the possible frequency shifts with reference to the strong mercury lines in the adjacent spectrum. The shifts selected as real were those which gave the same value if the Raman lines were caused by two or more exciting lines. In the relatively few cases in which there was no such coincidence in the values, the scattered line was assigned to the nearest mercury line of high intensity. A few doubtful selections are indicated by question marks. This is the usual method employed when the mercury arc, with its great number of lines, is used as the exciting source. Without doubt this method gives rise to the inclusion in tables of data, of frequency shifts which are not real, and to the omission of certain true shifts.

This is illustrated by Table I, which gives the Raman frequencies as determined by the writers (H.B.), by Dadieu and Kohlrausch[2] (D.K.), by Bhagavantam and Venkateswaren[3] (C.D.), and by Cleeton and Dufford[4]

[2] A. Dadieu and K. W. F. Kohlrausch, J. Opt. Soc. Am. **5,** 286–322 (1931).
[3] S. Bhagavantam and S. Venkateswaren, Proc. Roy. Soc. **A127,** 360 (1930).
[4] Cleeton and Dufford, Phys. Rev.

(C.D.) for allyl bromide ($CH_2=CHCH_2Br$), and for n-propyl bromide ($CH_3CH_2CH_2Br$).

TABLE I. *Wave numbers of bromides.*

Allyl bromide			Propyl bromide		
H.B.	D.K.	B.V.	H.B.	D.K.	C.D.
254 (3)	252	259	312 (2)	314	308
—	385	—	—	397	—
535 (2)	526	535	459 (2)	—	—
695 (2)	687	690	563 (1)	564	566
—	926	—	648 (2)	647	—
1000 (2)	—	—	778 (1)	773	—
1193 (2)	1190	—	—	836	—
1215 (2)	1212	1209	—	885	—
1296 (4)	1292	1301	—	—	968
1320 (2)	—	1321	1023 (2)	1024	—
1378 (2)	—	—	—	—	1079
1410 (2)	1406	1414	1143 (2)	1131	—
1638 (2)	1633	1641	1165 (2)	—	—
2157 (2)	—	—	1185 (2)	—	—
2986 (2)	2966	2975	1229 (2)	—	1254
—	3011	—	1435 (1)	1430	1456
—	3085	—	—	—	2736
			2896 (2)	2862	2875
			2933 (2)	2935	2923
			2965 (2)	2959	2976
			2993 (3)	3000	—

TABLE II. *Raman wave numbers for bromides. Average $\Delta\bar{\nu}$ values.*

iso-propyl bromide	n-butyl bromide		Secondary butyl bromide	iso-butyl bromide	Tertiary butyl bromide	n-amyl bromide	iso-amyl bromide
	H.B.	D.K.					
172 (1)	280 (2)	279	291 (4)	303 (4)	301 (6)	219 (1)	288 (2)
297 (3)	457 (2)		317 (1)	421 (2)	515 (5)	436 (1)	564 (2)
353 (2)	563 (2)	557	347 (2)	470 (2)	538 (2)	473 (1)	619 (2)
409 (2)	642 (3)	637	455 (2)	495 (2)	615 (2)	564 (3)	636 (2)
423 (1)	702 (2)	—	482 (2)	517 (2)	803 (2)	642 (3)	648 (2)
540 (4)	745 (2)	—	533 (2)	572 (2)	954 (2)	703 (2)	749 (2)
882 (2)	798 (3)	794	612 (1)	622 (3)	1141 (2)	747 (2)	822 (2)
964 (1)	867 (3)	853	635 (2)	653 (4)	1260 (2)	780 (2)	1297 (2)
1040 (3)	893 (2)	—	840 (2)	796 (1)	1456 (1)	1057 (2)	2872 (2)
	—	1057					
1096 (2)	1103 (3)		956 (1)	812 (2)	2923 (3)	1113 (2)	2932 (3)
	—	1139					
1227 (3)	1170 (2)		1077 (1)	1144 (2)	2970 (2)	1208 (2)	2962 (2)
	—	1257					
1284 (2)	1299 (2)	—	1103 (1)	1198 (2)	3025 (2)	1248 (3)	
1441 (2)	1362 (2)	—	1212 (2)	1234 (2)		1302 (3)	
	—	1440					
2927 (2)	1491 (2)	—	1263 (2)	1313 (1)		1436 (2)	
2958 (3)	2874 (2)	2865	1451 (2)	1454 (1)		1491 (2)	
2983 (2)	2935 (4)	2930	2877 (2)	2871 (2)		2824 (2)	
2993 (2)	2964 (4)	2962	2922 (3)	2962 (3)		2877 (2)	
			2974 (2)			2936 (2)	
						2968 (4)	
						3013 (2)	
						3068 (2)	

NOTE: The figures in parentheses give the number of values from which the average value was obtained.

For allyl bromide the values of Dadieu and Kohlrausch are from 2 to 9 wave numbers smaller than ours, while those of Bhagavantam and Venkateswaren vary from ours by from +5 to −6. Where the differences are much greater it is possible that the same lines were not measured.

The Raman wave number 459 for n-propyl bromide was found only by ourselves, and not by the two other workers. That it may correspond to a real frequency is indicated by its occurrence with the value 457 in n-butyl bromide and 455 in secondary butyl bromide. A vibration of about this wave number is attributed by Andrews to a transverse vibration in the –C–C–C– chain.

The wave numbers which correspond to the Raman shifts for other organic bromides are listed in Table II and Fig. 2. It may be seen that n-amyl bromide gives a surprisingly large number of values, but it is possible

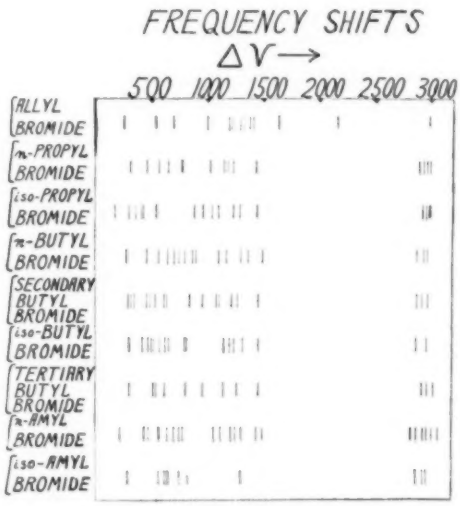

Fig. 2.

that some of them do not correspond to real shifts. One difficulty, which is not sufficiently recognized in connection with the Raman spectra of such compounds, is that it is exceedingly difficult to obtain such organic liquids free from isomers or other compounds similar in properties.

The data from which the mean values of the Raman shifts given in Tables I and II have been obtained, are given in Table III. The few anti-Stokes lines are designated by a negative $\Delta\bar{\nu}$. In general the variation in the value of $\Delta\bar{\nu}$ for what seems to be the same Raman shift is not more than 3 units.

4. The Carbon-Halogen Bond with a Single Carbon Atom

As is indicated in Table IV the frequency which corresponds to the carbon-chlorine bond is 2.13×10^{13}, to the carbon-bromine bond, 1.81×10^{13}, and to the carbon-iodine bond 1.60×10^{13} per second, when only one carbon atom is present. If more than one carbon atom is in the molecule these

characteristic frequencies are reduced by from 6 to 11 percent for bromides and probably somewhat more for chlorides, as is shown in the next section.

The equation for the Raman frequency ($\Delta\nu$) may be written in a simple approximate form as

$$\Delta\nu = \omega_0(v' - v'') = \frac{1}{2\pi}\left(\frac{f}{\mu}\right)^{1/2}(v' - v'')$$

TABLE III. *Wave-lengths of Raman and exciting lines.*

Raman line $\bar{\nu}$	Exciting line λ	Exciting line $\bar{\nu}$	$\Delta\bar{\nu}$	Raman line $\bar{\nu}$	Exciting line λ	Exciting line $\bar{\nu}$	$\Delta\bar{\nu}$
			Allyl bromide				
24451	4046.56	24705	254	21997	4347.50	22995	998
24174	4046.56	24705	531	21744	4339.24	23039	1295
24010	4046.56	24705	695	21744	4358.34	22938	1194
23514	4046.56	24705	1191	21721	4046.56	24705	2984
23514	4077.84	24516	1002	21721	4339.24	23039	1318
23492	4046.56	24705	1213	21721	4358.34	22938	1217
23408	4046.56	24705	1297	21699	4347.50	22995	1296
23328	4046.56	24705	1377	21642	4358.34	22938	1296
23296	4046.56	24705	1409	21617	4358.34	22938	1321
23068	4046.56	24705	1637	21617	4347.50	22995	1378
22786	4339.24	23039	253	21528	4077.84	24516	2988
22682	4358.34	22938	256	21528	4358.34	22938	1410
22546	4046.56?	24705	2159	21299	4358.34	22938	1639
22400	4358.34	22938	538	20885	4339.24?	23039	2154
22243	4358.34	22938	695				
			n-propyl bromide				
24394	3663.27	27290	2896	21830	4347.50	22995	1165
24394	3650.14	27388	2994	21809	4046.56	24705	2896
24394	4046.56	24705	311	21809	4339.24	23039	1230
24057	4046.56	24705	648	21809	4347.50	22995	1186
24057	4077.84	24516	459	21793	4358.34	22938	1145
22626	4358.34	22938	312	21774	4046.56	24705	2931
22536	4347.50	22995	459	21774	4358.34	22938	1164
22375	4358.34	22938	563	21742	4046.56	24705	2963
22291	4358.34	22938	647	21711	4046.56	24705	2994
22160	4358.34	22938	778	21711	4358.34	22938	1227
21970	4347.50	22995	1025	21503	4358.34	22938	1435
21918	4358.34	22938	1020	20003	4347.50	22995	2992
21855	4339.24	23039	1184	20003	4358.34	22938	2935
21855	4347.50	22995	1140	19972	4358.34	22938	2966
			iso-propyl bromide				
24407	3650.14	27388	2981	21897	4358.34	22938	1041
24407	4046.56	24705	298	21844	4358.34	22938	1094
24298	3663.27	27290	2992	21812	4339.24	23039	1227
24298	4046.56	24705	407	21778	4046.56	24705	2927
24165	4046.56	24705	540	21749	4046.56	24705	2956
24165	4077.84	24516	351	21711	4046.56	24705	2994
23975	4077.84	24516	541	21711	4347.50	22995	1284
23824	4046.56	24705	881	21711	4358.34	22938	1227
23664	4046.56	24705	1041	21556	4077.84	24516	2960
23477	4046.56	24705	1228	21556	4347.50	22995	1439
23477	4077.84	24516	1039	21495	4358.34	22938	1443
23232	4077.84	24516	1284	20011	4347.50	22995	2984
22641	4347.50	22995	354	20011	4358.34	22938	2927
22641	4358.34	22938	297	19980	4358.34	22938	2958
22528	4358.34	22938	410	18135	5460.74	18307	172
22399	4358.34	22938	539	18010	5460.74	18307	297
22056	4358.34	22938	882	17884	5460.74	18307	423
21974	4358.34	22938	964	17768	5460.74	18307	539
21897	4347 50	22995	1098				

TABLE III. (*Continued*)

Raman line $\bar{\nu}$	Exciting line λ	$\bar{\nu}$	$\Delta\bar{\nu}$	Raman line $\bar{\nu}$	Exciting line λ	$\bar{\nu}$	$\Delta\bar{\nu}$
			n-butyl bromide				
24425	3650.14	27388	2963	22197	4347.50	22995	798
24425	4046.56	24705	280	22139	4358.34	22938	799
24143	4046.56	24705	562	22070	4358.34	22938	868
24061	4046.56	24705	644	22045	4358.34	22938	893
24061	4077.84	24516	455	21891	4347.50	22995	1104
23961	4046.56	24705	744	21870	4339.24	23039	1169
23907	4046.56	24705	798	21836	4358.34	22938	1102
23877	4077 84	24516	639	21768	4046.56	24705	2937
23838	4046.56	24705	867	21768	4358.34	22938	1170
23813	4046.56	24705	892	21741	4046.56	24705	2964
23813	4077.84	24516	703	21741	4339.24	23039	1298
23650	4077.84	24516	866	21676	4339.24	23039	1363
23603	4046.56	24705	1102	21643	4077.84	24516	2873
23216	4046.56	24705	1489	21577	4077.84	24516	2939
23216	4077.84	24516	1300	21577	4358.34	22938	1361
22659	4358.34	22938	279	21553	4077.84	24516	2963
22480	4358.34	22938	458	21503	4347.50	22995	1492
22375	4358.34	22938	563	20064	4347.50	22995	2931
22294	4339.24	23039	745	20064	4358.34	22938	2874
22294	4347.50	22995	701	20004	4358.34	22938	2934
22294	4358.34	22938	644	19974	4358.34	22938	2964
			Secondary butyl bromide				
24414	3650.14	27388	2974	22406	4358.34	22938	532
24414	3663.27	27290	2876	22359	4347.50	22995	636
24414	4046.56	24705	291	22326	4358.34	22938	612
24224	4046.56	24705	481	22154	4347.50	22995	841
24224	4077.84	24516	292	22099	4358.34	22938	839
24171	4046.56	24705	534	21982	4358.34	22938	956
24171	4077.84	24516	345	21892	4347.50	22995	1103
23253	4046.56	24705	1452	21861	4358.34	22938	1077
23253	4077.84	24516	1263	21828	4046.56	24705	2877
23229	4358.34	22938	−291	21828	4339.24	23039	1211
22647	4347.50	22995	348	21783	4046.56	24705	2922
22647	4358.34	22938	291	21783	4347.50	22995	1212
22621	4358.34	2293	317	21732	4046.56	24705	2973
22586	4339.24	23039	453	21732	4347.50	22995	1263
22482	4358.34	22938	456	21593	4077.84	24516	2923
22455	4358.34	22938	483	21488	4358.34	22938	1450
22406	4339.24	23039	633	20018	4358.34	22938	2920
			iso-butyl bromide				
24401	4046.56	24705	304	22518	4358.34	22938	420
24283	4046.56	24705	422	22469	4339.24	23039	570
24235	4046.56	24705	470	22469	4358.34	22938	469
24212	4046.56	24705	493	22421	4347.50	22995	574
24212	4077.84	24516	304	22421	4358.34	22938	517
24189	4046.56	24705	516	22316	4358.34	22938	622
24083	4046.56	24705	622	22285	4358.34	22938	653
24052	4046.56	24705	653	22142	4358.34	22938	796
23893	4046.56	24705	812	22126	4358.34	22938	812
23893	4077.84	24516	623	21833	4046.56	24705	2872
23861	4077.84	24516	655	21796	4347.50	22995	1199
23590	4358.34	22938	−652	21796	4358.34	22938	1142
23560	4046.56	24705	1145	21741	4046.56	24705	2964
23470	4046.56	24705	1235	21741	4358.34	22938	1197
23392	4046.56	24705	1313	21705	4358.34	22938	1233
23239	4358.34	22938	−301	21555	4077.84	24516	2961
22634	4358.34	22938	304	21484	4358.34	22938	1454
22542	4339.24	23039	497	20068	4358.34	22938	2870
				19976	4358.34	22938	2962

TABLE III. (*Continued*).

Raman line $\bar{\nu}$	Exciting line λ	Exciting line $\bar{\nu}$	$\Delta\bar{\nu}$	Raman line $\bar{\nu}$	Exciting line λ	Exciting line $\bar{\nu}$	$\Delta\bar{\nu}$
			Tertiary butyl bromide				
25005	4046.56	24705	−300	22134	4358.34	22938	804
24403	4046.56	24705	302	21982	4358.34	22938	956
24214	4077.84	24516	302	21797	4358.34	22938	1141
24189	4046.56	24705	516	21781	4046.56	24705	2924
24167	4046.56	24705	538	21781	4339.24	23039	1258
24000	4077.84	24516	516	21734	4046.56	24705	2971
23903	4046.56	24705	802	21734	4347.50	22995	1261
23903	4077.84	24516	613	21594	4077.84	24516	2922
23564	4046.56	24705	1141	21482	4358.34	22938	1456
23564	4077.84	24516	952	20015	4339.24	23039	3024
23453	4358.34	22938	−515	20015	4358.34	22938	2923
23240	4358.34	22938	−302	19970	4347.50	22995	3025
22635	4358.34	22938	303	19970	4358.34	22938	2968
22422	4339.24	23039	617	18008	5460.74	18307	299
22422	4358.34	22938	516	17793	5460.74	18307	514
22400	4358.34	22938	538				
			n-amyl bromide				
24141	4046.56	24705	564	21882	4347.50	22995	1113
24062	4046.56	24705	643	21882	4358.34	22938	1056
23956	4046.56	24705	749	21830	4046.56	24705	2875
23923	4046.56	24705	782	21830	4339.24	23039	1209
23877	4077.84	24516	639	21768	4046.56	24705	2937
23811	4077.84	24516	705	21739	4046.56	24705	2966
23739	4077.84	24516	777	21739	4339.24	23039	1300
23647	4046.56	24705	1058	21692	4046.56	24705	3013
23499	4046.56	24705	1206	21692	4077.84	24516	2824
23454	4046.56	24705	1251	21692	4347.50	22995	1303
23403	4046.56	24705	1302	21692	4358.34	22938	1246
23403	4077.84	24516	1113	21637	4046.56	24705	3068
23269	4046.56	24705	1436	21637	4077.84	24516	2879
23269	4077.84	24516	1247	21637	4358.34	22938	1301
22719	4358.34	22938	219	21549	4077.84	24516	2967
22502	4358.34	22938	436	21549	4339.24	23039	1490
22465	4358.34	22938	473	21503	4077.84	24516	3013
22430	4347.50	22995	565	21503	4347.50	22995	1492
22375	4358.34	22938	563	21503	4358.34	22938	1435
22294	4339.24	23039	745	20068	4339.24	23039	2971
22294	4347.50	22995	701	20004	4358.34	22938	2934
22294	4358.34	22938	644	19971	4339.24	23039	3068
21882	4046.56	24705	2823	19971	4358.34	22938	2967
			iso-amyl bromide				
24142	4046.56	24705	563	22190	4358.34	22938	748
24055	4046.56	24705	650	22116	4358.34	22938	822
23955	4046.56	24705	750	21834	4046.56	24705	2871
23883	4046.56	24705	822	21768	4046.56	24705	2937
23883	4077.84	24516	633	21743	4046.56	24705	2962
22707	4347.50	22995	288	21743	4339.24	23039	1296
22651	4358.34	22938	287	21641	4358.34	22938	1297
22400	4339.24	23039	639	20065	4347.50	22995	2930
22374	4347.50	22995	621	20065	4358.34	22938	2873
22374	4358.34	22938	564	20008	4358.34	22938	2930
223 2	4358.34	22938	616	19976	4358.34	22938	2962
22292	4358.34	22938	646				

in which v represents a quantum number, μ the mutual mass, w_0 is sometimes considered as the fundamental mechanical frequency, and f as the force con-

stant. The values of f for the methyl halides are given in Table IV. It is assumed that in the emission of these intense Raman lines $v'-v''=\pm 1$.

The force constant (a) is calculated in the ordinary way, and it is considered that the methyl group vibrates as a unit with respect to the halogen atom. In (b) a slight, somewhat arbitrary allowance has been made for the fact that this is not strictly true.

TABLE IV. *Values for the carbon-halogen bond.*

Compound	Wave Number cm^{-1}	ν Frequency per Second $\times 10^{-13}$	Force Constant f $\times 10^5$ dynes a	b	Amplitude $\times 10$ cm $v=\frac{1}{2}$	$v=1\frac{1}{2}$	$\frac{1}{2}fa\times 10$ $v=\frac{1}{2}$	$v=1\frac{1}{2}$
CH_3Cl	712	2.135	3.136	3.02	6.7	11.6	2.0	3.5
CH_3Br	603	1.808	2.695	2.60	6.65	11.5	1.7	3.0
CH_3I	534	1.601	2.246	2.17	6.9	11.9	1.5	2.6

The force constant decreases from the chloride to the iodide. The values are much smaller than those of the single bonds listed by Dadieu and Kohlrausch which are, in 10^5 dynes per cm, equal to 4.31 for C·C in ethane, 4.96 for C·C in methyl alcohol, and 4.89 for C·N in methyl amine.

Thus if f represents the strength of the bond, the carbon-halogen bond seems to be much weaker than the most common of the other single bonds found in organic compounds. That the strength of the bond decreases rapidly from chloride to bromide to iodide, is in agreement, not only with the heats of dissociation, but also with the other known relations.

The meaning of the amplitude a' is definite in the classical quantum theory, but loses this definiteness in the newer quantum mechanics.

Since $\epsilon=fa^2/2=(v+\frac{1}{2})w_0h$

$$a=\left(\frac{2\epsilon}{f}\right)^{1/2}=\left(\frac{(2v+1)hw_0}{f}\right)^{1/2}$$

in which (ϵ) is the energy and w_0 is the mechanical frequency. The values for this amplitude for $v=\frac{1}{2}$ and $v=3/2$ are given in Table IV.

Dadieu and Kohlrausch give the mean value of the force as $\frac{1}{2}fa$, and consider this to be more characteristic of the bond than the force constant.

For $v=\frac{1}{2}$ the values of $\frac{1}{2}fa$ in 10^{-4} dyne cm are 2.0, 1.7, and 1.5 for methyl chloride, bromide, and iodide, respectively, while Dadieu and Kohlrausch give 2.04 for the C·C bond in methane, 2.27 for the C·O bond in methyl alcohol, 2.23 for the C·N bond in methyl amine, 4.13 for the double bond in ethylene, 4.4 for the carbonyl C·O bond, 4.14 for the oxygen bond in O_2, and 6.28 for the bond in carbon monoxide.

5. The Effect of a Lengthening of the Chain Upon the Carbon-Halogen Bond

The effect of a lengthening of the hydrocarbon chain upon the characteristic carbon-bromine frequency is exhibited in Table V.

This is the most intense line in the Raman spectrum of the bromides.

The remarkable fact revealed by our data is that while the carbon-bromine frequency is reduced by about 6 percent if the number of carbon atoms in the chain is increased from one to two, a further increase from two to five carbon atoms produces no appreciable effect.

TABLE V. *Characteristic wave numbers for the carbon-bromine bond in organic bromides.*

CH_3Br	603 (C.D.)	594 (D.K.)
C_2H_5Br	566 (C.D.)	557 (D.K.)
n$-C_3H_7Br$	563 (H.B.)	564 (D.K.)
n C_4H_9Br	563 (H.B.)	557 (D.K.)
$C_5H_{11}Br$	564 (H.B.)	
$(CH_3)_2CH\,(CH_2)_2Br$	564 (H.B.)	

If an attempt is now made to apply Eq. (1) to determine the value of the force constant f and thus, presumably, the strength of the bond, it is apparent that the equation cannot be solved without additional knowledge or an additional assumption. It seems to have been customary to assume that all of the hydrocarbon chain vibrates with respect to the bromine atom:—or more complicated equations are used which indicate a change of the single fundamental frequency into two values.

The constancy of the fundamental carbon-bromine frequency seems to suggest that neither of these assumptions is valid in this case.

Thus it seems apparent from the constant value of the frequency for normal compounds that *the organic radical cannot vibrate as a whole with respect to the bromine atom*, for such an assumption leads to an absurd value of the force constant for very long chains.

Thus, on the basis of the assumption that the effective mass of the methyl group with respect to the vibration toward bromine is 14.4 atomic weight units, the force constant for methyl bromide is 2.60×10^5 dyne/cm (or 2.70 if CH_3 vibrates as a single unit of mass 15). If now the amyl group vibrates as a unit the force constant for amyl bromide would be 7.0×10^5 dyne/cm, or more than two and a half times larger than for methyl bromide. This is much too large.

If the force constant in all of the normal bromides is assumed to be constant and equal to 2.60×10^5 dyne/cm, the effective mass of the portion of the hydrocarbon chain of two or more carbon atoms, which vibrates (with respect to the bromine) is 17. This indicates that the CH_2 group adjacent to the bromine possesses most of the mass which is effective. That is the CH_2 group vibrates, but its effective mass is increased by the constraint due to its union with the rest of the hydrocarbon chain.

If it is assumed that the force constant decreases with the length of the chain, then the amount of mass in the radical R which vibrates, also decreases with increase of mass of the radical, which seems to be improbable, except for the increase from one to two carbon atoms. Thus these facts, together with the equation $\nu=1/2\pi(f/\mu)^{1/2}(v'-v'')$, lead to the idea that (1) the force constant remains constant as the length of the chain increases, or

(2) the force constant increases as the length of the chain increases, and at the same rate as the mutual mass (μ) of the vibrating parts increases.

From what is known from the standpoint of organic chemistry, it seems that the strength of the carbon-halogen bond does not increase rapidly with the length of the chain.

Thus the final conclusions reached are: (1) The force constant either remains constant, or else it increases only slightly with an increase in length and mass of the normal hydrocarbon chain. (2) As indicated before, only a part of the radical R vibrates with respect to the halogen atom in the process in which the characteristic frequency is emitted.

The values of Dadieu and Kohlrausch suggest that the characteristic frequency of this bond may be higher if an odd number of carbon atoms is present in the molecule than if this number is even. The variation in value is, however, very small, and is not exhibited by our data.

The data of a recent paper by West and Farnsworth[5] indicates the probability that the chlorides exhibit the same relations as the bromides. Unfortunately for the purpose of the present paper, their work does not extend to chains of more than 3 carbon atoms.

TABLE VI. *Characteristic wave numbers for the carbon-halogen bond.*

1.	2. Cl	3. Br	4. I	5. Cl-Br	6. Br-I	7. Cl^2-Br^2 $\times 10^{-3}$	8. Br^2-I^2 $\times 10^{-3}$	9. $\frac{Br^2-I^2}{Cl^2-Br^2}$
Methyl	711 (W.F.)	603 (C.D.)	522 (D.K.)	108	81	142	91	.64
Ethyl	655 (W.F.)	556 (C.D.)	499 (D.K.)	89	67	109	71	.65
n-Propyl	650 (W.F.)	563 (H.B.)	—	87	—	105	—	—
n-Butyl		563 (H.B.)						
n-Amyl		564 (H.B.)						

Since, with a constant mutual mass, the force constant varies as the square of the frequency, it is apparent from column 9 of Table VI, that the decrease in the value of the force constant is only 65 percent as great between the bromide and iodide as it is between the chloride and bromide.

6. The Effect of a Branching of the Chain Upon the Fundamental Frequency Associated with the Carbon-Halogen Bond

The branching of the hydrocarbon chain seems to have no effect upon the fundamental frequency associated with the carbon-halogen bond, provided the branching occurs sufficiently distant from the halogen atom. Thus iso-amyl bromide ($(CH_3)_2 \cdot CH \cdot CH_2 \cdot CH_2 \cdot Br$) gives the wave number 564, which is the same as that associated with n-amyl, n-butyl, and n-propyl bromides. However, if the branching is considerably less distant, the frequency is reduced considerably. Thus with iso-compounds, or if the halogen atom is attached to a secondary or tertiary carbon atom, the wave number is reduced from 564 to about 537 cm^{-1} (Table VII).

[5] W. West and M. Farnsworth, Trans. Faraday Soc. **27**, 145 (1931).

Thus a branching of the chain sufficiently close to the substituted halogen atom either lowers the force constant and presumably weakens the bond, or else it lowers the effective mass of the part of the hydrocarbon chain which vibrates. The former of these seems the more probable.

The frequency for iso-butyl bromide (wave number 572 cm^{-1}) seems exceptional in that it is higher than for the normal compound. However, a lower frequency also appears.

TABLE VII. *Characteristic wave numbers for the carbon-halogen bond with branched chains.*

(Normal)	711	(564)
ISO propyl $(CH_3)_2$ CH X	616 (W.F.)	540
Secondary butyl CH_3CH_2CHX CH_3	—	537
Tertiary butyl $(CH_3)_3$ C X	564 (D.K.)	538
ISO amyl $(CH_3)_2$ CH CH_2CH_2 X		(564)
ISO butyl $(CH_3)_2$ CH CH_2 Br		(572) and (517)

7. A Lower Characteristic Frequency Seemingly Associated with the Carbon-Bromide Bond

A wave number of about 300 cm^{-1} has been found for all of the organic monobromides investigated by us, with the exception of allyl bromide, in which a double carbon bond is present. A similar value of about 330 cm^{-1} has been found for chlorides by West and Farnsworth, and with ethyl iodide a value of 260 cm^{-1} was found by Dadieu and Kohlrausch.

Table VIII gives a list of these wave numbers for different chlorides and bromides, and a single value for an iodide.

The values for the bromides (in the upper part of Table VIII) may be associated with some type of transverse vibration at the carbon-bromine bond. Unlike the frequency which the writers have associated with a longitudinal vibration at this bond, the values for iso- or secondary compounds do not exhibit any general differentiation from those of the normal compounds. A few examples are listed to show that if two or more halogen atoms are present the frequencies due to carbon-halogen bonds are greatly modified. Thus, according to Dadieu and Kohlrausch, carbon tetrachloride is represented by the wave numbers 216 (4), 313 (4), 455 (4), 755 (2), 782 (2), in which the numbers in parenthesis represent the intensities. The more intense lines have wave numbers which are smaller than the most characteristic of the carbon-halogen bond in aliphatic compounds. This is probably due in part at least to a greater mutual mass of the vibrating parts of the molecule.

8. Wave Numbers between 1400 and 1460 cm^{-1}

Almost all of the hydrocarbons of the paraffin series and their derivatives exhibit a Raman wave number between 1400 and 1460 cm^{-1}.

This has been attributed by Dadieu and Kohlrausch to a transverse vibration of the hydrogen atoms in the CH_2 group, and by Daure to the single carbon-carbon bond. There seems to be much evidence which indicates the probability that one of these points of view is correct, and certain different

details of evidence which seem to speak against each of these ideas. Present opinion seems on the whole more in favor of the former of these conclusions. Table IX lists frequencies in this range as found in monobromides.

TABLE VIII. *Lower wave numbers presumably characteristic of the carbon-halogen bond.*

	Cl	Br	I
Methyl	372 (W.F.)		
Ethyl	327 (W.F.)	290	260 (D.K.)
n-propyl	333 (W.F.)	312	
n-butyl	—	280	
Isopropyl	330 (W.F.)	297	
Isobutyl	—	303	
Isoamyl	—	288	
Secondary butyl	—	291	
β Chloropropylene	337 (W.F.)		
The above values are changed considerably if more than one halogen atom is present.			
CX_4	216–313 (D.K.)		
CHX_3	259–364 (D.K.)	154–221 (D.K.)	
CH_2X_2	283 (D.K.)	178 (D.K.)	119 (D.K.)
XH_2C-CH_2X	295 (D.K.)	188 (D.K.)	
$X_2HC-CHX_2$	287–351 (D.K.)	218 (D.K.)	
1–3 dibromopropane		371 (D.K.)	

TABLE IX. *Wave numbers of about 1450 cm^{-1} for monobromides.*

ethyl bromide	1439 (D.K.)		
n-propyl bromide	1435 (H.B.)	isopropyl bromide	1441
n-butyl bromide	1440 (D.K.)	isobutyl bromide	1454
	1491 (H.B.)	secondary butyl bromide	1451
n-amyl bromide	1436 (H.B.)	tertiary butyl bromide	1456
	1491 (H.B.)	allyl bromide	1410

9. Frequency Characteristic of the Double Bond Between Carbon Atoms

Dadieu and Kohlrausch have found 1639 cm^{-1} as the wave number characteristic of the double carbon bond in allyl chloride. The writers obtain the value 1638 for the bromide, so the increase of mass of the halogen has little effect upon the frequency. Dadieu and Kohlrausch point out that the frequency, characteristic of the double bond, is moderately constant. Thus their values for di-chlor, tri-chlor, and tetra-chlor ethylene indicate values of 1583, 1585, and 1569, respectively.

The writers are indebted to a Grant-in-Aid of the National Research Council which was used for the purchase of the spectrograph used in this work.

THE EMISSION OF SECONDARY ELECTRONS FROM TUNGSTEN

By A. J. Ahearn
Bell Telephone Laboratories, New York

(Received September 28, 1931)

Abstract

An apparatus is described for investigating critical potentials in the emission of secondary electrons from tungsten. Measurements on the velocity distribution in the primary beam show that secondary electrons from the electron gun are absent. Tube characteristics which might introduce spurious critical potentials in the secondary emission from tungsten appear to be absent. By heat treating the tungsten and cleaning up residual gases, maxima and critical slope changes were developed below 40 volts. With sensitive methods of measuring and plotting the data, critical potentials within the range from 40 to 500 volts were observed only at the following uncorrected voltages; 70, 108, 208, 297 volts. All but the 70 volt effect disappeared eventually after heat treatments of the tungsten target. Thus when the tungsten surface is most free from contamination, critical potentials persisted only at the following uncorrected voltages; maxima at about 3.5 and 8 volts and slope increases at 24, 33 and 70 volts. The phenomena may be associated with the diffraction of electrons or the production and absorption of characteristic soft x-rays. Regardless of the mechanism operating at the critical potentials, their decrease or elimination beyond 40 volts points strongly to effects of surface contamination rather than to characteristics of tungsten.

Introduction

MANY investigations[1] have been made on the secondary electron characteristics of metals. Critical potentials[2] have been observed in some of these researches. The most recent work on critical potentials in the secondary electron emission of tungsten is that of Krefft[3]. The present work was undertaken to investigate the reality of these as characteristic of clean tungsten.

The Experimental Tube

A beam of electrons was projected from an electron gun and struck a tungsten target. The secondary electrons emitted by the tungsten under bombardment were received on a collector. By measuring I_p the primary current which bombarded the target and I_s the secondary electron current emitted, the secondary electron emission I_s/I_p was obtained.

The essential details of the experimental tube which was used are drawn to scale in Fig. 1. The elements F, S, A and B constitute an electron gun. The filament F is a tungsten ribbon $27\times0.5\times0.06$ mm operated at about 4.5

[1] Soller, Phys. Rev. **36,** 1212 (1930); Rudberg, Roy. Soc. Proc. **A127,** 111 (1930); Farnsworth, Phys. Rev. **31,** 405 (1928); Brinsmade, Phys. Rev. **30,** 494 (1927).

[2] Stuhlman, Phys. Rev. **25,** 234A (1925); Petry, Phys. Rev. **28,** 362 (1926); Rao, Roy. Soc. Proc. **A128,** 57 (1930); Rao, Roy. Soc. Proc. **A128,** 41 (1930); Hyatt and Smith, Phys. Rev. **32,** 929 (1928); Farnsworth, Phys. Rev. **34,** 679 (1929).

[3] Krefft, Phys. Rev. **31,** 199 (1928); Krefft, Ann. d. Physik **84,** 639 (1927).

amperes. D_1 is a square aperture 3.0 mm on each side. D_2, D_3, D_4, D_5 are circular apertures of diameters 1.5, 1.0, 1.0 and 2.0 mm respectively. The target T, which is the source of the secondary electrons is of tungsten sheet 0.06 mm thick supported on tungsten rods. The filament H is a flat spiral of tungsten ribbon supported on tungsten rods. It serves to heat the target T by bombardment and radiation. The element C serves to collect the secondary electrons emitted by T. The aperture D_6 is 4.5 mm in diameter. The elements S, A, B and C are of nickel sheet 0.3 mm thick. An ionization gauge is attached to the experimental tube. A 6 cm length of 4 mil thoriated tungsten filament is included for use as a getter to clean up residual gases after removal of the tube from the pumps. Guard rings prevent electrical leakage over short glass paths between the electron gun and the element C.

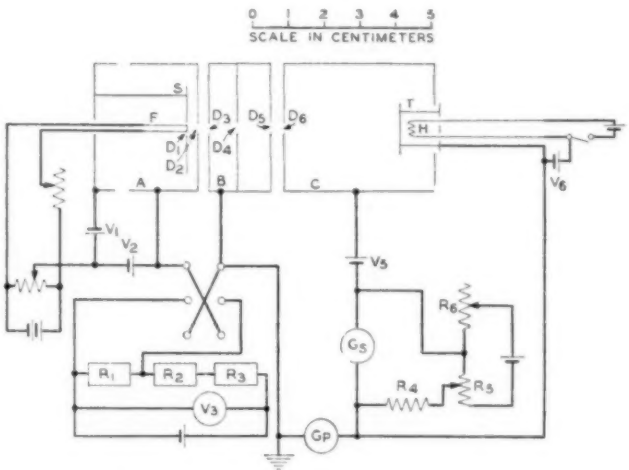

Fig. 1. Apparatus and electrical circuit.

The experimental tube was exhausted by a four-stage mercury diffusion pump. There were two liquid air traps between the diffusion pumps and the tube. Liquid air was maintained continuously on the one next to the pumps. During the twenty four hours preceding the seal off, the trap next to the tube was immersed in liquid air. The entire tube up to its seal off constriction was maintained at about 450°C in an electric furnace until the pressure was reduced to about 1×10^{-6} mm Hg. The elements, S, A, B and C were then maintained at a bright red heat by high frequency induction for several hours until in this condition the pressure was again reduced to about 1×10^{-6} mm Hg. The filament F, and the "getter" were then outgassed, and the target T heated at a bright red heat until again the pressure was about 1×10^{-6} mm Hg. This entire outgassing process was then repeated. Thus the condition was finally reached where the target could be heated to a temperature (yellow color) sufficient to heat the element C to a visible red color without increasing the pressure of about 1×10^{-7} mm Hg. After this condition was established with the filaments and target glowing, the glass was torched for about one hour and then the tube was sealed off from its pumps. During the course

of the pumping of the tube some measurements were made and so it was on the pumps continuously for about three weeks.

Method of Measurements

Fig. 1 shows the circuit used. V_p, the potential of T and C with respect to F, was varied by adjusting the value of R_1, keeping $R_1+R_2=10{,}000$ ohms and having $R_1+R_2+R_3=100$ V_3. In this way, potential changes can be made and reproduced easily and accurately.

G_S and G_P were galvanometers each of 10,000 megohms sensitivity. During most of the measurements, both the primary and the secondary currents were measured with the galvanometers at full sensitivity by means of annulling current circuits one of which is shown in Fig. 1. R_4 had a constant value of 100,000 ohms. The annulling current was adjusted by varying R_5 and R_6 whose maximum values were 10 and 10,000 ohms respectively.

In order to use the galvanometers as described above, it is essential that the filament F be maintained at a constant temperature. To this end, all connections in the filament heating circuit were either welded, soldered or tightly clamped and the rheostat was water cooled.

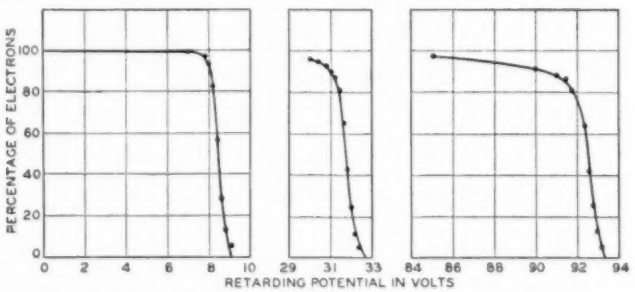

Fig. 2. Electron velocity distribution in primary beam.

In critical potential measurements it is important that the primary beam of electrons have a uniform velocity distribution not only to secure sharp slope changes but also to avoid spurious ones. With this in view the electron gun shown in Fig. 1 was patterned after that of Davisson and Germer[4] in order to obtain a beam of electrons in which secondary emission from the metal of the electron gun was absent. Fig. 2 shows velocity distribution curves for the primary electrons for bombarding potentials of 7, 30 and 90 volts. In the 90 volt case 91 percent and 97 percent of the original beam are present with a retarding potential of 90 volts and 85 volts respectively. If secondary electrons were present they would be largely eliminated by a retarding potential of a few volts. Therefore it seems reasonable that secondary electrons are absent in all three cases and that the differences between the three curves of Fig. 2 are probably due to the distribution of the retarding field.

During some early measurements with S 15 volts negative and A 50 volts

[4] Davisson and Germer, Phys. Rev. **30**, 705 (1927).

positive with respect to F, a sharp increase in the measured value of the secondary emission was observed as the potential V_p of the primary beam passed through that of A. The value of V_p at which this slope increase occurred varied along with variations in the potential of A. The effect, although a small one, was quite clearly a characteristic of the tube rather than of the tungsten target. It may have been caused either by a sudden spreading of the primary beam or by a migration of electrons to C from the rear of the electron gun as the electric field between A and B was reversed. To avoid this difficulty, the electron gun was operated as follows. The element S was a few volts negative with respect to the center of F while A was a few volts positive to F. The velocity of the electrons emerging from B was adjusted by an electric field of the proper value between A and B.

When the experimental tube was first constructed, a Faraday cylinder about 5 cm long and slightly smaller in diameter than the target was mounted in the place of the target. Measurements then made showed that the ratio of currents measured by the G_S and G_P galvanometers was as small as could be expected from the dimensions of the Faraday cylinder. Thus with the target mounted in the tube, the current measured by the G_S galvanometer consisted of secondary electrons from tungsten.

Varying the potential V_5 from zero to 3 volts had no influence on the appearance or magnitude of critical potential effects and produced a negligible increase in the emission coefficient. For part of the results shown $V_5=0$ and for the rest $V_5=3$ volts.

Results

The results presented are divided into four states according to the temperature, heat treatment and gas content of the target and general vacuum conditions in the tube. State 1 denotes the condition which existed after the tube had been removed from the pumps for one month with no treatment of any kind since its removal. The pressure was about 1×10^{-7} mm Hg. The measurements were made with the target at tube temperature. State 2 represents the following conditions. By means of the thoriated tungsten getter the pressure was reduced to about 3×10^{-8} mm Hg. The target was heated at about 1450°K for ten or fifteen hours. All temperatures given in this paper are based on pyrometer measurements made on the outer end of the element T. Being farthest from H this is the coldest part of T. No correction was made for the absorption by the glass walls of the tube. The actual temperatures reached will therefore be higher than the values given. The measurements were made with the target at about 1200°K. It is assumed that the tungsten is more free from surface contamination than in state 1. State 3 designates the following conditions. The target was heated to about 1700°K for an hour. This temperature did not increase the tube pressure of about 2×10^{-8}mm Hg. The tube then remained undisturbed for one month. The measurements were made with the target at tube temperature. State 4 represents the following conditions. After the measurements corresponding to state 3 were obtained, the target was heated at about 1400°K continuously for fifty hours. Then each

day before measurements were made at about 1300°K, the target was heated intermittently for a total of one hour at about 1800°K. After the day's measurements were over, the target was operated at about 1400°K until the 1800°K heat treatment preceding further measurements was given. It is thought in this work that the tungsten target is most free from contamination in state 4. In Figs. 3 to 16 the curves are marked 1, 2, 3, 4 corresponding to the above states.

The curves of Fig. 3 show the general secondary emission characteristics of tungsten, details of which are shown in Figs. 4–16. Curve *A* was obtained during the pumping of the tube described in section 2 before the target had been heated beyond about 900°K, while curve *B* resulted just after the target was first heated to about 1300°K for one hour. Both curves *A* and *B* were obtained with the target at tube temperature. Curves 1, 2, 3 correspond to

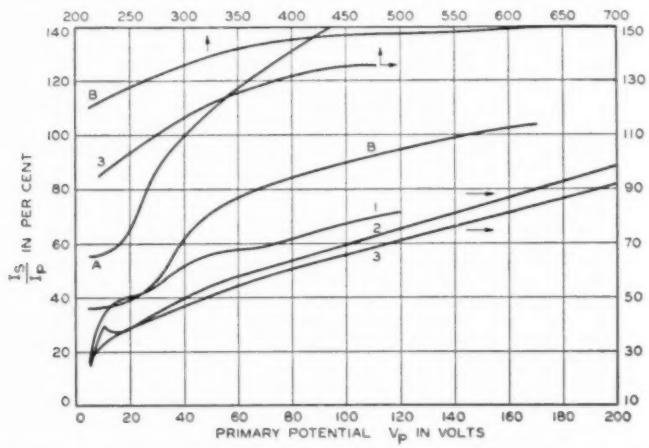

Fig. 3. General secondary electron characteristics of tungsten. The arrows indicate the special scales for the curves.

states 1, 2, 3 respectively. The curve corresponding to state 4 agreed well with curve 3. It is to be noted that on curve *A* the emission factor reaches 100 percent at 40 volts compared to 230 volts on curve 3. Fig. 4 contains curves 1, 2, 4 corresponding to states 1, 2 and 4. Curves corresponding to state 3 agree well with those of state 4. The nature of the changes which occur from state to state is obvious. During state 1 no measurements below 5 volts were made.

Fig. 5 shows the experimental curves between 20 and 40 volts corresponding to states 1, 2, 3, 4. Beyond the low voltage range of Fig. 4, with the exception of state 1 it was not satisfactory to determine slope changes by plotting the data as in Fig. 5. The following method due to Thomas[5] was used to magnify small slope changes. Straight lines were selected whose slopes were approximately that of the first portion of the curves of Fig. 5. A derived curve was then drawn whose ordinates were the differences between the ordinates of the experimental curve and those of the straight line. In this way slope changes of the experimental curve appear either magnified or as a minimum

[5] Thomas, Phys. Rev. **26**, 739 (1925).

on the derived curve. The lower half of Fig. 6 contains these derived curves corresponding to the experimental data of Fig. 5. These differences are

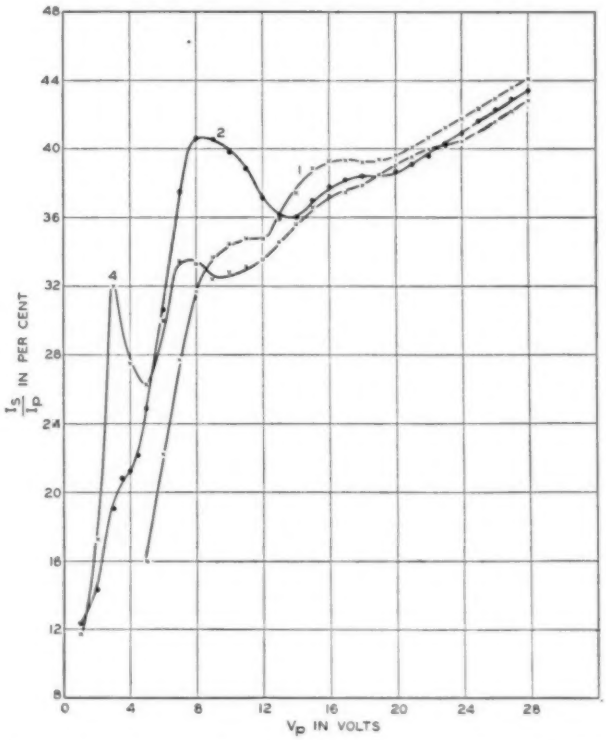

Fig. 4. Secondary electron characteristics of tungsten from 0 to 28 volts.

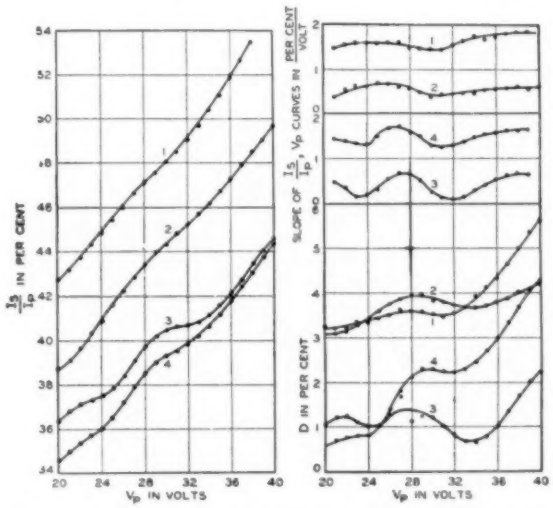

Fig. 5. Secondary electron characteristics of tungsten from 20 to 40 volts. Curve 1: Subtract 3 from ordinate. Curve 3: Add 2 to ordinate. Curve 4. Add 5 to ordinate.

Fig. 6. Secondary electron characteristics of tungsten from 20 to 40 volts. For slope curves: Curve 1: Subtract 1 from ordinate. Curve 4: Subtract 1 from ordinate.

marked D, the ordinates being expressed in the same units as in the experimental curves. For convenience in plotting, the derived curves have been separated from each other so that their relative ordinates are without significance. One sees for example that the small slope change near 33 volts in curve 1, Fig. 5, readily appears in derived curve 1 of Fig. 6 as a maximum and minimum. For comparison with the derived curves, the slopes of the experimental curves are given at the top of Fig. 6. An inspection of Figs. 5 and 6 shows that the slope change near 33 volts is greater in state 1 than in state 2, and that the slope changes near 24 and 33 volts are larger in state 3 than in state 4.

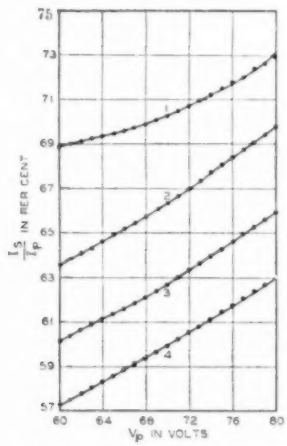

Fig. 7. Secondary electron characteristics of tungsten from 60 to 80 volts. Curve 1: Subtract 11 from ordinate. Curve 2: Subtract 6 from ordinate. Curve 3: Subtract 6 from ordinate.

Figs. 7 and 8 contain the experimental curves, their slopes, and the corresponding derived curves from 60 to 80 volts. With the possible exception of curve 1, the data of Fig. 7 are ambiguous as to the presence of critical changes of slope. However, the derived curves in Fig. 8 clearly reveal a critical slope increase at about 70 volts. Again as in Figs. 5 and 6, the curves of Fig. 8 show that the slope increases for states 1 and 3 are much longer than for states 2 and 4 respectively. By comparison with curve 1 the slope change in curve 4 has almost disappeared. No slope changes were observed from 40 to 60 volts, nor from 80 to 90 volts.

Fig. 9 reveals very little whereas curves 1, 2 and 3 of Fig. 10 reveal a definite slope increase at about 108 volts. Again the change of slope is larger in states 1 and 3 than in states 2 and 4 respectively. In fact in curve 4 of Fig. 10 the change of slope at 108 volts seems definitely to be absent.

Fig. 11 contains derived curves of two runs from 120 to 190 volts. In comparing the magnitude of the changes of slope in Fig. 10 with the variations between $4A$ and $4B$, the differences in the scale factors should be noted. These curves show no significant critical changes of slope in state 4. In Figs. 12 and 13, the slope change which appeared at about 207 volts in state 3 has disappeared in state 4.

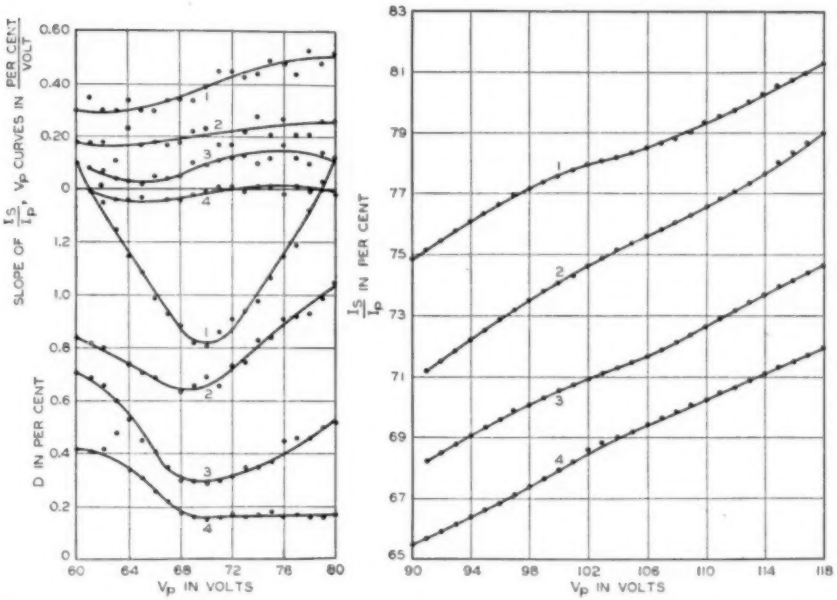

Fig. 8. Secondary electron characteristics of tungsten from 60 to 80 volts. Slope curves: Curve 1: Subtract 0.2 from ordinate. Curve 2: Add 0.1 to ordinate. Curve 3: Add 0.2 to ordinate. Curve 4: Add 0.3 to ordinate.

Fig. 9. Secondary electron characteristics of tungsten from 90 to 118 volts. Curve 1: Subtract 10 from ordinate. Curve 2: Subtract 4 from ordinate. Curve 3: Subtract 2 from ordinate.

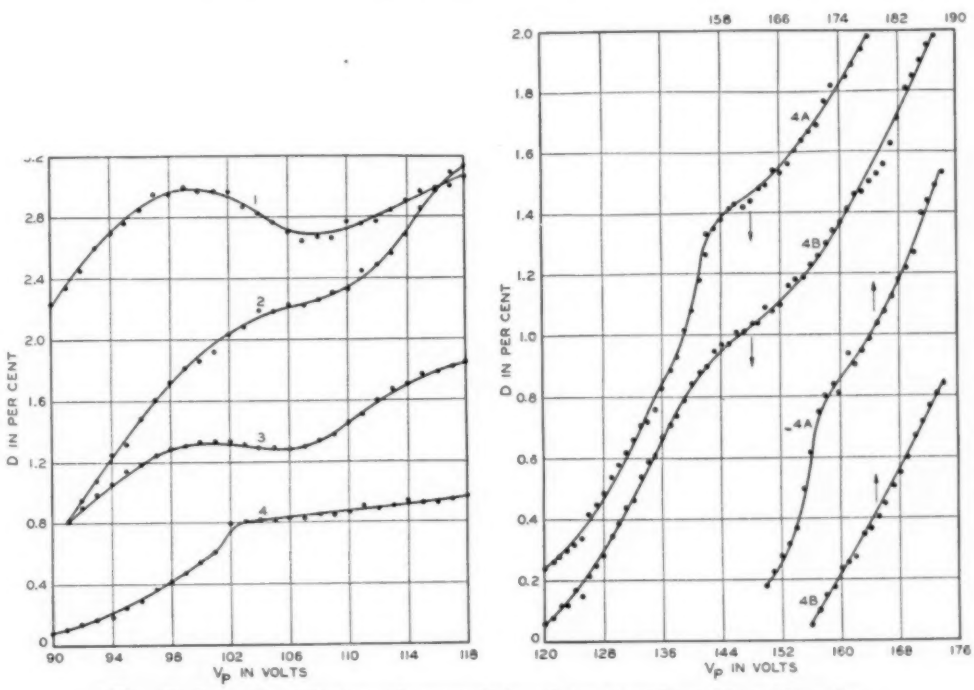

Fig. 10. Secondary electron characteristics of tungsten from 90 to 118 volts.
Fig. 11. Secondary electron chacteracteristics of tungsten from 120 to 190 volts.

Fig. 14 contains derived curves for two runs in the state 4 from 220 to 276 volts and from 310 to 364 volts. In Figs. 13, 14, 15 and 16, there are some places where different portions of the curves do not fit together. As shown in the curves, these discontinuities are not reproduced in the same place when the scale is shifted. The points on the voltage axis at which the galvanometer readings were shifted by means of the annulling current circuit of Fig. 1 from one end of the galvanometer scale to the other are marked on the curves with short vertical lines. They agree nicely with the discontinuities in the curves and it therefore seems reasonable that the latter are the result of slight de-

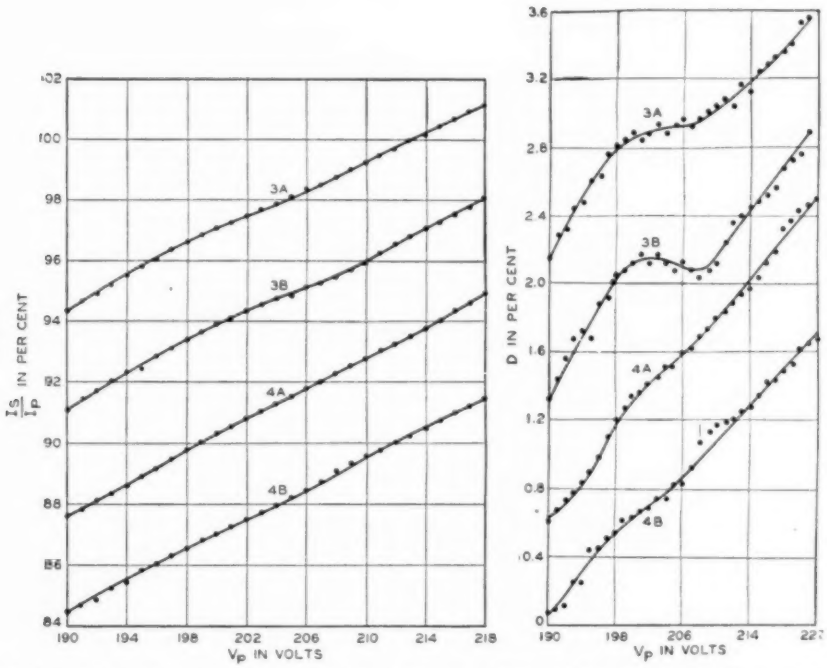

Fig. 12. Secondary electron characteristics of tungsten from 190 to 218 volts. Curve 3A: Subtract 7 from ordinate. Curve 4B: Add 3 to ordinate.

Fig. 13. Secondary electron characteristics of tungsten from 190 to 218 volts.

partures from linearity between galvanometer deflection and current at the extreme ends of the scale. The curves of Fig. 14 show no significant critical potentials. Fig. 15 shows a change of slope at about 297 volts in state 3, but it is absent in state 4.

The curves of Fig. 16 show no significant changes of slope between 360 and 490 volts. The measurements given in Fig. 16 were made with the target at tube temperature. The filament *H* burned out in giving the 1800° heat treatment of state 4 as described at the beginning of section 4. However, the measurements were completed within six hours after the target was reduced to tube temperature.

As discussed early in this section, in states 1 and 3 the measurements were made with the target at tube temperature and after it had stood for a long

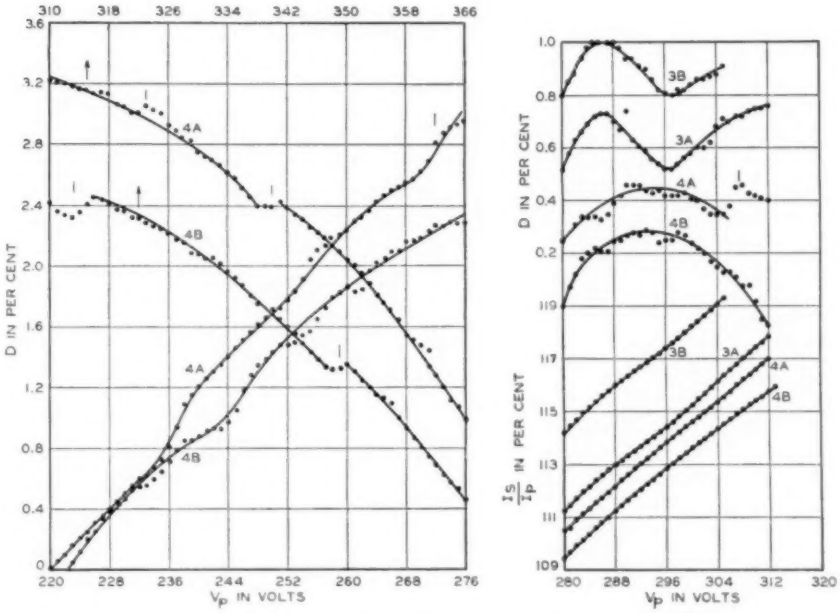

Fig. 14. Secondary electron characteristics of tungsten from 220 to 276 and from 310 to 364volts. See discussion of Fig. 14 in section on results for meaning of short vertical lines.
Fig. 15. Secondary electron characteristics of tungsten from 280 to 312 volts.

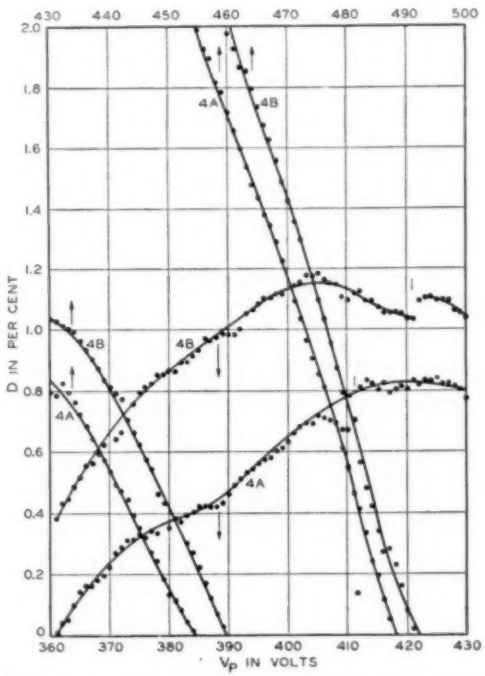

Fig. 16. Secondary electron characteristics of tungsten from 360 to 490 volts.

time without any heat treatment whatever. On the other hand, in states 2 and 4 the measurements were made with the tungsten target at about 1200 and 1300°K after certain heat treatments had been given. It seems most probable that states 1 and 3 correspond to a relatively contaminated surface as compared with states 2 and 4, and that the tungsten surface is most free from contamination in state 4.

In summarizing the observed effects, their variation from state to state is to be emphasized. In the low voltage region, as we progress from state 1 to state 2 and likewise from state 2 to state 4 (state 3 agreeing well with state 4) maxima are observed near former slope changes.

Proceeding from states 1 and 3 to states 2 and 4 respectively, the magnitude of the slope change at about 33 volts decreased as shown by Fig. 6. Also, the transition from state 2 to state 3 has increased the change of slope of curve 3 over curve 1 as well as curve 4 over curve 2. It is to be noted that in the transition from state 2 to state 3 the increase in slope at about 20 volts disappears and another appears at about 24 volts.

The data from 40 to 500 volts may be generalized as follows. In going from state 1 to state 2 and also from state 3 to state 4 the magnitude of the slope changes were always decreased. In this region only 4 critical potentials were observed even with the sensitive methods of measuring and graphing the data, and all but one of these disappeared in state 4.

Thus critical increases of slope at 70, 108, 208 and 297 volts were the only ones ever observed beyond 40 volts. Of these, only the 70 volt one persisted in state 4, and it was greatly weakened in intensity.

Thus in state 4, the state in which the tungsten surface is most free from contamination, only the following critical potentials have persisted; maxima at about 3.5 and 8 volts and slope increases at 24, 33 and 70 volts. These values are merely the applied voltages uncorrected for contact potential, etc

Discussion

It seems reasonable that the critical potentials observed in this work are characteristic of the tungsten target and are not caused by peculiarities of the tube. If in the primary beam there were secondary electrons which were emitted from the nickel of the electron gun, any critical potentials for nickel would introduce critical potentials in the measurements which would not be characteristic of tungsten. The curves of Fig. 2 indicate that the primary beam is free of secondary electrons from the nickel and therefore this possibility seems eliminated.

In contrast to these results, in the work of Krefft[3] on the secondary electron emission of tungsten between 25 and 500 volts, 25 critical potentials are indicated on his curves, 16 of which are indicated as remaining in measurements with the tungsten target at 1450°K. He used only one galvanometer to measure both the primary and secondary current. It was not operated at maximum sensitivity in the measurements. His slope changes were indicated on the experimental curves rather than on derived curves which are more

sensitive to slope changes. Thus, due to the more sensitive methods of measuring and plotting the data, slope changes, which in Krefft's curves are just noticeable would be quite prominent in the present work if they occurred. Moreover slope changes would have to be considerably smaller than in Krefft's work in order to escape detection.

Krefft states that secondary electrons from the metal of the electron gun were present in the primary beam. As pointed out at the beginning of this section, these might introduce spurious critical potentials.

Critical potentials in the emission of secondary electrons have been associated with the diffraction of electrons and the production of characteristic soft x-rays. The most recent measurements on the production of characteristic soft x-rays of tungsten are those of Richardson and Rao.[6] The characteristic soft x-rays were detected photoelectrically. The experimental arrangements were such that the x-rays were produced by electrons some of which had the distribution in velocity characteristic of the electrons coming from the thermionic source and the others the distribution which is characteristic of secondary electron emission of the x-ray target. Thus any critical potentials in the emission of secondary electrons, in reflection of electrons with or without energy losses, or in the diffraction of electrons by the x-ray target would produce slope changes in the excitation of continuous x-rays which might be observable. These in turn would be interpreted as critical potentials for the production of characteristic x-rays. It would seem that before a relation between secondary electron and soft x-ray critical potentials could be established, these ambiguities must be eliminated. Unfortunately there are as yet little spectroscopic data on soft x-rays of tungsten to compare with these photoelectric measurements on soft x-rays.

From about 25 to 500 volts, Richardson and Rao report about 60 critical potentials for the production of soft x-rays in tungsten. Over the same voltage range Krefft reported 25 critical potentials for the production of secondary electrons 9 of which disappeared after certain heat treatments. In the present work only 6 critical potentials were observed in this range and only three of these survived the heat treatment described in section 4. So far as the number of critical potentials is concerned, the marked difference between the three experiments makes any connection between them improbable.

Data on the diffraction of electrons from polycrystalline tungsten are not yet known. It may be that in state 4 the maxima at 3.5 and 8 volts and the critical increases of slope at 24 and 33 volts as well as other low voltage effects are diffraction phenomena.

Regardless of the mechanism producing the slope changes, their diminution or elimination beyond 40 volts points strongly to effects of surface contamination rather than to characteristics of tungsten.

This work was begun at the University of Minnesota. With an experimental tube which was kept on the pumps, consistent results were not ob-

[6] Richardson and Rao, Roy. Soc. Proc. **A128,** 16 (1930).

tained. Time did not allow the improvement in vacuum technique which was thought necessary.

The author is indebted to Drs. M. J. Kelly and H. E. Mendenhall for the opportunity and facilities to continue the work at Bell Telephone Laboratories and for helpful discussions of the work and to Dr. C. J. Davisson for suggestions and criticisms. The general problem was suggested by Professor John T. Tate to whom the author is grateful for suggestions and criticisms given during the progress of the experiments.

THE DETERMINATION OF THE PHOTOELECTRIC THRESHOLD FOR TUNGSTEN BY FOWLER'S METHOD

By A. H. Warner
University of California at Los Angeles

(Received October 12, 1931)

Abstract

The photocurrent per unit intensity curves for two different tungsten surfaces have been replotted by means of the method suggested by R. H. Fowler. The points all fit the theoretical curve very well, although the thresholds for the two surfaces are different. For one surface the data were obtained at temperatures of 1100, 900 and 790°K. The average value of the threshold at 0°K was 2632A, or 4.69 volts, with a greatest difference between individual values of 1.3 percent. The thermionic work function of this surface was 4.71 volts. The second surface was investigated at room temperature, and was formed by evaporation after very careful outgassing. The threshold for this surface was 2720A or 4.54 volts at 0°K, which agrees with Dushman's value of 4.54 volts for the thermionic work function at the same temperature. This should be regarded as the most reliable value.

IN AN earlier paper by the author[1] a value of the photoelectric threshold for tungsten was reported, based upon photocurrent per unit intensity curves made at various temperatures up to 1100°K. The value there given was 2575A, or 4.79 volts.

This value was of necessity based upon the measurements made at temperatures above 700°K, since below this the currents were too small to be determined accurately. This increase in current with temperature was apparently not accompanied by a shift in threshold, and was ascribed to the elimination of a contaminating gas layer from the surface.

In order to obtain larger currents at room temperatures, a tube was constructed with two central tungsten filaments, from one of which tungsten was evaporated upon the wall of the tube after the utmost precautions had been taken to eliminate all traces of gas, and the tube had been sealed off from the pump. The evaporation acted as a further clean up and it is felt that any contamination that may exist must be due to impurities contained in the tungsten itself.

The second filament and the evaporated coating are both illuminated through a quartz window, which is fastened to the Pyrex tube by means of a graded seal. The reaction of the filament which is of small area is too small to be detected at any temperature by a Dolazalek electrometer. Excellent results are obtained from the coating on the walls, which is maintained at room temperature. A more sensitive electrometer has been obtained and further work with the filament should be possible.

[1] A. H. Warner, Phys. Rev. **33**, 815 (1929).

It is the purpose of this paper to reexamine the data from both tubes by means of the method suggested by Fowler,[2] and to compare the results obtained.

Tungsten Filament

The current per unit intensity curves for the first tube are shown in Fig. 1. A Hilger quartz monochromator was used, with 0.05 inch slit width. This did not provide as monochromatic a beam as is desirable, but smaller slits gave too small currents. Readings taken at ten Angstrom intervals between 2350A and 2600A show that there was considerable overlapping of the lines.

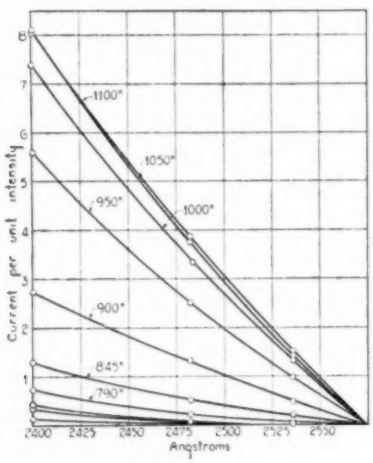

Fig. 1.

The intensities of the lines were governed by adjusting the current, voltage and temperature of the arc to agree with conditions under which Kazda[3] made a careful determination of relative line intensities. This method is subject to error unless the optical path is also identical with the one used by Kazda. While the same type of monochromator was used, there undoubtedly were small differences in the quartz windows of the cell, and the quartz of the arc itself.

In accordance with Fowler's method log I/T^2 has been plotted against $h\nu/kT$ for 1100°K, 900°K and 790°K. (Fig. 2.) The horizontal shifts necessary to bring the experimental curves into concidence with the theoretical are given in Table I.

Table I.

°K	$h\nu_0/kT$	$\lambda_0 A$	ϕ_0 (volts)	Average
1100	49.8	2619	4.71	$\lambda_0=2632$
900	60.0	2650	4.65	$\phi_0=4.69$
790	69.0	2626	4.70	

[2] R. H. Fowler, Phys. Rev. **38,** 45 (1931).
[3] C. B. Kazda, Phys. Rev. **26,** 643 (1925).

It can be seen that the points agree very well with the theoretical curve, and that the variation in λ_0 is small.

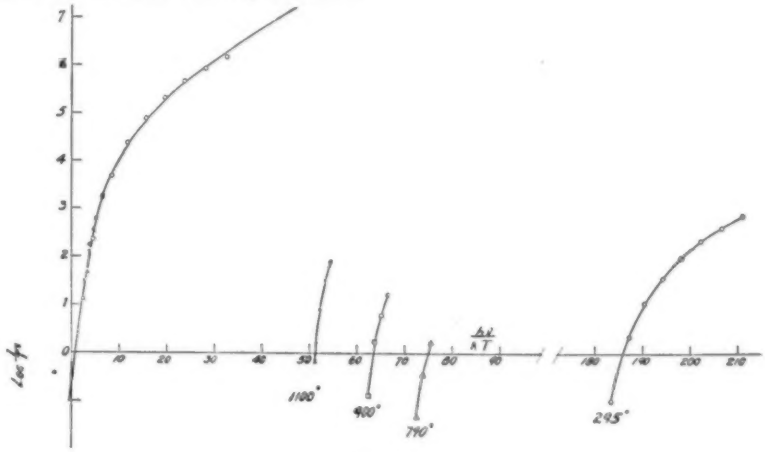

Fig. 2.

Evaporated Surface

The current per unit intensity curve for the evaporated surface in the second tube is shown in Fig. 3, which also shows the photoelectric response of

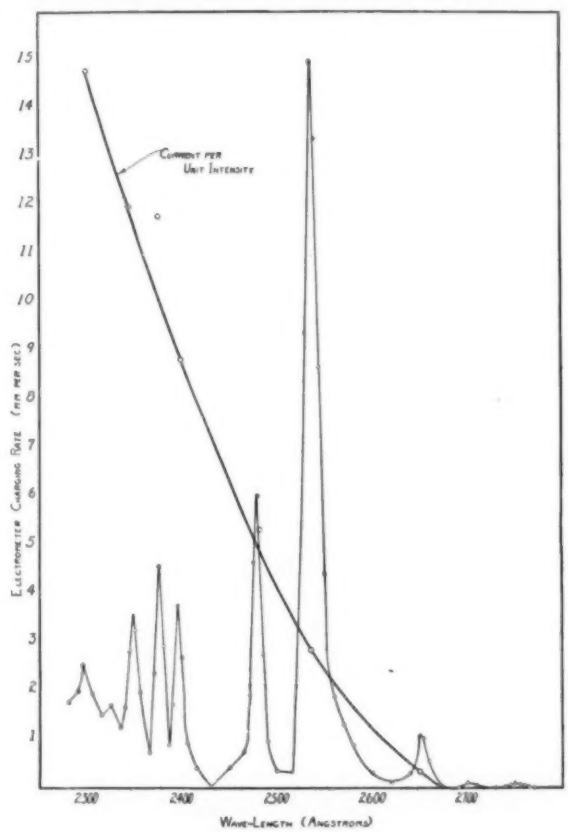

Fig. 3.

the surface as a function of wave-length. A Bausch and Lomb monochromator was used, with both entrance and exit slits set at 0.002 inch. As a result a very monochromatic beam was obtained, as is shown by the resolution of the lines of the mercury arc.

The intensities of the lines were determined by using Kazda's technique. The use of fine slits to obtain a highly monochromatic beam reduces the energy in the transmitted beam to such a low value that some method of extrapolation from a determination with wider slits is necessary. The use of Kazda's values, uncorrected for the change in type of monochromator introduces some uncertainty in the values of the intensities. The points of the current per unit intensity are quite consistent in spite of this.

The plot of these data according to Fowler's method is also shown in Fig. 2. The points fall very nicely upon the theoretical curve, and the $h\nu/kT$ shift gives the value of the threshold as 2720A, or 4.54 volts. The value from the current per unit intensity curve is between 2675A, or 4.61 volts, and 2750A, or 4.49 volts.

There was still a measurable current at 2700A, and investigation revealed that the surface was slightly sensitive to wave-lengths as long as 5600A. This is to be ascribed to traces of thorium. A sample of the wire used for the filament was mounted in a tube in which its thermionic properties could be investigated. It was found possible to activate it so that the work function agreed with the values given by Kingdon for a tungsten wire covered with thorium. (2.76 volts, 4470A.) The threshold for thorium on a tungsten surface is being studied and will be reported in a later paper.

It is to be expected from theoretical grounds that the photoelectric and thermionic work functions are equal. Dushman's[4] very careful thermionic work gave a value of 4.54 volts for pure tungsten. The photoelectric value (4.54 volts) for the evaporated surface, calculated by Fowler's method, is in complete agreement with this. The value given by Dushman is b_0 and should be independent of temperature. The photoelectric value obtained by Fowler's method should also be independent of temperature. These values then may be considered to be the work function at 0°K, and are found to be equal where the photoelectric measurements were made upon a tungsten surface formed by evaporation in a high vacuum.

The accuracy of the photoelectric determination depends upon the measurement of the current and the line intensities, upon the precision with which the $h\nu/kT$ shift can be determined when the experimental curve is superimposed upon the theoretical one, and upon the measurement of the temperature.

The positions of the points on the curve showing the photoelectric response as a function of wave-length were determined by taking several readings for each wave-length used and averaging. The readings never differed by more than a few percent. The values of the currents for the various lines were taken from the maxima exhibited by the final curve. The sharpness of

[4] S. Dushman, Phys. Rev. **25**, 338 (1925).

these peaks introduces some uncertainty, but it is thought their heights can be determined within two percent.

The determination of line intensities introduces an uncertain error. Two points of the current per unit intensity curve fall off the best curve through the other points. A redetermination of the intensities is being made.

The $h\nu/kT$ shift can be made quite accurately. In this case the shift is large (178.8), and should be accurate to better than one percent. The temperature was also determined quite accurately.

The accuracy of the current per unit intensity determination of the threshold depends largely upon the points in the vicinity of the intercept. If the small currents for 2700A and 2750A are included, the curve becomes parallel with the axis. The presence of the sensitive impurity is largely responsible for these currents, but it is probable that the tungsten also contributes slightly to the current at 2700A. From these considerations it would seem that the threshold should lie in the region between 2675A and 2750A with its most probable value at 2720A, as given by the Fowler method.

Conclusions

The value given by the work at higher temperatures (2630A, 4.69 volts) must be considered as less reliable, due to the presence of a contamination that inhibited the activity of the surface. This threshold was undoubtedly characteristic of the surface, as the thermionic work function agreed very closely. The variance of the latter from the commonly accepted value may be accepted as conclusive evidence that the surface was not perfectly clean.

The data from both tubes are seen to fit the Fowler theoretical curve. The threshold for the evaporated surface of tungsten at 0°K calculated by Fowler's method agrees extremely well with the value to be expected from the thermionic work function at the same temperature as determined by Dushman. This value is 4.54 volts, or 2720A.

The author is greatly indebted to Dr. R. A. Millikan for his generosity in placing the facilities of the Norman Bridge Laboratory of the California Institute of Technology at his disposal.

THE TEMPERATURE OF THE LOWER ATMOSPHERE OF THE EARTH*

By E. O. Hulburt
Naval Research Laboratory

(Received October 9, 1931)

Abstract

From the known amounts of the various gases of the atmosphere from sea level to about 20 km, from the observed light absorption coefficients of the gases and from the albedo of the earth's surface the temperature of the atmosphere in radiative equilibrium is calculated on the assumption that the sunlight is the only source of energy. The calculation is perhaps more rigorous than has hitherto been attempted, although it contains a number of approximations. The sea level temperature comes out to be about 19° above the observed world-wide average value 287°K, and the temperature above about 3 km falls many degrees below the observed temperatures. The temperature gradient in levels from 3 to 6 km is greater than that of convective equilibrium and hence the atmosphere would not be dynamically stable if radiation equilibrium prevailed. Therefore air currents take place to bring about convective equilibrium. Continuing the calculation it is found that only when the convective region extends to about 12 km (as is observed), with radiative equilibrium above 12 km (as is observed), does the atmosphere satisfy the conditions of dynamic stability and thermal equilibrium with the received solar energy. For this case the calculated sea level temperature is 290°K in good agreement with the observed value 287°K. Calculation shows that doubling or tripling the amount of the carbon dioxide of the atmosphere increases the average sea level temperature by about 4° and 7°K, respectively; halving or reducing to zero the carbon dioxide decreases the temperature by similar amounts. Such changes in temperature are about the same as those which occur when the earth passes from an ice age to a warm age, or *vice versa*. Thus the calculation indicates that the carbon dioxide theory of the ice ages, originally proposed by Tyndall, is a possible theory.

Introduction

1. IT IS generally accepted that the most important source of heat energy on the surface of the earth is the light of the sun. The only other known source of possible importance, namely, the leakage of heat to the surface by conduction from the interior of the earth, is relatively small, being less than one ten-thousandth of the energy of sunlight. It should therefore be possible to calculate the surface temperature of the earth and the temperature of the atmosphere to various heights above sea level on the assumption that the earth and the atmosphere radiate away to space an amount of energy equal to that received from the sun. Such a calculation requires a knowledge of the amounts of the gases of the atmosphere at all levels from sea level upward, the absorption coefficients of the gases throughout the optical spectrum, the reflecting power of the surface of the earth, the mixing action of winds, and other quantities. The problem has never been worked out completely. In the present paper an attempt at a fairly rigorous solution is presented, although

* Published with the permission of the Navy Department. Read before the National Academy of Sciences April 27, 1931.

it contains a number of approximations, and fair agreement is found with the observed temperatures of the earth and the atmosphere. In the process of working out the problem one is led to an understanding of the effects of radiation and convection on the values of the temperatures. In important papers on the subject Gold[1] discussed types of atmospheres which could be in convective and radiative equilibrium and Maris[2] derived conclusions about the temperatures, mainly of the high atmosphere, from calculations of the rates of energy absorption and radiation in various levels of the atmosphere.

The Observed Temperatures of the Atmosphere

2. The sea level temperature averaged over the earth is 287° Kelvin, or 14° Centigrade. The average temperatures t°K of the atmosphere are plotted as abscissas against the height z above sea level in the dotted curves 1′ and 1″, Fig. 1, which refer to summer and winter conditions, respectively. The

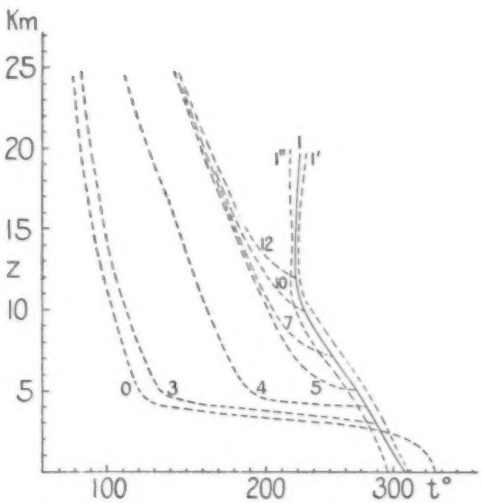

Fig. 1. Curves 1′ and 1″ give the observed temperatures t of the atmosphere at various heights z above sea level, for summer and winter, respectively, curve 1 is the average of 1′ and 1″ and the other curves are theoretical.

data[3] were obtained from 416 souding balloon flights in the years 1900 to 1912 in Europe and hence refer to a north latitude of about 50°. Curve 1, Fig. 1, is the average of the abscissas of curves 1′ and 1″ with the exception of the point at sea level which was plotted at 287°. We assume that curve 1 represents the world-wide average temperatures of the atmosphere, a questionable assumption, but perhaps not far wrong.

It is seen from curve 1, Fig. 1, that t falls off rapidly to about 220°K at $z=10$ or 12 km and is roughly constant from $z=12$ to 20 km. From $z=0$ to about 12 km the winds are relatively swift; this is known as the "convective

[1] Gold, Proc. Roy. Soc. **82,** 43 (1909); later discussed by Emden, Sitz. d. K. Akad. Wiss. zu München, page 55 (1913), and by Milne, Phil. Mag. **44,** 872 (1922).

[2] Maris, Terr. Mag. and Atmos. Elec. **33,** 233 (1928); **34,** 45 (1929).

[3] Humphreys, "Physics of the Air," 2nd Ed., 55 (1929).

region" (or the "troposphere"). From $z=12$ to 20 km, spoken of as the "isothermal region" (or the "stratosphere"), the winds are relatively slow. The temperature of the isothermal region over the equator is usually around 200° K and over polar regions is around 230°K. The height where the isothermal region sets in is about 15 km at the equator and decreases with increasing latitude. At any locality it may vary up and down 5 km or so with weather or other conditions, in polar regions it may descend to the surface of the earth.

In the convective region the atmosphere is in adiabatic equilibrium, but only approximately so. The theoretical adiabatic temperature gradient[4] is about 10 degrees km^{-1}, which gives a temperature of 187° at 10 km for a sea level temperature 287°. The observed value at 10 km is about 220° so that the atmosphere is warmer than it would be if adiabatic equilibrium prevailed. There are a number of factors which together are probably adequate to account for this,[2] such as the heat carried upward by water vapor, the effect of winds blowing from warm to cold regions, the direct absorption of the incoming sunlight by the atmosphere, etc. Hereafter we shall use the portion of curve 1, Fig. 1, from $z=0$ to 12 km as the curve of adiabatic or convective equilibrium. In so doing we take into account after a fashion the transport of heat energy by moisture and the other factors.

The present paper grew out of an attempt to find the answer to three inter-related questions, (1) why is the average sea level temperature about 287°K, (2) why does convection hold sway to about 10 or 12 km and not above, and (3) why is the temperature constant with height from about 12 to 20 km? In their pioneer papers Humphreys[5] and Gold[1] from considerations of radiation equilibrium showed that the average-in-height temperature of the absorbing layers of the atmosphere would not be below 212°K. Gold went a step farther and showed that if the atmosphere consists of two shells, the inner in the adiabatic and the outer in the isothermal state, the inner must extend to a level above 0.5 km but not greatly above 1 km. No detailed answers to the three questions were presented; the answers arrived at in the present paper are given in sections 11 and 12.

The Light Absorption Coefficients of the Gases of the Atmosphere

3. The absorption coefficient α of a gas for light of wave-length λ is defined by

$$I = I_0\epsilon^{-\alpha x},$$

where I_0 is the original intensity of the light and I is the intensity after passing through x cm of the gas at standard conditions, i.e. 0°C and atmospheric pressure. In the present calculations we are interested primarily in the infrared region of the spectrum and the only gases of the atmosphere which are known to have important absorption bands in this region are water vapor, carbon dioxide and ozone. The values of α for these gases, taken from the tabulations of Maris[2], are plotted in Fig. 2 as ordinates against λ in μ as abscissas. Maris obtained the values of α for water vapor and carbon dioxide by

[4] See, for example, Jeans "The Dynamical Theory of Gases," page 336 (1925).

[5] Humphreys, Astrophys. J. 29, 14 (1909).

calculation from the tables of Gold[1] who summarized the measurements of Paschen, Rubens and Aschkinass, Angström, Langley and others, made over 30 years ago. In the case of carbon dioxide only the average values of α across the various absorption bands are known, hence the flat tops of the carbon dioxide curve of Fig. 2. The shape of the absorption curve across several of the carbon dioxide bands has been observed, for example the 12.5 to 16μ band is given[6] roughly by the dotted curve *a*, Fig. 2, but the data are not sufficient to enable one to calculate with any certainty the exact values of α across the bands. Maris calculated the values of α for ozone given in Fig. 2 from rather

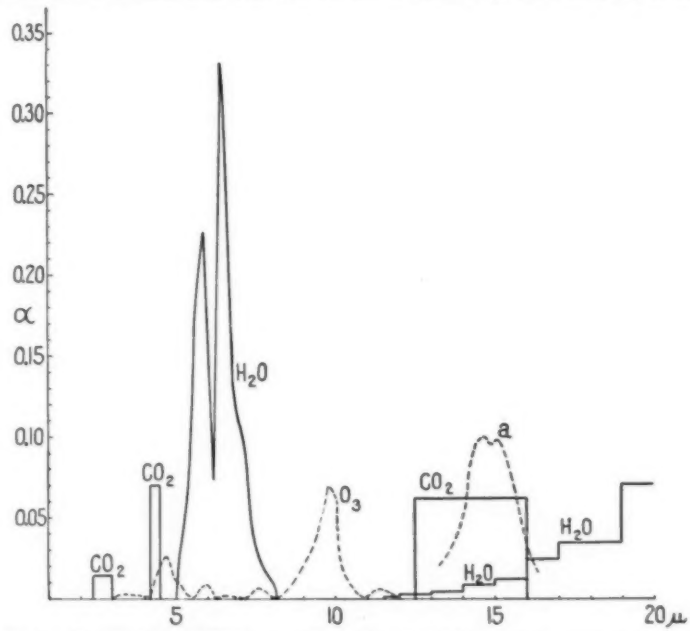

Fig. 2. The light absorption coeffieicnt α of carbon dioxide, water vapor and ozone; for ozone the scale of ordinates must be multiplied by 10.

conflicting measurements of Fabry[7] and of Ladenburg and Lehmann.[8] In general recent investigators have been interested in determining the fine structure, etc., of the bands and not in getting accurate absorption coefficients. It may be hoped that more exact values of α will be obtained with modern infrared spectrographic technique. This would enable the calculations of this paper to be improved, not however very easily. Several approximations, perhaps permissible under the present circumstances, would no longer be so, and to carry out the mathematical analysis without the approximations will be a matter of some labor.

The Distribution of Carbon Dioxide, Water Vapor, and Ozone Up Through the Atmosphere

4. Denote by x cm the equivalent thickness, reduced to standard condi-

[6] Burmeister, Verh. d. Deutsch. Phys. Gesell. **15**, 589 (1913).
[7] Fabry, Proc. Phys. Soc. London **39**, 1 (1926).
[8] Ladenburg and Lehmann **21**, 305 (1906).

tions, of a gas in the atmosphere from sea level to a height z. Let x_b cm be the thickness from sea level to infinity, i.e. outside of the atmosphere; x_b may be spoken of as the thickness to the "top" of the atmosphere. Then $x_b - x$ is the thickness of the gas from any level to infinity. The values of x and $x_b - x$ for carbon dioxide and water vapor are given in Table I. The values for carbon dioxide were calculated from standard tables, e.g. those of Maris[2], of the partial pressures of the gases of the atmosphere; the tables were of course based on direct observations. The values for water vapor were calculated from the pressures of saturated water vapor at the temperatures of the atmosphere given by curve 1, Fig. 1. $x_b = 3300$ cm, which amounts to 2.56 grams of water in a 1 cm vertical column of the atmosphere; this is in agreement with the value 2.6 grams deducible from Arrhenius' values of average humidity.[9] It is assumed that the values of Table I represent world-wide averages. This is satisfactory for carbon dioxide, which is very constant over the earth, but is perhaps questionable for water vapor, which varies tremendously with the weather, etc.

TABLE I.

	Carbon dioxide		Water vapor		Average
z	x	$x_b - x$	x	$x_b - x$	$\alpha(x_b - x)$
0 km	0 cm	252 cm	0 cm	3300 cm	145
3	102	150	2590	410	60
5	142	110	3080	220	5.2
7	164	88	3250	50	3.8
10	192	60	3276	24	2.3
12	207	45	3285	15	1.67
15	225	27	3291	9	1.00
20	239	13	3295	5	0.44
∞	252	0	3300	0	0

For ozone x_b is about 0.3 cm. Ozone exists in the levels above about 50 km[7]. Its distribution with height is not known, but we do not need to know the distribution, for in the present paper we are content to deal with the effects of ozone in a very simple way, as described in section 13.

THE TEMPERATURE OF THE SURFACE OF THE EARTH WARMED BY THE SUN AND ASSUMED TO HAVE NO ABSORBING ATMOSPHERE

5. The solar constant S, i.e. the energy of the sunlight falling on the outside of the atmosphere in the spectrum region from 0.3 to about 3μ, is 1.35×10^6 erg cm^{-2} sec.$^{-1}$. Of this energy about 30 percent is absorbed in the atmosphere[10], mainly in the levels below 10 km, so that only about 70 percent reaches sea level. However, for reasons given in section 10, we assume that the atmosphere is perfectly transparent to the incoming solar radiation and thus treat the 30 percent on the same basis as the 70 percent. The clouds and surface of the earth reflect away to space about 32 percent of the sunlight (reference 3, page 84). Therefore a fraction 68 percent, denoted by A, of the solar energy is absorbed by the earth.

[9] Arrhenius, Phil. Mag. **41**, 264 (1896).

[10] Abbott and Fowle, Annals Astrophys. Obs., Smithsonian Inst., **2**, 173 (1908).

The Stefan-Boltzmann law for the energy E erg cm^{-2} sec.$^{-1}$ radiated by a black body at a temperature t°K is

$$E = \sigma t^4, \tag{1}$$

where $\sigma = 5.71 \times 10^{-5}$ erg deg.$^{-4}$. If the earth had no atmosphere and were in thermal equilibrium with the sun's radiation we have, since the earth receives the sunlight as a disk and radiates as a sphere,

$$4\pi r^2 \sigma t_0^4 = \pi r^2 SA, \tag{2}$$

where r is the radius of the earth, t_0 the temperature of the surface and A is 68 percent. This gives

$$t_0^4 = SA/4\sigma, \tag{3}$$

or

$$t_0 = 252°.$$

t_0 is the black-body temperature. The true temperature t_0' of the earth's surface is given by

$$at_0'^4 = t_0^4, \tag{4}$$

where a is the fraction of the radiation of a black body at temperature t_0 absorbed by the surface (a is also known as the "emissive power"). If $a = 1$ the surface is a black body and $t_0' = t_0$; if $a < 1$ the surface is not a black body and $t'_0 > t_0$. Although a for the surface of the earth, including the clouds, is about 0.68 for radiation from 0.2 to 3μ, the value of a for radiation of longer wave-lengths is not known. The longer wave-lengths are of importance because t_0 is actually about 287°K and a black body at this temperature radiates mainly in the range from 3 to 30μ (see Fig. 4). We shall assume that $a = 1$, so that $t_0' = t_0$. The assumption is probably not far from the truth because 7/8 of the earth's surface is water and water is absorbent to the longer infrared radiations. The variation of a for the land with changes in climate may be important (see section 14).

The Temperature of the Atmosphere and of the Surface of the Earth in Radiative Equilibrium

6. It is assumed that heat energy is transferred through the atmosphere only by radiative processes. This amounts to assuming that convection is absent, for conduction is on the whole negligibly small compared to radiation or convection. Take the pressures of the atmosphere and the amounts of the component gases at various heights to be those observed, i.e., as given in Table I. Assume, as in section 5, that the atmosphere is transparent to the incoming solar radiation of which 32 percent is reflected out to space by the surface of the earth and the clouds. Thus on the average each cm^2 of the earth's surface absorbs $SA/4$ erg sec.$^{-1}$, where A is 68 percent. The surface is assumed to radiate this energy in the form of black-body radiation (see section 5) upward to the atmosphere which transmits some of the radiation and absorbs some of it. The atmosphere is heated by the radiation which it absorbs and reradiates the energy upward and downward, the downward radia-

tion warming the earth. Thus each layer of the atmosphere is subjected to an upward and a downward stream of radiation. The condition of radiative equilibrium is that the temperature distribution out through the atmosphere be such that each level of the atmosphere radiate as much energy as it absorb and that the energy leaving the top of the atmosphere be equal to $SA/4$.

The first step in expressing the foregoing ideas in mathematical terms is to make an approximation by replacing the complicated absorption bands of Fig. 2 by a single equivalent absorption band of average absorption coefficient α across the band. This simplifies the equations very much. The conclusions which we reach are not appreciably troubled by the approximation. A more exact treatment is hardly justified at the present time in view of the uncertainties in the values of the absorption coefficients and other quantities.

Let the energy emitted from the surface of the earth be E erg cm^{-2} sec.$^{-1}$. Let ϕ be a fraction such that ϕE be the portion of E comprised in those wave-lengths of the spectrum to which the atmosphere is perfectly transparent. Then $(1-\phi)\,E$ is the energy in the wave-lengths absorbed by the atmosphere. The quanities are shown diagrammatically in Fig. 3a, in which the area under the black body curve is E and the shaded portion is $(1-\phi)E$. The earth receives and absorbs $SA/4$ erg cm^{-2} sec.$^{-1}$ from the sun and a certain amount of energy sent down by the atmosphere, and radiates ϕE directly to space and $(1-\phi)E$ which is absorbed by the atmosphere (see Fig. 3).

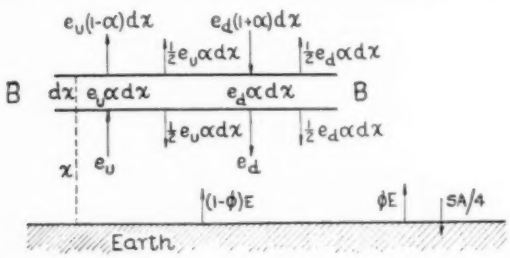

Fig. 3. Diagram showing energy absorbed, transmitted and emitted by an elementary layer BB of the atmosphere.

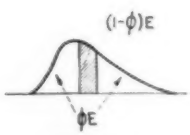

Fig. 3a.

Consider a horizontal layer of the atmosphere at a height x or z cm above sea level, shown by BB, Fig. 3. Let the thickness of the layer be dx. At the layer there is an upward stream of radiation e_u erg cm^{-2} sec.$^{-1}$ and a downward stream e_d, the streams of radiation comprising only the wave-lengths in the single equivalent absorption band of the atmosphere. Of e_u an amount $e_u\alpha dx$ is absorbed by the layer, and an amount $e_u(1-\alpha dx)$ passes through. The absorbed energy is reradiated, $e_u\alpha dx/2$ upward and an equal amount downward (see Fig. 3); similarly for e_d. For radiation equilibrium the temperature t of the layer is expressed by the relation, obtained from the Stefan laws of radiation embodied in (1) and (4),

$$\tfrac{1}{2}(e_u + e_d)\alpha dx = f\sigma t^4 \alpha dx, \tag{5}$$

or

$$e_u + e_d = 2f\sigma t^4,$$

where f is the fraction of the energy of a black body at temperature t in the

region of the absorbed wave-lengths. In general f, e_u and e_d are functions of x.

Since the atmosphere can radiate only in the spectrum region of the absorption bands, the difference between the upward and downward radiation streams is constant at all heights. Hence

$$e_u - e_d = \text{constant} = SA/4 - \phi E. \tag{6}$$

Denote by de_u the change in e_u in the distance dx measured positively upward. Then de_u is equal to the upward radiation leaving the top side of the layer minus the upward radiation entering the lower side of the layer. Therefore, referring to Fig. 3,

$$\begin{aligned} de_u &= \tfrac{1}{2}e_u\alpha dx + e_u(1 - \alpha dx) + \tfrac{1}{2}e_d\alpha dx - e_u, \\ &= -\tfrac{1}{2}\alpha(e_u - e_d)dx. \end{aligned}$$

Substituting (6)

$$= -\tfrac{1}{2}\alpha(SA/4 - \phi E)dx.$$

Integrating

$$e_u = -\tfrac{1}{2}\alpha(SA/4 - \phi E)x + C, \tag{7}$$

where C is a constant of integration. At the top of the atmosphere $x = x_b$ and $e_u = SA/4 - \phi E$. Hence $C = (1 + \alpha x_b/2)(SA/4 - \phi E)$ and (7) becomes

$$e_u = (SA/4 - \phi E)[1 + \alpha(x_b - x)/2]. \tag{8}$$

Either by a similar derivation, or directly from (6) and (8), we find

$$e_d = (SA/4 - \phi E)[\alpha(x_b - x)/2]. \tag{9}$$

From (5), (8) and (9)

$$2f\sigma t^4 = (SA/4 - \phi E)[1 + \alpha(x_b - x)]. \tag{10}$$

Equation (10) gives t in terms of quantities all of which are known except E. To find E we make use of the fact that at sea level $x = 0$ and $e_u = (1 - \phi)E$. Substituting these values into (8) gives

$$E = \frac{SA}{4}\,\frac{1 + \alpha x_b/2}{1 + \phi\alpha x_b/2}. \tag{11}$$

From (1) $E = \sigma t_0^4$, where t_0 is the temperature of the surface of the earth, and (11) becomes

$$t_0^4 = \frac{SA}{4\sigma}\,\frac{1 + \alpha x_b/2}{1 + \phi\alpha x_b/2}. \tag{12}$$

Introducing (11) into (10) yields

$$t^4 = \frac{SA}{8\sigma f}\,\frac{1 - \phi}{1 + \phi\alpha x_b/2}[1 + \alpha(x_b - x)]. \tag{13}$$

Equations (13) and (12) are the desired relations which give the temperatures of the atmosphere and of the surface of the earth for the condition of radiation equilibrium. In the foregoing derivation we have neglected the curvature

of the earth, which introduces no appreciable error, and have regarded the atmosphere as sufficiently homogeneous so that reflection or scattering of the radiation does not occur, which is probably permissible above the cloud region. Further, we have dealt with the streams of radiation as though they flowed only in the vertical direction. Actually, the radiation is everywhere diffuse radiation, but the case of diffuse radiation is very closely given by the vertical radiation derivation for relatively great absorption such as occurs in the infrared bands of the water vapor and the carbon dioxide of the atmosphere. Maris (reference 2, page 245) proved this by a calculation using Gold's evaluation of a certain integral (reference 1, page 62).

7. We must distinguish between the temperatures of the bottom of the atmosphere and the surface of the earth; these of course are not necessarily the same when the energy exchanges occur only by radiation as is assumed in the present case. The temperature t_0 of the surface of the earth is given by (12), which, when the numerical values are substituted for S and A, reduces to

$$t_0 = 252\left(\frac{1+\alpha x_b/2}{1+\phi\alpha x_b/2}\right)^{1/4}. \tag{14}$$

The temperature of the bottom of the atmosphere, denoted by t_0'', is found by putting $x=0$ and $f=1-\phi$ in (13). This gives

$$t_0'' = 252\left(\frac{1}{2}\,\frac{1+\alpha x_b}{1+\phi\alpha x_b/2}\right)^{1/4}. \tag{15}$$

For an atmosphere which does not absorb at all, this being the same as the case of no atmosphere as far as radiation processes are concerned, $\phi=1$ and from (14) $t_0=252°\text{K}$. This agrees, as it should, with (3). For a weakly absorbing atmosphere αx_b and $\phi\alpha x_b$ are small compared to unity and (14) and (15) yield approximately

$$t_0 = t_0''(2)^{1/4}, \tag{16}$$

which is the well-known Schwartzchild[11] relation. For an atmosphere which absorbs strongly in its bands, as is the case of the water vapor and the carbon dioxide of the atmosphere, αx_b and $\phi\alpha x_b$ are large compared to unity, being of the order 10^2, and (14) and (15) give approximately

$$t_0 = t_0'' = 252(1/\phi)^{1/4}. \tag{17}$$

8. To determine ϕ and f of (12) and (13) the black-body energy curves for a number of temperatures were plotted in Fig. 4. Referring to Fig. 2 we see that there are three important regions of absorption, the first from about 5 to 8μ due to water vapor, the second from about 12 to 16μ due both to carbon dioxide and water vapor, and the third from about 16 to 20μ due to water vapor. In the curves of Fig. 4 these regions are shaded. The ratio of the shaded areas to the total area under the black-body curve, denoted by f_1, f_2 and f_3, respectively, are plotted as ordinates in Fig. 5 against the temperature t as

[11] Schwartzchild, Gött, Nach. page 41 (1906).

abscissa. The three absorption areas together make up the assumed equivalent single absorption band and hence from the definition of f (section 6) we have $f=f_1+f_2+f_3$. f is also plotted in Fig. 5. ϕ is one minus the value of f at sea level.

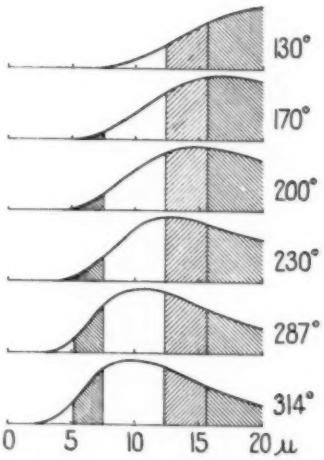

Fig. 4. Spectral energy curves of a black body at various temperatures.

We have left out of account the region of wave-lengths beyond 20μ simply because there are no observations of the absorption coefficients for this range of the spectrum. For example, it is not known whether water vapor is opaque or transparent to these wave-lengths. The method of calculating f

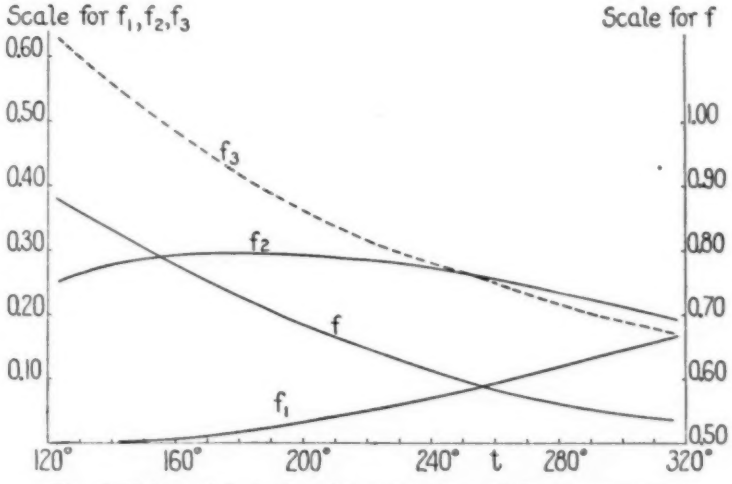

Fig. 5. Values of f_1, f_2, f_3 and f as functions of the temperature.

from the curves up to 20μ amounts to assuming that the atmospheric gases absorb in the region above 20μ to about the same extent as they do below 20μ; it is a sort of compromise between assuming that the atmosphere is either completely transparent or completely opaque to the longer wave-lengths.

The average values of the quantity $\alpha(x_b-x)$ which occurs in (13) were calculated approximately at each height z by combining the values for water vapor and carbon dioxide of Fig. 2. and Table I, weighing them according to the relative amounts of the two gases, the widths of the absorption bands and the average values of α across the bands. The values of $\alpha(x_b-x)$ are given in the last column of Table I. The "top" of the atmosphere is the region above which there is not enough atmosphere to cause appreciable absorption. From the values of α (x_b-x) it is seen that light in the wavelengths absorbed by the single equivalent absorption band is reduced to about 1/5, 1/2.7 and 1/1.5 of its original intensity in getting out to space from 12, 15 and 20 km levels, respectively. Therefore the "top" of the atmosphere is around 25 km.

From the values of $\alpha(x_b-x)$ and from (12) and (13) t and t_0 were calculated in the following way: t_0 was guessed and $1-\phi$ corresponding to t_0 was read off the f curve of Fig. 5. The values of t_0 and ϕ were substituted in (12) (or in (14) or (15)) and if the equation was satisfied t_0 was correct. If not, t_0 was guessed again and the procedure repeated until the correct values of t_0 and ϕ were obtained. These were put into (13) and the same method of successive approximations was used to determine t and f for each height z. The values of t are plotted in curve 0, Fig. 1, which gives the temperatures which would exist in the atmosphere if radiation equilibrium prevailed. The curve does not agree with the observed temperatures of curve 1, Fig. 1, giving a sea level temperature of 306° which is 19° above the observed value, and at levels above 5 km giving temperatures many degrees below those observed.

9. We digress for the moment to consider the effect on t_0 of changes in the carbon dioxide content of the atmosphere. From (14) it is found that doubling, or tripling, or reducing to zero the carbon dioxide of the atmosphere changes t_0 by less than 1° Centigrade. This same conlusion was reached by Angström,[12] Abbott,[13] Humphreys,[3] and others, as the result of qualitative discussions of terrestrial radiation which were perfectly correct as far as they went. However, the assumption of radiation equilibrium has led to atmospheric temperatures at variance with those observed. And we conclude, what was perhaps obvious from the start, that the physics of the atmosphere is not governed by radiation processes alone. So that any calculation of the possible effects on climate of changes in the carbon dioxide of the atmosphere must be left to a later section (section 14) after convection has been considered.

The Temperature of the Atmosphere Taking Into Account Convection and Radiation

10. If the temperature of the atmosphere were that of the radiation equilibrium curve 0, Fig. 1, the atmosphere would be dynamically unstable. The air above 3 km would be so dense, because of its low temperature, that it would descend rapidly; convective equilibrium would be brought about and the t, z curve would approach curve 1, Fig. 1. In general, if the t, z curve at

[12] Angström, Ann. d. Phys. **6**, 173 (1901).
[13] Abbott, reference 10, page 173.

any point is less steep than the convective equilibrium curve at that point, the atmosphere is dynamically unstable and a flow of air occurs in such a direction as to bring about convective equilibrium more or less completely. The t, z curve may of course be steeper than the adiabatic curve in a dynamically stable atmosphere. Convection is of course, also promoted by horizontal winds blowing from night to day areas, from warm to cold regions, etc.

Therefore curve 0, Fig. 1, shows that radiation equilibrium cannot exist in the atmosphere below about 5 km; it might, however, exist at greater heights, for above 5 km curve 0 is steeper than curve 1, Fig. 1. Assume that below a level, denoted by z_1, convective equilibrium exists, as given by curve 1, Fig. 1, and that above z_1 radiation equilibrium prevails. The two states will merge into each other through a region of transition, but for simplicity we regard the transition as abrupt. The assumption means that the energy leaving the earth advances upward through the atmosphere by the process of convection until a level z_1 is reached above which it advances by the process of radiation. We take various values of z_1 and investigate the stability of the atmosphere by calculating t_0 and the t, z curve above z_1 for each value.

Let the equivalent thickness of the absorbing gases, reduced to standard conditions, from z_1 to a higher level z be x_1 and to infinity be x_{b1}. At z_1 the temperature is t_1 as given by curve 1, Fig. 1, and the upward energy stream is e_{u1} where

$$e_{u1} = f\sigma t_1^4. \tag{18}$$

In the region above z_1 we have corresponding to (8) and (9), putting in (1),

$$e_u = (SA/4 - \phi\sigma t_0^4)[1 + \alpha(x_{b1} - x_1)/2], \tag{19}$$

and

$$e_d = (SA/4 - \phi\sigma t_0^4)[\alpha(x_{b1} - x_1)/2]. \tag{20}$$

Substituting $x_1 = 0$ and (18) into (19) and solving for t_0 gives

$$\phi t_0^4 = \frac{SA}{4\sigma} - \frac{f\sigma t_1^4}{1 + \alpha x_{b1}/2}. \tag{21}$$

From (5), (19), (20) and (21) we obtain

$$2f\sigma t^4 = (SA/4 - \phi\sigma t_0^4)[1 + \alpha(x_{b1} - x_1)]. \tag{22}$$

$x_{b1} - x_1$ is the same as $x_b - x$ so that the last column of Table I can be used in calculations from (22). In passing it may be noted that the temperature of the bottom of the part of the atmosphere in radiation equilibrium, obtained by putting $x_1 = 0$ in (22) and using (21), is not exactly equal to t_1 the temperature of the top of the part of the atmosphere in convective equilibrium. This is not an inconsistency, but merely results from the assumption that the convective region merges abruptly into the radiative region. A similar case was discussed in section 7.

For the case $z_1 = 3$ km, t_1 from curve 1, Fig. 1, is 269° and from (21) t_0 comes out to be 305°. With this value for t_0, t was calculated from (22) for z

above 3 km and is plotted in curve 3, Fig. 1. Just as in the case for curve 0, the atmosphere is dynamically unstable for the lower part of curve 3. Further, the value $t_0 = 305°$ is inconsistent with the assumption of $z_1 = 3$ km. For the assumption that t below 3 km be given by curve 1, Fig. 1, requires that t_0 be about 287°. Whereas the radiation equilibrium requirements laid down in (21) call for $t_0 = 305°$. Thus the assumption that $z_1 = 3$ km leads to an atmosphere dynamically unstable and one for which the radiation of energy to space is less than the energy received from the sun.

In a similar manner curves 4, 5, 7, 10 and 12, Fig. 1, were obtained corresponding to the cases $z_1 = 4$, 5, 7, 10 and 12 km, respectively. The respective values of t_0 were 301, 294, 293, 291 and 290°. For $z_1 = 15$ km t_0 was 296°. It is seen that only for z_1 between 7 and 14 km, and better still for z_1 between 9 and 12 km, does the atmosphere satisfy the conditions of dynamic stability and equilibrium with solar radiation. Such an atmosphere agrees closely with the observed atmosphere, for example, the calculated and observed values of t_0 are 290° and 287°, respectively. The agreement is no doubt better than is warranted by the accuracy of the data on which the calculations are based. Apparently the uncertainties and omissions have conspired to counteract each other to some extent.

The reason for treating the 30 percent of the incoming solar radiation, which is mostly absorbed in the levels below 10 km, (see section 5) as though it actually reached sea level is now clear. Since the thermal energy received from the sun by the surface of the earth and the atmospheric levels to about 12 km is spread around and transferred upward by convection, it makes little difference whether the energy is supplied to the earth's surface or to some level in the convective region.

Summary

11. We may summarize the conclusions thus far reached and in so doing give the answers to the first two questions in section 2. If the atmosphere were in radiative equilibrium at all heights the average temperature at sea level would be 306°K, or about 19° hotter, and at levels above 3 km more than 100° colder than it is. Such an atmosphere would be dynamically unstable and vertical convection currents would be set up. These would stir up the atmosphere in the lower levels to give the temperatures of convective equilibrium, thereby cooling the atmosphere at sea level and warming it above. If the convective region extended only to, say, 5 km we find that the atmosphere again is dynamically unstable and in addition that the total radiation emitted from the earth and the atmosphere is less than the energy received from the sun. When the convective region extends to 10 or 12 km (as is observed) the atmosphere is found to be stable, the calculated sea level temperature is about 290° (close to the observed value 287°) and the total radiation emitted from the earth and the atmosphere is equal to the received solar energy. If the convective region extended to a level greater than 12 or 15 km the outgoing radiation is less than the incoming solar radiation. Thus we have proved that the only type of atmosphere, of the types considered, which satisfies the

conditions of dynamic stability and thermal permanence is the type of atmosphere which is observed.

12. Nothing in the foregoing analysis has led to the answer to the third question of section 2, namely, why is the temperature of the atmosphere approximately constant with height from 12 to 20 km? True, it has been shown that, in agreement with the observed lack of winds, the conditions in this region are those of radiative and not of convective equilibrium. But equilibrium with outgoing terrestrial radiation calls for a decreasing temperature with increasing height. The constancy of t with z therefore requires some additional hypothesis. The obvious hypothesis, emphasized by Maris,[2] is that the incoming solar radiation is absorbed in the isothermal region in such a way that, together with the absorbed outgoing terrestrial radiation, t is constant with z. The constancy of t with z instead of being commonplace is in reality strange and unexpected and probably to be explained as the result of the combined action of two or more causes.

The Effect of Ozone

13. A simple calculation shows that the ozone, which exists in levels above about 50 km, has a slight effect on the temperature of the earth; it cools the earth about 1°. Ozone has two general regions of absorption, one in the ultraviolet extending from about λ2300 to 2900A and one in the infrared of which the most important portion is the band from about λ8.5 to 10.5μ, see Fig. 2. The solar energy curve in the ultraviolet below 2900A is of course not known, but if it be extrapolated into the ultraviolet on the assumption that the sun radiates as a black body at 6000°K the energy from 2300 to 2900A is about 4 percent of the solar constant S. The 3 mm of ozone is sufficiently thick to absorb completely this ultraviolet energy. If the ozone were not present and the ultraviolet energy came through to the earth S would be increased by 4 percent and t_0, instead of being 287°, would be $287 \times (1.04)^{1/4} = 289.8°$.

If the ozone is present in the atmosphere it absorbs the 4 percent ultraviolet energy and reradiates it equally upward and downward. Because the ozone is not very hot, probably not above 500°K, the reradiation is almost entirely in the infrared and mainly in the 8.5 to 9.5μ band. This band happens to be in a region which is little absorbed by water vapor and carbon dioxide, see Fig. 2. Therefore the ozone energy either reaches the surface of the earth or at least enters well into the convective region of the atmosphere, and adds 2 percent to S. The earth radiation at 287° passes out to the ozone where 2 percent is absorbed. The 2 percent is got by calculation from the values of α of Fig. 2 (or see Fig. 4, ref. 2). Of this 1 percent, which amounts to 0.3 percent of S, is reradiated downward to the earth. Thus the radiation received by the earth is equal to S increased by 2.3 percent, and t_0 becomes $287 \times (1.023)^{1/4} = 288.6°$, which is 1.2° less than 289.8°. Therefore the earth is about 1° cooler, *ceteris paribus*, than it would be if the ozone were removed from the atmosphere.

The Carbon Dioxide Theory of the Ice Ages

14. The sea level temperature t_0 was calculated in section 10 to be 290° by means of (21) with $z_1 = 12$ km, $t_1 = 219°$ and $\alpha x_{b1} = 1.67$ from Table I. To determine the changes in t_0 with changes in the amount of carbon dioxide in the atmosphere we may, to a first approximation, assume that αx_{b1} varies, the other quantities remaining constant. The value $\alpha x_{b1} = 1.67$ was the arithmetical average of $\alpha x_{b1} = 2.83$ for the 12.5 to 16μ band of carbon dioxide and $\alpha x_{b1} = 0.52$ for the 14 to 20μ band of water vapor, the 5 to 8μ band of water vapor being of no importance for 219° radiation (see the 200° curve of Fig. 4). If the carbon dioxide of the atmosphere were doubled $\alpha x_{b1} = (2 \times 2.83 + 0.52)/2 = 2.59$; if the carbon dixide were halved, $\alpha x_{b1} = (2.83/2 + 0.52)/2 = 0.92$. With these values in (21) t_0 comes out 294° and 286°, respectively. Thus doubling or halving the carbon dioxide in the atmosphere changes t_0 by 4°. Similarly, tripling or reducing to zero the carbon dioxide increases or decreases t_0 by 7°. Such changes as these in the world-wide average surface temperature of the earth are of about the same amount as occurred during the ice ages.[14] The calculation is thus in support of the carbon dioxide theory of the ice ages advanced long ago by Tyndall.[15] It is perhaps well to mention the essence of the physics underlying the calculation. In the convective region of the atmosphere the outgoing thermal energy is passed upward by convection to the radiative region above 12 km. So that the radiative region controls to a considerable extent the temperatures in the lower lying convective region. And the radiative region owes its optical properties more to the carbon dioxide than to the water vapor there.

Further, an increase or decrease in the world-wide average atmospheric temperatures of a few degrees would give rise to other changes. The water vapor in the atmosphere would be increased or decreased, this would accentuate the temperature changes. At the same time changes in the areas covered by vegetation and snow fields would take place, thus changing the optical properties, that is, the emissive power a, section 5, of the surface of the earth. Whether a would increase or decrease can not be said at the present time, for the reflecting powers, etc., of snow, sand, vegetation, etc. in the infrared to 40μ are not known. In general so many other changes may be thought of, such as a change in the carbon dioxide content of the sea, etc., that speculation as to the exact consequences of an increase or decrease in the average world-wide temperatures of a few degrees seems fruitless.

About all we can conclude is that the carbon dioxide theory of the ice ages is at least a possible one, and that objections which have been raised against it by some physicists[3,12,13] are not valid. We can not conclude that objections may not crop up in the future. Geologists[14] apparently have come upon no evidence, and have no unanimous opinion to offer, as to the fundamental causes of the ice ages. And we let it go at that.

[14] See any treatise on geology, for example, Coleman, "Ice Ages, Recent and Ancient," MacMillan (1926), or the excellent article on glacial periods by Howe, Encyclopaedia Brittanica, 13th ed., 12, 56 (1926).

[15] Tyndall, Phil. Mag. **22,** 277 (1861).

SPARKING POTENTIAL AND ELECTRODE MATERIAL

By Leonard B. Loeb
Department of Physics, University of California

(Received September 19, 1931)

Abstract

A consideration of the character of the normal spark breakdown in air with external ionization and involving time lags of greater than 10^{-4} seconds indicates that with the assumption of space charges the original Townsend theory of sparking can be maintained and that the spark mechanism as is experimentally found will be independent of electrode material. It is shown that the results of Duffendack, Wolfe and Randolph in which they find a dependence of sparking potential on the work function of the electrodes is due to their special experimental arrangement and in no sense contradicts the Townsend theory as asserted by them. It is shown that short time (less than 10^{-5} seconds) surge impulse breakdown in gaps of small area with insufficient ionization necessitates a new breakdown mechanism involving probable impact ionization at the cathode by positive ions to replace the deficient ionization. On the basis of this point of view further much needed investigations are indicated.

Introduction

THE countless investigations on the sparking potentials in air and other gases at atmospheric pressures and above have all been unanimous in ascribing a relatively unimportant role to the electrode material [1,21] and considerable importance to the nature of the gas and the gas density. This of course assumes the absence of thick nonconducting oxide films or water films on the electrodes. It also applies largely to conditions where the *potential of the gap is gradually raised to the sparking potential* so that overvoltages are not involved. If the cathode is illuminated by ultraviolet light or the gas in the gap is ionized these *sparking potentials are closely the same* for a given shape of electrodes and are remarkable constant. If no ionization is provided the results may be erratic and average possibly one or two percent above the values for the same gaps when electrons or ions are present, the variation depending on how the potentials are raised. In fact the constancy of these phenomena is such that this method is a *standard* method for measurement of high potentials *without any specification as to electrode material.*

Recent investigations of Duffendack, Wolfe and Randolph[2] using spark plugs and an induction coil or magneto discharge led these observers to

[1] J. J. Thomson, Conduction of Electricity through Gases, 2nd Edition, Cambridge Press' 1906, Chapter 15, especially p. 437; W. O. Schumann, Elektrische Durchbruchsfeldstärke von Gasen, Julius Springer, Berlin, 1923, pp. 17, 20, 156, 159; J. S. Townsend, Electricity in Gases, Oxford Press, 1914, Chapter X; E. Warburg, Handbuch der Physik (Geiger and Scheel) Vol. XIV, Chapter 7, page 367; R. Seeliger, Einführung in die Physik der Gasentladung, Barth, Leipzig, 1927, p. 85.

[2] O. S. Duffendack, R. A. Wolfe and D. W. Randolph, Development of an Electron Emitting Alloy, paper delivered before the Electrochemical Society April 23–25, 1931, printed in preprint form only.

results which appear to disagree with the above common observation. They found by an oscillographic study of the spark between wires in a spark plug that the sparking potential at breakdown, measured over short time intervals was high and very variable with ordinary spark plug wires of nickel alloy. When, however, alloys were used with about 0.04 percent of Ba or Mg present these sparking potentials became uniform and as much as 30 percent lower than before. At the same time they found that the work function of the metal was materially lowered, and in fact that the sparking potentials *as measured by them* were definitely connected with the work function. They therefore asserted that the work function of the metal does influence the sparking potential of the metal and that the overwhelming mass of previous data must be in error.

That an *apparent* contradiction exists in unquestionably correct. However, *this contradiction is in reality only apparent* and inasmuch as it involves questions of considerable importance in theory it may not be amiss to point out the obvious cause for the discrepancy, which in itself is not uninteresting.

Effect of Electrode Material on Sparking

The previous investigations have all been carried out as stated by slowly raising the potential until a spark occurred and by measuring the potential. The lack of dependence on electrode material indicated, as Townsend[3] had long ago shown, that the essential spark mechanism depended on the production near the cathode of electrons through ionization of the gas molecules by some mechanism, presumably by positive ions.[21] At very low pressures (less than 1 cm) in inert gases Holst[4] and Oosterhuis and also James Taylor[5] had shown a dependence on electrode material, the sparking potential being the lower the lower the work function. Neuman[6] in this laboratory confirmed these findings but found that between 1 and 2 cm pressure in argon the mechanism changed and the potential became independent of the electrode material. He there pointed out the obvious conclusion that when the gas density is so low that the electron formation near the cathode essential to a self-sustaining discharge can only come from bombardment of the cathode by positive ions the work function of the cathode must play an important role. As the pressure reaches a point where the probability of ionization of the gas in the high space charge near the cathode by positive ions becomes commensurate with that at the cathode surface, the discharge mechanism changes to one independent of cathode material. This view is doubtless correct. All these experiments were performed by the gradual raising of the potential up to sparkover.

[3] J. S. Townsend, Electricity in gases, Oxford Press, 1914, Chap. IX, pp. 322 and 30; Phil Mag. **45,** 444 (1923); Marx: "Handbuch der Radiologie" Vol. I, p. 241.

[4] G. Holst and E. Oosterhuis, Phil. Mag. **46,** 1117 (1923); Physica **1,** 78 (1921); C. R. **175,** 577 (1922).

[5] J. Taylor, Phil. Mag. **3,** 753 (1927); **4,** 505 (1927); Proc. Roy. Soc. **A114,** 73 (1927); also H. G. L. Huxley, Phil. Mag. **3,** 1056 (1927).

[6] L. J. Neuman, Proc. Nat. Acad. Sci. **15,** 259 (1929).

The Time Lag in Spark Discharge

In the work of Duffendack, Wolfe and Randolph the potential was raised in a small fraction of a second (the time scale was in 10^{-5} of a second) and the breakdown potential was measured by oscillograph. Further no source of ionization was furnished at the cathode, unless in some experiments the cathode was at red heat due to gasoline explosion.* Hence their experimental procedure constitutes an obviously new approach to the problem, which involves as its chief feature the rate of rise of potential. In other words, a time element is introduced into this investigation which was absent in other investigations. This time element brings into consideration a different aspect of spark discharge, i.e. that of the well-known time lag. This is a factor which has been little studied and still less discussed in its bearing on the breakdown potential. Since the time element has certain interesting features it will repay one to consider the role of time in spark discharge.

A study of the effect of time on the breakdown of spark gaps reviewing past literature was made by Zuber[7] in 1925 and was mathematically discussed by Laue.[8] Since Zuber's work some new features have been added in the work of Rogowski[9] and others using the high speed cathode-ray oscillograph, and by others, essentially Lawrence and Dunnington[12] and Beams [10,11] using the Kerr cell shutter. Zuber studied the spark lag, i.e. the time between the point where the potential reaches the sparking value, or some small overvoltage of one or two percent, and the time at which the spark passes. He finds that down to about 0.1 second the number of time intervals, between arriving at the sparking potential and the passage of the spark, which exceed t seconds is given by $n_t = n_o e^{-p\beta t}$. Here β is the chance that an electron is formed in the gap by ultraviolet light, radiation from radium or by natural processes and p is the chance that such an electron can in the gap lead to a spark discharge. Thus the average time lag of the spark is $\bar{t} = 1/p\beta$. The quantity p depends on overvoltage, the nature of the gas and the spark gap. Zuber did not go to shorter time intervals because of the physical limitations of his measuring circuit. He also found that $\bar{t}$ was in reality a function of β, and for *very small* overvoltages that it was about proportional to the intensity of ionization. He further found that overvoltages also reduced $\bar{t}$ and that moist air acted in a similar fashion. The interpretation of these results in terms of later knowledge is of considerable importance.

* In their paper before the Electrochemical Society no accurate description of the spark chamber was given, an omission which makes discussion somewhat difficult.

[7] K. Zuber, Ann. d. Physik **76,** 231 (1925).

[8] M. von Laue, Ann. d. Physik **76,** 261 (1925).

[9] W. Rogowski, Archiv. f. Elektrotechnik **20,** 19 (1928); and O. Beyerle, Archiv. f. Elektrotechnik **25,** 267 (1931); P. O. Pedersen, Ann. d. Physik **71,** 317 (1923); R. Tamm, Archiv. f. Elektrotechnik **20** (1928); Burroway, Archiv. f. Elektrotechnik **16,** 14 (1926); J. J. Torok, Trans. A.I.E.E. **47,** 177 (1928); **48,** 46 (1930).

[10] J. W. Beams, Jour. Franklin Inst. **206,** 809, 1928; Phys. Rev. **28,** 475 (1926); Phys Rev. **35,** 24 (1930).

[11] J. C. Street and J. W. Beams, Phys. Rev. **38,** 416 (1931); L. von Hamos, Ann. d. Physik **7,** 857 (1930).

[12] E. O. Lawrence and F. G. Dunnington, Phys. Rev. **35,** 396 (1930).

With the limitations of his apparatus Zuber could not determine whether there was *a real lower limit to the time t* at which a spark could occur. The writer[13,17] had in 1928 postulated that a space charge mechanism was required to cause a spark to occur according to the Townsend theory; and assuming the charge due to positive ion migrations in a long gap he indicated that below $t=10^{-5}$ to 10^{-4} seconds such a mechanism could not take place. It was accordingly predicted that *the minimum spark lag must lie at time intervals of this order of magnitude.* This point in fact has never been investigated. It is the writer's belief that the space charge mechanism is probably correct for what will be termed the *normal spark breakdown.* Shortly thereafter the work on *surge impulse breakdown* of spark gaps of Pedersen,[9] Rogowski, Tamm, Burroway, Torock and Beams[10,11] indicated that for considerable overvoltages the time lag lay in periods of 10^{-8} or even 5×10^{-9} seconds. The later researches of Lawrence and Dunnington,[12] and Dunnington[14] show, however, that for actual breakdown without overvoltage and the electrodes illuminated with ultraviolet light the time lag is always finite and large, as observed by Zuber. Once, however, breakdown started it was found to be accomplished in time intervals of the order of 5×10^{-9} seconds up to 10^{-7} seconds. The results of Pedersen, Rogowski, *et al* led the writer[15] to abandon the positive ion mechanism for the space charge accumulation *especially in the case of surge impulse breakdown* and to formulate a mechanism of space charge formation based *entirely on the movement of mobile electrons.* Independently Franck and von Hippel[16] formulated a similar theory using a slightly different idea requiring longer time intervals. Schumann[17,18] later developed the Franck and von Hippel idea quantitatively by equations which in the main agree well with Dunnington's[14] observations concerning the mechanism of breakdown. Both the Franck and von Hippel and the Schumann theory apply beautifully to the case of *normal breakdown with time lag,* although they are probably not completely essential. It is further probable that the *electron ionization mechanism* as postulated by the writer and Franck and von Hippel may not be *completely adequate for short time surge breakdown* of spark gaps and that an *added factor to be discussed later may enter with inadequate ionization.*[21]

The Mechanism of the Normal Spark Breakdown

The new developments lead one to the following conclusions. Spark discharge in gases in the atmospheric pressure range, when occurring near the minimum sparking potential, occur essentially on the basis of the mechanism assumed by Townsend. That is electrons must be generated by *positive ion impact on gas molecules* near the cathode in such numbers that the discharge becomes self-sustaining. *This mechanism only can account for the independence of the work function of the electrode surfaces universally observed* for spark dis-

[13] L. B. Loeb, Jour. Franklin Inst. **205,** 305 (1928).
[14] F. G. Dunnington, Phys. Rev. **38,** 1535 (1931).
[15] L. B. Loeb, Science **69,** 509 (1929), also Jour. Franklin Inst. 1930.
[16] J. Franck and A. von Hippel, Zeits. f. Physik **57,** 696 (1929).
[17] W. O. Schumann, Zeits. f. Technische Physik **11,** 131 (1930).
[18] W. O. Schumann, Zeits. f. Technische Physik **11,** 194 (1930).

charge of this character. In order, however, that the Townsend mechanism can occur space charges must be produced near the cathode of such magnitudes that the Townsend mechanism can take place (i.e. space charges giving gradients of the order of five to ten times the initial uniform sparking potential gradient). The consequences of the existence of space charges have actually been observed in the early periods of spark discharge under minimum sparking potential conditions by Dunnington.[14]

The space charges require for their formation 10^{-4} to 10^{-5} seconds if they are to be produced by positive ions and 2×10^{-8} to 10^{-7} seconds if they are to be formed by electron movement only, provided they can be and are so produced. It is quite possible that to form the space charges by electron movement only, overvoltages are required.[17,18,19] It is in fact only in surge impulse breakdown with overvoltages that we have any definite knowledges of time lags less than 10^{-4} seconds. It may therefore be that for space charges and breakdown in less than 10^{-4} seconds considerable overvoltages, electron ionization and possibly a new mechanism for causing this process may be required, especially in the absence of ultraviolet light, while this is not essential for normal breakdown. Consequently while the time lags in spark breakdown measurements for the minimum sparking potential are such as to always insure the space charge formation and the Townsend mechanism,[21] this may in no sense hold for shorter time intervals.[17,18,19]

Returning to the question of space charge formation in longer time intervals, it is clear that under the conditions of minimum spark potential investigations the actual limit for space charge formation and for breakdown is of the order of 10^{-4} seconds or a bit less. The question then arises as to what causes the observed statistical lags of Zuber extending in some cases into minutes. The essential feature that affects the time lag and makes classical sparking potential measurements differ from the overvoltages breakdown *must depend on some rare fortuitous combinations of circumstances whose occurrence ends in the building of a space charge under the minimum potential conditions*. Since high fields exist across the gap any ionization occurring in such a fashion as not to lead to an appropriate space charge will be swept away and one must await the occurrence of the right combination of events to give a spark. As Zuber showed, the occurrence of appropriate conditions is a most complex phenomenon. It depends first on the occurrence of at least one electron in the gap where the then undistorted field is highest. In addition it must depend on whether this electron is near enough to the cathode to be effective in building up a space charge. This is influenced by the sort of gas, by the small overvoltage, by gap design and by the pressure of the gas. It may as postulated by Franck and von Hippel and by Schumann not depend on *one electron, but on a succession of electrons liberated in proper time sequence near the cathode*. It may again depend on a proper spatial orientation of electrons in the gap as postulated by the writer's chain mechanism; or it may depend on a proper space time sequence. In the limit if no artificial ionization is present such a fortuitous combination of events may on the average occur very rarely

[19] W. O. Schumann, Zeits. f. Technische Physik **11**, 58 (1930).

and we observe time lags which preclude any accurate approach to the true sparking potential (i.e. such lags that owing to human impatience the potentials appear 2 percent high). With ionization at the cathode the results are more uniform, the time lags are shorter and conditions are much improved so that the potentials are slightly lower. In spite of this, however, there are time lags of a finite amount (exceeding 0.1 of a second) indicating definitely a spatial, or temporal spatial, succession of electronic events which is not too common. Once, however, these occur the space charges are built up, the ionization by positive ions begins and the spark takes place in a very short time.

The Surge Impulse Breakdown Mechanism

One may now turn to the problem presented by Duffendack, Wolfe and Randolph's method. These observers measure the actual potential at breakdown of presumably an *un*illuminated spark plug gap whose actual minimum breakdown potential as it occurs in air is not measured by the static method. Such gaps have so small a volume of air to be ionized by the normal atmospheric processes that the chance of a proper occurrence of circumstances leading to a normal spark is most remote. In addition the fields between spark plug terminals are far from uniform and it can occur that, with considerable overvoltages, fields far greater than those causing sparking under ordinary conditions obtain. These observers measure at what potential in a rapidly rising potential wave the gap actually breaks down. The time between that when the true minimum potential on the spark coil wave is reached and that when due to a considerable overvoltage (of the order of several tens of percent) the spark passes at the observed potential is of the order of 10^{-5} seconds. Hence they observe a phenomenon that depends on just the type of surge breakdown mechanism in which the electronic space charge mechanism is completely unknown and has at best only been conjectured. There is in this operation no time for the *fortuitous and apparently efficient set of occurrences* which give the true minimum sparking potential. Instead on a rapidly rising potential wave the field strength at the points on the electrodes rises to absolutely unknown values. It continues to rise until conditions of ionization in the gap are such that perhaps just any one electron or ion located anywhere in or near the gap can start a space charge building mechanism. The impulse may even pass without a spark. It is most probable that the intense fields near points on the cathode catch the first positive ion appearing due to natural ionization, and if this when accelerated can produce on *impact with the cathode* a new electron, a mechanism for space charge formation of the Franck and von Hippel type is set up. It is unlikely that in such intense radial fields the field at any distance from the minute point on the cathode would be great enough to generate ions by collision of the positive ion and gas molecule. This is emphasized first by the fact that for ionization of a gas by positive ions with any efficiency much higher fields are needed than those for liberation of electrons from the cathode surface by positive ions; and secondly by the fact that the high fields probably lie about *rough points* on the cathode and are not of sufficient intensity at several ion free paths to give the positive ion a chance to ionize other gas molecules. It therefore appears not unreasonable to assume

that in this *forced discharge at very high fields* the space charge mechanism is built up by electrons from the positive ion bombardment of the electrode surface. This mechanism then replaces the adequate ionization obtaining in other sparks. Such an electron and space charge source must depend on the work function of a particular spot on the cathode. A similar conclusion was also reached independently in one of Schumann's splendid papers.[21] If the work function for this spot is low the potential needed for a spark will be lower than for a point of high work function. By making electrodes of uniformly low work function the surge impulse breakdown potential will be markedly lower and more uniform. It will, however, never be really uniform (as can be seen by the photographs of Duffendack, Wolfe and Randolph) for the potential rises quickly and the points are not uniform. It is most probable that considerable uniformity could be introduced into such experiments with perhaps even lower potentials, if really intense ionization at the cathode is introduced by an external agent (e.g. ultraviolet light on the cathode). In this case the potential should be independent of work function, except insofar as the photoelectric efficiency of the source varies markedly with this quantity. This condition has been studied to some extent by Rogowski and Tamm[20] and is in accord with the above.

It thus appears that the work of Duffendack, Wolfe and Randolph in no sense invalidates the generally accepted theory of the ordinary spark breakdown mechanism, nor does it cause us to revise it in the least. Their work deals with conditions radically different from the ones used in classical studies. In fact they have discovered that *by removing almost all natural chances of ion formation between the electrodes* by short time intervals and small electrode area *it takes a new mechanism requiring much higher fields to produce a space charge and a spark.* In the absence of ionization and under their special conditions as to electrode form it is probable that the most efficient mechanism depends on electron emission from the cathode by positive ion bombardment.[21] This is definitely dependent for its effectiveness on the work function of the metal. It is conceivable by still further altering conditions in shortening time intervals and using smaller electrodes that one might be able to suppress sparking entirely until one reached field strengths leading to the well-known field currents. This would also depend on work functions and yield still another spark mechanism. It may be that recent results of Street and Beams[11] apply to just this situation. This phenomenon would hardly, however, disprove the Townsend interpretation of the spark under entirely different conditions.

It is imperative as seen from this discussion that experiments be made to really measure the shortest time limit in normal spark discharge. It would also be of great interest to find for what time intervals and fields the new electrode-material dependent mechanism begins to manifest itself. It should also be of interest to see whether in all short time surge impulse breakdown the nature of cathode material does not play a role, and to determine the effect of intense external ionization on such breakdown.

[20] W. Rogowski and R. Tamm, Archiv. f. Elektrotechnik **20**, 107 (1928).
[21] W. O. Schumann, Zeits. f. Technische Physik **11**, 143 (1930).

THOMAS-FERMI EQUATION SOLUTION BY THE DIFFERENTIAL ANALYZER

By V. Bush and S. H. Caldwell
Massachusetts Institute of Technology

(Received September 25, 1931)

Abstract

A numerical solution of the Thomas-Fermi equation $d^2\phi/dx^2=\phi^{3/2}/x^{1/2}$, with the boundary conditions $\phi(0)=1$ and $\phi(\infty)=0$, is presented, as obtained mechanically by means of the Differential Analyzer. This device for solving ordinary differential equations is described in a separate paper in the Journal of the Franklin Institute. The results are given for larger values of argument than have previously been reported, and at high values of argument precision has been improved. Over a part of the range, previously published results are checked, and the entire range is checked by an independent integration.

A MACHINE recently developed at the Massachusetts Institute of Technology is capable of the solution of many forms of ordinary differential equations.[1] This paper presents the results obtained by its use in the solution of the Thomas-Fermi[2,3] equation, which was picked as one of the first problems for attack largely because it brought out certain interesting points in connection with the operation of the machine.

The equation with dimensionless variables introduced is

$$\frac{d^2\phi}{dx^2}=\frac{\phi^{3/2}}{x^{1/2}} \tag{1}$$

and the boundary conditions are

$$\phi(0)=1 \tag{2.0}$$

$$\phi(\infty)=0. \tag{2.1}$$

An equation of this type, with boundary conditions as given, is inherently difficult to solve by any method. It is nonlinear and involves a singularity at $x=0$. Moreover, the boundary conditions are such that they cannot be satisfied directly; one must be satisfied at the point of singularity at $x=0$, and the other at infinity. It is also characteristic of this equation that small errors introduced when solving with x increasing have a cumulative effect as the solution proceeds.

The second derivative in Eq. (1) becomes infinite for $x=0$, so the solution for the region from $x=0$ to $x=0.2$ was taken from an expansion given by Baker.[4] The remainder of the problem was divided for solution into two parts,

[1] V. Bush, Jour. Franklin Inst. **212,** 447 (1931).
[2] L. H. Thomas, Proc. Camb. Phil. Soc. **23,** 542 (1927).
[3] E. Fermi, Zeits. f. Physik **48,** 73 (1928).
[4] E. B. Baker, Phys. Rev. **36,** 630 (1930).

corresponding to the regions from $x=0.2$ to $x=10$ and from $x=10$ to $x=\infty$.

In the region from $x=0.2$ to $x=10$, in order to keep the ordinates in the result large and hence maintain precision, there was introduced in Eq. (1) a new variable

$$\psi = \phi\epsilon^{x/2} \tag{3}$$

which gave the equation

$$\frac{d^2\psi}{dx^2} = \frac{d\psi}{dx} - \frac{\psi}{4} + \frac{\psi^{3/2}}{x^{1/2}\epsilon^{x/4}} \tag{4}$$

Moreover, it was found advisable to operate the machine with x decreasing in order to minimize the effect of casual errors, which in this region produced a cumulative effect with increasing x. The required starting conditions at $x=10$ were obtained by running a family of solutions in the region from $x=10$ to $x=\infty$, using a range of values for $\phi(10)$ within which the correct value was known to lie. Each of these solutions satisfied Eqs. (1) and (2.1), and was extended back by means of Eq. (4) to $x=0.2$. At that point the values of ϕ and ϕ' were read and plotted, together with points computed from Baker's expansion for different values of $\phi'(0)$. The intersection of the two curves established by interpolation the values of $\phi(10)$ and $\phi'(10)$ for which the solution satisfied the original equation and both boundary conditions.

In the region from $x=10$ to $x=\infty$, a change of variables was made, introducing

$$u = \frac{1}{x}, \quad q = \phi u \tag{5}$$

after which Eqs. (1) and (2.1) became

$$\frac{d^2q}{du^2} = \frac{q^{3/2}}{u^4} \tag{6}$$

and

$$q(0) = 0. \tag{7}$$

The procedure here was to assume a value of q at $u=0.1$ and to adjust by trial the corresponding values of q' so that Eq. (7) was satisfied when the machine was run with q decreasing. This was repeated for a number of values of q covering the desired range. This procedure, while exceedingly laborious when using formal methods, is not unduly time consuming on the analyzer, for a single solution can be run in a few minutes when once the machine is set up.

For the solution of Eqs. (4) and (6), the differential analyzer was connected as shown in Figs. 1 and 2 respectively.[5] In these diagrams scales, signs

[5] For explanation of symbols used, see reference 1.

and gear ratios are disregarded. The revolutions of each shaft are proportional to the quantities indicated.

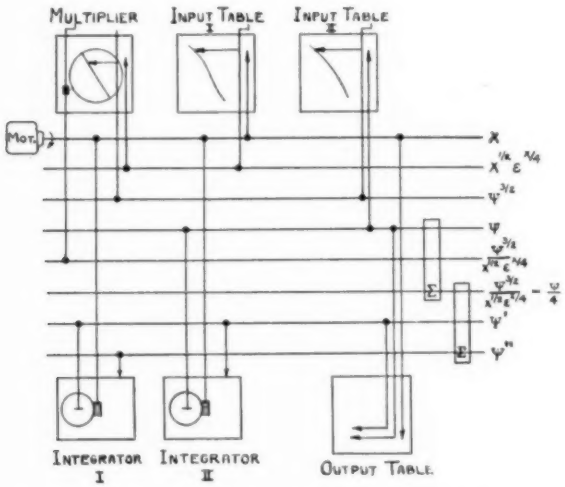

Fig. 1. Connections of the Differential Analyzer to solve the equation

$$\frac{d^2\psi}{dx^2} = \frac{d\psi}{dx} - \frac{\psi}{4} + \frac{\psi^{3/2}}{x^{1/2}e^{x/4}}.$$

Table I shows the numerical solution obtained for the region from $x = 0.2$ to $x = 36.92$. These values agree to within less than one percent with those re-

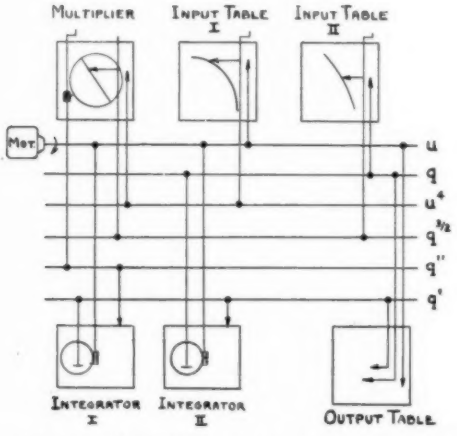

Fig. 2. Connections of the Differential Analyzer to solve the equation

$$\frac{d^2q}{du^2} = \frac{q^{3/2}}{u^4}.$$

ported by Baker,[4] whose table covers the range up to $x = 14.88$. In the region from $x = 15$ to $x = 20$, Fermi[3] gives values of one significant figure; the present

table gives two significant figures for all values beyond $x=16$. The initial slope was found to be -1.589 and thus agrees with Baker's value.

TABLE I.

x	ϕ	x	ϕ	x	ϕ
0	1.000*	2.500	0.193	10.44	0.0225
0.010	0.985*	2.708	0.176	10.67	0.0216
0.030	0.959*	2.918	0.162	10.92	0.0206
0.060	0.924*	3.125	0.150	11.16	0.0198
0.080	0.902*	3.333	0.138	11.43	0.0189
0.100	0.882*	3.542	0.127	11.72	0.0180
0.150	0.835*	3.750	0.118	12.01	0.0171
0.200	0.793	3.960	0.110	12.31	0.0163
0.250	0.755	4.167	0.102	12.63	0.0155
0.292	0.727	4.375	0.0956	12.97	0.0147
0.333	0.700	4.583	0.0895	13.33	0.0139
0.375	0.675	4.792	0.0837	13.72	0.0131
0.417	0.651	5.000	0.0788	14.12	0.0123
0.458	0.627	5.209	0.0739	14.55	0.0116
0.500	0.607	5.418	0.0695	15.01	0.0109
0.542	0.582	5.625	0.0656	15.48	0.0102
0.584	0.569	5.834	0.0619	16.00	0.0094
0.625	0.552	6.042	0.0587	16.56	0.0088
0.667	0.535	6.250	0.0554	17.14	0.0081
0.709	0.518	6.458	0.0526	17.78	0.0075
0.750	0.502	6.667	0.0500	18.46	0.0069
0.792	0.488	6.875	0.0473	19.20	0.0064
0.833	0.475	7.083	0.0450	20.00	0.0058
0.875	0.461	7.292	0.0430	20.87	0.0053
0.917	0.449	7.500	0.0408	21.82	0.0048
0.958	0.436	7.708	0.0389	22.85	0.0043
1.000	0.425	7.917	0.0371	24.00	0.0038
1.042	0.414	8.125	0.0355	25.26	0.0034
1.083	0.406	8.333	0.0340	26.67	0.0030
1.125	0.393	8.542	0.0321	28.24	0.0026
1.167	0.382	8.750	0.0310	30.00	0.0022
1.208	0.374	8.958	0.0298	32.00	0.0019
1.250	0.364	9.167	0.0287	34.29	0.0016
1.458	0.322	9.375	0.0275	36.92	0.0011
1.667	0.287	9.583	0.0265		
1.875	0.259	9.792	0.0255		
2.083	0.234	10.000	0.0244		
2.292	0.212	10.22	0.0235		

* Computed points.

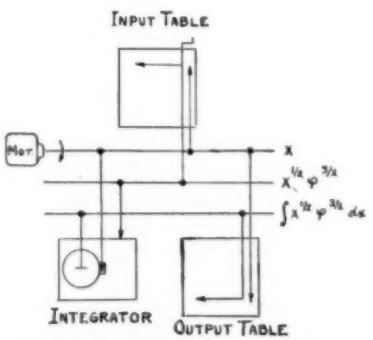

Fig. 3. Connections of the Differential Analyzer to perform the integration

$$\int x^{1/2}\phi^{3/2}dx.$$

A condition which ϕ must satisfy and which was not used in making the solution is given by

$$\int_0^\infty \phi^{3/2} x^{1/2} dx = 1. \tag{7}$$

This was used as a final check on the work, with the machine connected as in Fig. 3. The integral between the limits $x = 0$ to $x = 30$ had the value 0.994.

This problem was suggested by Professor R. M. Langer of the Department of Physics, and we are greatly indebted to him for his many suggestions and the active interest he took in the solution. Messrs. S. E. Caldwell, G. B. Hoadley, and J. R. Outt assisted in the operation of the machine and the measurement of final results.

LETTERS TO THE EDITOR

Prompt publication of brief reports of important discoveries in physics may be secured by addressing them to this department. Closing dates for this department are, for the first issue of the month, the twenty-eighth of the preceding month; for the second issue, the thirteenth of the month. The Board of Editors does not hold itself responsible for the opinions expressed by the correspondents.

On Inhomogeneities in the Magnetization of Ferromagnetic Materials

For some time work has been in progress on a method for detecting slight inhomogeneities in the magnetization of ferromagnetic materials and as a result of a good deal of experimenting the conclusion has been reached that qualitative observations are best made with small magnetized particles in suspension in a liquid. If such a suspension is allowed to settle on a magnetized surface, the pattern of the deposit reveals those points at which irregularities in the magnetic flux occur. The first successful attempts were made with finely divided iron obtained by sparking between iron electrodes under alcohol. This material was, however, very poor, and revealed only one pattern, namely, that obtained near saturation, as in Fig. 1, and that only with some uncertainty. Since starting this investigation Hámos and Thiessen[1] have published observations similar to those mentioned above.

Fig. 1. Patterns obtained on an iron-silicon alloy in large fields. Magnification ×16.

The technique for observing inhomogeneities has, however, been carried considerably farther, and though the procedure may still be regarded as a crude first attempt, very pretty results have been obtained. The essential improvement results from using particles having a larger permanent moment. So far the best have been small Fe_2O_3 particles, and I am greatly indebted to Mr. L. McCulloch of these Laboratories for preparing the suspension with which the following results were obtained.

The first observations were made on crystals of iron and of an iron-silicon alloy having large grains. The samples had been ground and annealed. For large magnetizations the deposits found were like that shown in Fig. 1, the field being perpendicular to the striations. The markings do not show any relationship to the grain structure. For somewhat smaller magnetizations, however, various systems of evenly spaced straight parallel lines appear, as in Fig. 2, the lines being usually more or less perpendicular to the magnetization, but varying slightly in direction and spacing from grain to grain. As the sample is rotated in the field, the lines gradually disappear, and new sets of lines having a new orientation take their place. At very low magnetizations no detectable patterns have been found. Similar results have been observed on an iron-silicon alloy melted in H_2. Its surface was quite smooth and clean, and as free from strains as is possible in material having more than one grain.

Observations were made on the untouched surface of samples of nickel and cobalt melted in H_2 with similar results, except that in nickel a new aspect of the phenomenon manifested itself. Instead of showing single parallel lines of like intensity, the microscope revealed

[1] L. v. Hámos and P. A. Thiessen, Zeits. f. Physik **71**, 422 (1931).

rather complicated patterns whose detail changed with the degree of magnetization. Three representative deposits are shown in Figs. 3 to 5. The last two differ only in intensity of magnetization. Many cases have been observed in which both the periodicity of the

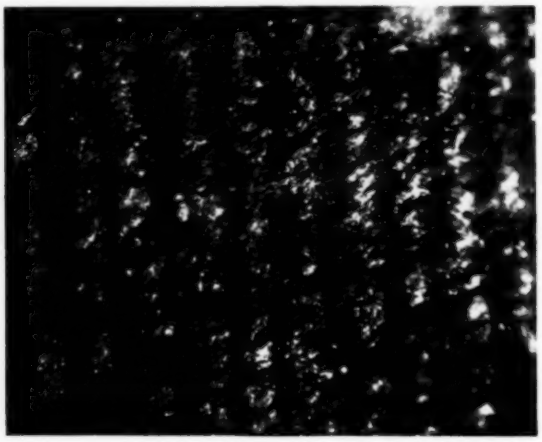

Fig. 2. Pattern obtained on the same sample as that shown in Fig. 1, but at smaller magnetizations. The width of the lines is probably due to surface irregularities. Magnification ×47.

intensity and the spacing of the lines made various complex but regular patterns. There are indications that the regularity of the patterns depends on the homogeneity of the mag-

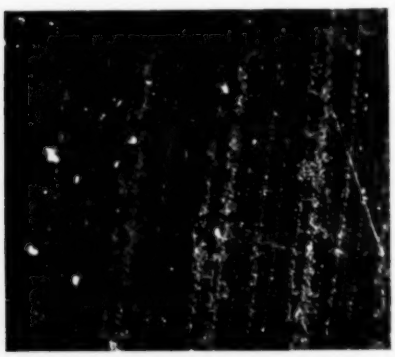

Fig. 3. Pattern obtained on a sample of nickel. Magnification ×47. On the original photograph some of the lines are distinctly seen to be double, while others are single.

netization, and that inhomogeneous magnetization gives rise to several superimposed patterns.

As to the interpretation of these results, little can be said at present with any confidence. The periodicity of the patterns makes it convenient to describe them in terms of periodic functions. It is of some interest to observe that the energies J associated with the spin-spin interactions would give rise to a wave phenomenon of the observed order of magnitude if the usual relations $J=h\nu$, and $\lambda\nu=c$ are applicable. If z is the number of nearest neighbors that an atom has, then zJ is of the order of $2\,\theta K$, θ being the Curie temperature and K the Boltzmann constant. This gives for iron with $z=8$ and $\theta=1060°$K, and for nickel with $z=12$ and $\theta=630°$K, the following wave-lengths:

Fe	Ni
0.055 mm	0.14 mm

Fig. 4. The narrow lines are the deposit obtained on a crystal of nickel. Magnification ×16.

Fig. 5. Pattern obtained on the same grain as that shown in Fig. 4, but at a slightly higher magnetization. Magnification ×16.

In all figures the magnetic field is in this → direction.

In addition, the work of Wolf[2] indicates that iron is a comparatively homogeneous material in which almost all the atoms are in the same state, whereas nickel is made up of two states in the ratio of 3 : 1. In a qualitative way, therefore, if standing waves of some sort, such as Bloch's spin-waves for instance, are associated with magnetization, one would expect them to be more simple in a uniform material like iron than in a material like nickel in which at least three values of J are present.

A more detailed report will appear shortly in this journal.

F. BITTER

Research Laboratories,
Westinghouse Elec. and Mfg. Co.,
East Pittsburgh, Pa.

[2] A. Wolf, Zeits. f. Physik, **70,** 519 (1931).

The Absolute Values of the Mobilities of Gaseous Ions

The necessity of establishing the absolute values of the mobilities of gaseous ions under conditions of high purity and exact control of experimental conditions has long been recognized. The marked effect of extremely minute traces of impurities on the observed mobilities, as well as the unknown complications introduced in those methods which employ gauzes, air streams of possible turbulence and volumes of ionization vaguely defined make it imperative that a method be employed which is free from all these objections. Prior to the development by Tydall and Grindley (Proc. Roy. Soc. **A110,** 341, 1926) of a mobility method of considerable resolving power, the only method for studying ion mobilities free from experimental uncertainties was that employing ultraviolet light for the production of negative ions. By use of this method Loeb has obtained 2.21 as the absolute value of the mobility of the negative ion in air. The method of Tyndall and Grindley, however, permits ions of both signs to be studied, is free from all the objections mentioned above, and can be adapted to studies where high gaseous purity is maintained. It is, therefore, being employed in these measurements of the absolute mobilities of ions in pure gases.

In the experiments which are at present being carried out, the ionization is produced by intense, hard x-rays from a Coolidge tube under a potential of 80 kv pure D.C. The ionization chamber is of glass, with all metal parts reduced as far as possible in dimensions. The whole may be baked out under vacuum before filling with the gas to be studied which has been passed through a carefully constructed purifying train. A slight adaptation made in the potential cycle applied to the plates of the ionization chamber permits the study of positive ions in gases where free electrons exist.

Under these conditions of purity, the absolute values of the mobility of the positive and negative ions in air have been determined and found to be the same as those obtained by Loeb, Tyndall and Grindley. At normal temperature and pressure, the values obtained are 2.21 cm/sec. per volt/cm for the negative ion and 1.60 cm/sec. per volt/cm for the positive ion, the average age of the ions being 0.05 seconds.

A study of the mobility of the positive ion in hydrogen is of particular interest in view of the results of Loeb (Phys. Rev. **38,** 549, 1931). For Na^+ ions of extremely short age (10^{-5} seconds) he has found an initial mobility of 17.5, which after 10^{-4} seconds, changes abruptly to a value of 13.5. A subsequent change reduces the mobility to 8.4 at which value it becomes independent of the age of the ion. The correctness of these observations, as well as a slight refinement of the absolute values obtained, is most interestingly obtained from experiments made under the conditions described above. A typical curve showing the existence of two distinct classes of ions in hydrogen is shown in Fig. 1. The age of the

slower ion is approximately 0.07 seconds. It is the normal ion in hydrogen and has an absolute mobility of 8.25 cm/sec. per volt/cm. The hump on the high mobility side of the curve is definite evidence of the presence of an ion of age equal to 0.04 seconds and mobility 13.1 cm/sec. per volt/cm. While this latter value is not exact owing to the lack of resolving power of the method under such conditions, particularly with the low current intensity obtained in hydrogen ionized by x-rays, the agreement with the value obtained by Loeb is extremely good in view of the uncertain temperature correction in his calculations. These experiments thus obtain a slightly more accurate absolute value for the mobility of the normal ion in hydrogen, and entirely substantiate the existence of one ion of much higher mobility as observed by Loeb. The detection of the 17.5 mobility ion is beyond the limits of this method.

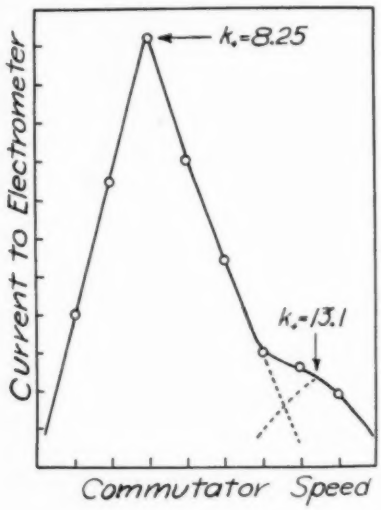

Fig. 1.

The experiments are being continued for ions in other gases.

NORRIS BRADBURY

Department of Physics,
University of California,
Berkeley, California,
October 19, 1931.

The Nuclear Moments of Indium and Gallium

The nuclear moment of indium was reported about a year ago by Jackson (Proc. Roy. Soc. **128,** 508, 1930) to be 1 from a study of the hyperfine structure of the resonance lines. Almost simultaneously McLennan and Allin (Proc. Roy. Soc. **129,** 208, 1930) reported it to be $\frac{1}{2}$ by studying practically the same lines. A more recent communication by Jackson (Nature **127,** 924, 1931) pointed out that the difference between his results and those of McLennan and Allin is just what one would expect from the difference in the resolving powers of their analyzing apparatus. A still more recent paper by McLennan, Allin, and Hall (Proc. Roy. Soc. **133,** 333, 1931) which continues their former investigation, again arrives at the conclusion that the nuclear moment is $\frac{1}{2}$. We have studied the resonance lines of indium using a Fabry-Perot interferometer and find indeed that λ4101 ($5p\ ^2P_{\frac{1}{2}} - 6s\ ^2S_{\frac{1}{2}}$) has four distinct components as reported by Jackson, which, while it does not determine the nuclear moment, requires that it be greater than $\frac{1}{2}$. Microphotometer curves of this line show that the outside components are of equal intensity (which would be expected for any value of the nuclear moment) and that the inner components are both of smaller intensity. From the intensity rules this latter would be expected only if the nuclear moment were greater than $1\frac{1}{2}$. The line λ4511 ($5p\ ^2P_{1\frac{1}{2}} - 6s\ ^2S_{\frac{1}{2}}$) was reported by Jackson to have four components but as the lines could not be fitted to a level scheme where both initial and final states were split into two, he concluded that he did not have the complete pattern and that one more line existed which he did not resolve. We have found a fifth component which is present very weakly and furthermore a strong indication of broadening in one of the more intense components, showing that the pattern consists of six lines, again in agreement with only those values for the nuclear moment which are greater than 1. The measured intervals are somewhat different from those reported by Jackson and these also point to the higher nuclear moment, the value $2\frac{1}{2}$ giving good agreement with the interval rule. The hyperfine-structure components of this line fall into two groups of three each and it must be that McLennan, Allin and Hall in observing only two lines have not separated the members of the groups. While it does not seem possible to say with certainty at present what the value of the nuclear moment for indium is, it

seems quite certain that it is greater than $1\frac{1}{2}$.

The resonance lines of gallium were examined with the same apparatus and the line $\lambda 4032$ ($4p\,^2P_{\frac{1}{2}}-5s\,^2S_{\frac{1}{2}}$) was found to consist of three components at -0.083, 0, $+0.098$ cm^{-1}. In order to make certain that the central component was single the interferometer plates were separated 3.6 cm, causing the outside, components of adjacent orders to overlap, but the central component showed no signs of broadening, and one may conclude that the gallium nucleus has a spin moment $\frac{1}{2}$ as this is the only value which would give three components. The intensities as estimated visually are also in good agreement with the expected ratio of 2 to 1 for the central component with respect to either of the outer ones. The other resonance line is more difficult to resolve and we have succeeded in obtaining only partial resolution. There does not seem to be any doubt, however, that the same difficulty exists for gallium that also exists for thallium and indium regarding the relative hyperfine structure separations of the two members of the doublet arising from a single p electron. Here again the separation of the state with $J=\frac{1}{2}$ is comparable to the S state with which it combines but the state with $J=1\frac{1}{2}$ has a much smaller separation than that to be expected theoretically.

J. S. Campbell
R. F. Bacher

National Research Fellows,
California Institute,
October 15, 1931.

Current-Intensity Relation of the λ600 Band of Helium

Sommer (Nat. Acad. Sci. Proc. **13,** 213, 1927) identified as a helium band a diffuse line occurring at λ600 on some of Lyman's plates. This identification has been confirmed by subsequent investigators but its relation to the rest of the helium molecular spectrum has remained undetermined. An investigation has been carried on at Princeton University in an attempt to determine the origin of the band. The extreme ultraviolet spectra of low voltage arc, Schuler cathode, and uncondensed capillary discharged have been obtained with a vacuum spectrograph. The band at λ600 appeared strongly only under such conditions of pressure and purity of the helium as permitted the appearance of the visible bands of helium. It has a distinctly sharp edge at the short wave-length side and shades away to the red. By using an approximate method of photometry it was found that in the uncondensed capillary discharge the intensity of λ600 varied directly with the current, whereas Weizel (Zeits. f. Physik **95,** 320, 1930) has observed that the visible bands of helium vary in intensity as the square of the current. An intensity varying as the first power of the current has generally been interpreted as signifying a primary, or one-stage process, while an intensity varying as the square of the current has been interpreted as a secondary, or two stage process, such as excitation by an electron of an atom which has been excited by a preceding electron. This suggests the possibility of a difference in the mechanism of excitation between the λ600 band and the visible bands. A more detailed discussion will be published later. Grateful acknowledgement is made to the Carnegie Institution of Washington for financial assistance.

John L. Nickerson

Mount Allison University,
Sackville, New Brunswick, Canada,
October 17, 1931.

Production of Second and Third Spark Spectra in a Hollow Cathode Lamp

The normal operation of a hollow cathode discharge tube with argon gas usually excites only the arc and a portion of the first spark spectra of the cathode material, while its operation with helium gas gives the arc and first spark spectra, and usually no more, the limit being approximately the energy available from the singly ionized gas. The introduction of a spark gap in series with the lamp removes this limitation and lines from higher stages of ionization are obtained. Lines of doubly ionized carbon and copper and of doubly and triply ionized germanium have been identified in spectrograms thus produced. Pulsating direct current was supplied to the Schuler Lamp by a full-wave rectifier consisting of two hot cathode mercury rectifier tubes, a filter choke and a 3 mfd condenser shunting the output. The lamp was normally operated at 0.4 to 1.2 amperes and at 500 to 2000 volts.

In normal operation with helium as the circulating gas the Ge II spectrum was strongly

excited when the carbon cathode containing about ½ gram of metallic germanium was operated at red heat. Ge I and C II lines were moderately strong, and lines of C I and gaseous impurities were rather weak, while a few of the most easily excited Ge III lines were present weakly.

After the adjustable spark gap had been placed in series with the lamp and closed, the lamp was operated normally until the Ge II was strongly excited. The spark gap was then opened slightly so that sparking occurred and the condenser gave an oscillatory discharge. An air blast on the spark gap reduced the tendency to arc. When sparking was taking place the lines appeared as follows: Ge I was little affected, Ge II was considerably intensified, Ge III and C III were brought out strongly and Ge IV only weakly excited. A spectrogram of the usual high potential hot spark without inductance usually shows certain Ge IV lines as the strongest lines in all of the Ge spectra. With the series spark gap bands, near 4000A, due to gaseous impurities, were much reduced in intensity. The helium bands 5500A to 6500A apparently were unaffected. When copper was used as the cathode the spark gap produced many strong lines that do not belong to the spectra of Cu I and Cu II, among these being the lines so far attributed to Cu III. Exposures of 15 minutes to 2 hours have been used for the region 500 to 2500A in a 1½ meter vacuum spectrograph.

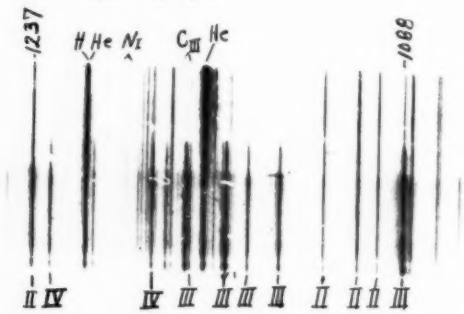

Fig. 1

The reproduction, Fig. 1, shows a portion of the germanium-helium spectrum taken with and without the use of the series spark gap. At the top two wave-lengths are indicated along with some impurities present. The stage of ionization of some of the germanium lines is indicated at the lower edge. Fig. 2 shows two germanium-helium spectra in the 4200A region. The wave-lengths and identifications are indicated at the top. It should be noted that when the spark gap is used the Ge III lines appear while the band *B* disappears.

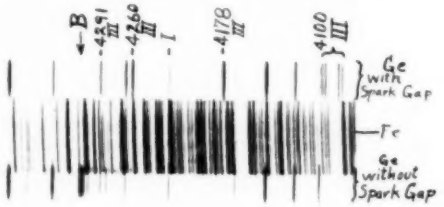

Fig. 2

This method of using a Schuler lamp is described because it provides a convenient method of exciting (apparently) all of the first and second spark spectra with scarcely any lines from higher stages of ionization present. By using argon to excite the arc spectrum, then helium with and without the spark gap all the lines may be identified as to stage of ionization. In addition the lines produced are very sharp, the source can be made sufficiently large to fill the angle subtended by any grating, and the sputtering is much less than with the hot spark. Since it is difficult to prevent arcing at the spark gap it is possible that a quenched gap of few sections, a make-and-break spark gap, or a magnetic blow-out might be employed to advantage. The spark gap must dissipate a large amount of heat.

It may be possible to excite still higher stages of ionization by a high potential condenser discharge through the lamp during an interruption of the direct current.

This technique has resulted from a suggestion by Dr. P. G. Kruger that a spark gap be employed to reduce the intensity of bands which had been troublesome.

C. W. Gartlein
R. C. Gibbs

Physics Department,
Cornell University,
Ithaca, N. Y.
October 26, 1931.

BOOK REVIEWS

Counting and Measuring. H. VON HELMHOLTZ, translated by CHARLOTTE LOWE BRYAN, with an introduction and notes by HAROLD T. DAVIS. Pp. xxxiv+39. D. Van Nostrand, New York, 1930. Price $2.50.

This little book contains a translation, with introduction and notes of Helmholtz' "Zählen und Messen," a paper which first appeared in the jubilee volume of philosophical papers dedicated to Eduard Zeller in 1887. More recently it has been reissued in the collection of Helmholtz' "Schriften zur Erkenntnistheorie" edited by P. Hertz and M. Schlick and published by Springer (Berlin 1921) to commemorate the hundredth birthday of Helmholtz. Through a strange oversight the volume under review nowhere gives an explicit reference to the original paper.

It is interesting to have this essay brought to attention at a time when physicists are devoting so much thought to the method of mathematical physics and its philosophical implications. That geometry, as referring to the actual space in which physical observations are made, is an empirical science, is now well recognized everywhere. Helmholtz takes us back even farther and shows how even the axioms of arithmetic are grounded in a physical empiricism. An illuminating quotation in this connection is:

"The first axiom, 'If two magnitudes are equal to a third, they are equal to each other,' is therefore not a law of objective significance, but it determines only what physical relations we can recognize as relations of equality."

In the introduction Professor Davis has traced the main course of thought on the problem of number and continuity from the Zeno paradoxes, through Cantor and Dedekind to the modern conflict between the schools of Hilbert and Brouwer. Unforuntately the space allotted to this task is too small for the fullest clarity to be attained in dealing with such a range of topics.

E. U. CONDON
Princeton University

Physics for Students of Pharmacy. C. J. SMITH. Pp. 287, figs. 194. Edward Arnold and Company, London, 1929. Price, $3.50.

A small book of two hundred and eighty-seven pages, with subject matter very highly selected from the standpoint of pharmacy students. The treatment is mainly with reference to the properties of matter, and classical apparatus encountered in laboratory experience. No attempt is made to discuss any of the so-called "modern physics," or modern mechanical devices. The properties of fluids occupy about one half of the section on mechanics. Sound is omitted. Heat and geometrical optics are treated quite fully. Bar magnets (the positions of Gauss are discussed at length) are given undue prominence, being allotted eighteen pages, while electromagnetic induction, x-rays, and radioactivity are covered in seven pages. Very few of the illustrations are taken directly from pharmaceutical experience. The author writes accurately and concisely, occasionally injecting practical details in manipulation, and frequently inserting historical statements.

R. C. WILLIAMSON
University of Florida

Physics of the Home. F. A. OSBORN. Pp. 391. figs. 221. McGraw-Hill Book Company, New York City, 1929, Second edition. Price $3.00.

The title of the book is apt. The book is written from the standpoint of students in Home Economy. The topics are selected with reference to their bearing in the home. Principles are stated briefly and concisely, and applications, (with numerous illustrations appealing to feminine experience) are discussed. Because of limitations in time, little space is devoted by the author to theoretical developments, or modern physics. One occasionally finds errors such as,

"tensile strength of steel wire equals 0.175 lbs. per square inch," or awkward expressions such as, "some notes have been sharped and flattened," or, "a vacuum of not less than one inch of mercury." But on the whole, the book should fill its place very well, and one will find much of interest in turning through its pages and noting the author's illustrations.

R. C. WILLIAMSON
University of Florida

Soap Films. A. C. S. LAURENCE. Pp. 141, figs. 61. G. Bell and Sons, Ltd., London. 1929. Price 12s 6d.

This book gives a good picture of the investigations which have been conducted on soap films. The author for several years assisted Sir James Dewar in his studies of soap films and later carried out independent investigations in this field. There are seven chapters to the book. Chapter I briefly discusses surface tension. Chapter II considers the characteristics of soap solutions and the preparation of soap and soap solutions to be used in making films and bubbles. Chapter III takes up the subject of soap films, their preparation and life history. Abnormal development, critical fall of soap films, and stratified films are also discussed in this chapter. Chapter IV is devoted to the black film. Chapters V, VI, and VII respectively discuss the subjects of soap solutions, soap molecules and the composition and structure of the soap film. Appendix I is devoted to the subject of oleic acid while appendix II deals with the color and thickness of soap films.

The author has presented the subject in a clear and pleasing manner. Students and investigators will obtain from this book a good picture of the subject of soap films and the physical behavior of soap solutions. Sixteen plates as well as other figures excellently illustrate the subject matter.

L. H. REYERSON
University of Minnesota

Analytical Mechanics. H. M. DADOURIAN, Pp. 427, figs. 148, D. Van Nostrand Company, New York, 1931. Price $4.00.

In this edition, as the author points out in the preface, much has been rewritten and one whole chapter almost entirely revised. This review, however, is not a comparison of the present edition with the previous ones but a consideration of the book as it now stands.

The scope of work covered is that of a good introductory course. In mode of development the author has first treated the mechanics of equilibrium and then proceeded to dynamics. In this choice he has been guided by the laudable aim, as he says, of introducing as few new concepts at a time as possible and of leading the student from the simpler to the more complex. There is too the advantage that if a student is taking a first course in calculus simultaneously the first portions of this text contain little calculus and so he should not be much called upon to anticipate results from the calculus course.

On the other hand there are, in the opinion of the reviewer, some real weaknesses. The concept of force is introduced on page 15, but without any statement there or elsewhere of how it is to be measured (by definition). Our ideas of its nature from muscular effort can surely not supply this need. Again on page 17 the kinetic reaction of a particle is defined as the product of its mass by its acceleration, although mass itself has not been previously mentioned. The mass idea is not discussed until page 122 and its nature and measurement are not treated until page 150. When this treatment is finally given it is based on force measurement which remains undefined. Surely such procedure cannot be conducive to clarity of ideas. Moreover, the experiments described on pages 151, 153 and 162 to clarify the ideas of mass and force are ideal, and incapable of verification to a degree that would afford reasonable confirmation. That on 162 is even theoretically unsatisfactory in that the motion is unstable. Would it not be preferable to have the evidence underlying fundamental ideas presented in such a form that the student could convice himself if he desired by trying the experiments out, or by reading the accounts of experiments that have actually been performed?

In the matter of notation the usual black face type for vectors is used. There is inconsistency however in many of the figures. Thus, in Fig. 98, page 242, the two arrows labelled $\boldsymbol{T}$ are

not the same force, the directions being different. If both are to be labelled by the same letter that letter can only denote magnitude and so should not be in bold face type. Again, in the figure on page 178 the arrow labelled $m\dot{v}$ should be labelled $-m\dot{v}$; and the same is true of every figure in which the kinetic reaction is represented.

There is no mention made of significant figures and some results imply an accuracy which is not obtainable. Thus, on pages 254 and 256, the answers are given to four figures while in each case the last digit has no significance.

On the other hand it is refreshing to find a text that is really consistent in the matter of units. Symbols everywhere represent physical quantities, units included. This consistence is a pleasant contrast with the practice of so many books where, in the same problem, the same letter is indifferently used to denote both an abstract number and a physical quantity.

The author also makes a good point in stressing that every force is associated with the action of some body. Such association is very helpful in the drawing of adequate figures for the solutions of problems.

The figures are well drawn and the type is good.

J. W. CAMPBELL
University of Alberta

Scientific Inference. HAROLD JEFFREYS. Pp. 247. The Macmillan Company, New York, 1931. Price $3.25.

Where all physical laws describing and explaining phenomen whose observation or appreciation lies within the ken of human experience are being reduced from the firm, "exact" basis of old to a system of probabilities, it is coming to be of more and more importance that the methods of derivation of such laws be subjected to rigorous analysis,—logical as well as mathematical. This is especially so because of the misconception, still somewhat prevalent, that results, derived by reasoning from probabilities, are therefore, *ipso facto* of an inferior nature to those obtained by using more "exact" methods.

Jeffrey's book forms indeed a most welcome addition in this rather neglected field, and its thorough treatment of the major and fundamental concepts at the basis of all scientific endeavor should make it a valuable aid to many of us who have been taking the ways and means of nature a little too much for granted. The author's primitive postulate is that it is possible to learn from experience, and that from this assumption and its logical consequences alone, there can be developed a justification for the adoption of *simple* quantitative laws, a justification which proves to be, plainly, that the *simple* law has a vastly greater inherent probability of being "true" than a more complicated one.

As one might expect from the author the treatment throughout is not only rigorous, but at the same time illuminating and stimulating. It does seem to this reviewer, however, that in some instances the rigor is too much on the side of the mathematical analysis, and he feels also that where so many of the fundamentals of Science involved have been subjected to the most careful and painstaking scrutiny, other, equally important fundamental concepts or results of observation have been passed over by *ex-cathedra* statements. One might mention: "But when the error arises as the resultant of a large number of independent errors of comparable importance, the normal law (of error) *is* right," and "We *know* . . . that light *is* a wave motion." As far as the former statement goes, one might, perhaps with more justification, say that if the normal law of error is found to hold in practice, then it would appear reasonably probable that the assumption concerning the existence of a large number of independent errors might have been right. Furthermore, this reviewer is not convinced that the question of the rejection of observations is quite as simple as it can be made to appear mathematically.

W. J. LUYTEN
University of Minnesota

Standard Four-Figure Mathematical Tables. L. M. MILNE-THOMSON, and L. J. COMRIE. Pp. 245. Macmillan and Company, England, 1931. Price 10/6 net.

This new volume of four-figure mathematical tables is not only one of the most useful books of its kind that has come to the reviewer's notice in recent years, but its form of presenta-

tion and general appearance make it a delight to the eye as well,—perhaps too obvious a thing to say where it concerns a work by such experienced calculators as Messrs. Milne-Thomson and Comrie. In addition to the usual tables of logarithms, antilogarithms, roots, powers, and reciprocals of numbers, and the natural and logarithmic tables of the trigonometric functions, natural logarithms, the gamma—and the error function, there are many others, such as those for trigonometric functions in radians, and for the inverse trigonometric and hyperbolic functions. The addition, at the end, of a table of integrals, both definite and indefinite, a revision of practically all the important formulae which occur in practical work, and a table of frequently used constants, gives the work a completeness as to render it almost indispensable to any research worker who ever has occasion to indulge in computations.

In choosing a type in which some figures extend above, and others below the general horizontal level of the majority, these new tables continue a practice which publishers of mathematical tables in this country would do well to follow—there can be no question but that the newer type is much easier on the eyes.

The work is available in two editions. In edition A the logarithms of numbers less than unity have been increased by 10. In edition B the logarithms of numbers less than unity are printed with negative characteristics.

W. J. Luyten
University of Minnesota

Astrophysik. (No. XI of **Strucktur der Materie.**) Svein Rosseland. Pp. 252, figs. 25. Julius Springer, Berlin 1931. Price RM 21.20.

The great advances made, as well as the revolutionary ideas introduced into astrophysics in the last decade or so, have made the want of an up-to-date, comprehensive survey of this important field felt very acutely in recent years. The appearance of Rosseland's Astrophysik, as No XI in the series: Struktur der Materie, edited by Born and Franck, fills this lacuna admirably.

After a short introductory review of the observational data of astrophysics and a thorough treatment of the fundamental physical and concepts underlying modern astrophysics, and with a view especially to their application to stellar interiors, the author divides the field in four main divisions. The first of these stellar hydrodynamics, includes Eddington's theory and the pulsation hypothesis. Energy problems, and stellar evolution, covering the problem of the source of stellar energy and the cosmogonic evolution of the universe forms the next part. The following division treats of the constitution of the atmospheres of the stars, and the problems arising in the interpretation of stellar specta. The last part considers the problems of the gaseous nebulae and the identification of "nebulium."

Considering the small amount of space at his disposal the author has succeeded remarkably well in presenting his subject in a manner at once comprehensive, authoritative, and well-documented, and for these reasons the book should appeal to a large class of physicists and astronomers. Owing to the limitations of space, no doubt, there are several points which are not as fully treated as they deserve,—at least from this reviewer's point of view. One might wish, e.g. that the spectral differences between giants and dwarfs and their relation to absolute magnitude determination had been given a more adequate space, and that the fundamental facts of observation had been given a less hurried survey. This applies to the first section as well as to the introductory parts to later discussions, where e.g. all irregular variable stars and novae together are dismised in one sentence, and the casual reader might well get the impression that the main division of all nebulae is in galactic nebulae and planetaries, while no mention is made of a possible observed change of period of the Cepheids beyond the fact that the lengthening demanded by Eddington has not been confirmed.

Another ciriticism might be levelled at the editorial make-up of the book, and its general appearance. It is particularly disconcerting to find that the entire book has been written as one chapter; and to have the first section of a new main division being in the middle of the same page where the last section of the previous main division left off. Furthermore, the index which is rather incomplete, does not differentiate between subjects and authors.

W. J. Luyten
University of Minnesota

Die elliptischen Funktionen von Jacobi. MILNE-THOMSON. Pp. 69, figs. 3. Julius Springer, Berlin 1931. Price RM 10.50.

The subtitle of the book, "Five-place Tables, with differences, of *sn u*, *cn u*, *dn u*, with the natural numbers as argument, arranged according to values of $m(-k^2)$, together with formulas and curves" gives a concise statement of the purpose and scope of the work. It is to be emphasized that these are *direct* tables of the functions *sn u*, *cn u*, *dn u*, in contrast to the ten-place tables of the elliptic integrals given by Legendre, *Traité des fonctions elliptiques*, Paris, 1825, Vol. II, and to the shorter five place tables such as in Hancock, *Elliptic Integrals*, New York, 1917, taken from Legendre's work. From Legendre's table the values of *sn u*, *cn u*, and *dn u* can be obtained only indirectly.

Each of the functions $sn(u, k)$, $cn(u, k)$, $dn(u, k)$ is tabulated to five places for real values of the variable u at intervals of 0.01, ranging from $u=0$ to $u=2$ or to $u>K$ if $K>2$. The largest value of u required is $u=6.5$ for $sn(u, 1)$. Instead of k, the quantity $k^2=m$ is used as the parameter, and the functions are tabulated for eleven values of m, at intervals of 0.1 ranging from $m=0$ to $m=1$. The first differences with respect to u are given in small type between the corresponding entries. Interpolation with respect to u requires the use of second differences, which are all small and easily obtained. Interpolation with respect to m is linear provided $u<\frac{1}{2}K$, while if $u>\frac{1}{2}K$ the function may be expressed in terms of functions of $K-u$ by appropriate formulas.

In addition to the tables just described a supplementary table gives the values of K, K', E, E', and $q(=e-\pi K'/K)$ to eight significant figures for values of $m=k^2$ ranging from $m=0$ to $m=1$ at intervals of 0.01. Altogether the tables, which occupy 66 pages, are well printed, conveniently arranged, and easily legible.

The introduction of eight pages consists of numerical examples illustrating the use of the tables; a list of the periods, zeros, poles, and residues; a group of fundamental formulas, including the trigonometric series, the power series, the addition formulas and the like; a table of some thirty integrals involving elliptic functions or their inverses; and finally a paragraph on the Weierstrass θ-function. It is to be regretted that formulas involving the theta-functions were not included, and that the list of integrals is not more complete.

Nevertheless the book satisfies a long-felt want on the part of many who have desired direct tables for the elliptic functions, and the author is to be complimented on having undertaken the work and on the excellent manner in which he has accomplished it.

W. E. MILNE
University of Oregon

Vorlesungen über Differential—und Integralrechnung. R. COURANT. Erster Band: **Funktionen einer Veränderlichen.** Pp. xiv+140, figs. 127. Berlin, Julius Springer, 1927. Price, RM 18.60.

This book, by one of the foremost of German mathematical scholars, is a first course in the differential and integral calculus—for students of suitable preparation and maturity. For readers trained under American conditions, and already acquainted with the essentials of the calculus, it is a valuable supplementary treatise, presenting familiar principles in a new light, and offering much additional material for which it would ordinarily be necessary to refer to more advanced texts.

Such chapter headings as differential and integral calculus of the elementary functions, Further development of the integral calculus, applications, Taylor's formula and the approximation of functions by polynomials, digression on numerical methods, infinite series and other limiting processes, call for no special comment. Partial differentiation and multiple integrals are reserved for a second volume, on functions of more than one variable; the subject of differential equations, as a separate major topic, is represented only by a short chapter on "The differential equations of the simplest oscillatory phenomena," with a note to the effect that the differential equations of more general phenomena of this sort will be taken up in the second volume.

Passages going beyond the minimum content of an ordinary course in the calculus are the chapter on Fourier series and trigonometric interpolation, and sections on polynomial interpolation, with special reference to the formulas of Newton and Lagrange, Wallis's infinite prod-

uct for π, Stirling's formula for the factorial, special functions illustrating peculiarities of continuity and differentiability, the multiplication and division of power series, the evaluation of the probability integral, the Bernoulli numbers, etc. A section on applications of the exponential function discusses continuously compounded interest, radioactive disintegration, the cooling or heating of a body in a surrounding medium, the dependence of atmospheric pressure on height above the earth's surface, the progress of chemical reactions, and the switching on and off of an electric current.

There are noteworthy differences between this course and those with which the American student is familiar. Exercises are not provided, except for an occasional statement in the frank and informal language of direct address that "I can leave it to you to prove so-and-so." The chapter on the "differential and integral calculus of the elementary functions" begins on page 109, being preceded by a 50-page chapter on "fundamental concepts of the integral and differential calculus," in which the definite integral is introduced first, then the derivative, and then the indefinite integral as inverse of the derivative; and this in turn is preceded by an introductory chapter of approximately equal length, discussing in some detail the notions of number, function, limit, and continuity. The reader will find much here which he has ordinarily thought of as belonging in a course in the theory of functions; but he will find the essential significance of this material, as an explanation of the fundamental principles of the calculus, more apparent than it sometimes is when the theory of functions is presented as a separate subject. The calculus is treated throughout as an analysis of relations of number and quantity, rather than as a technique for the manipulation of formulas.

The book is admirably printed and neatly bound, convenient to the hand and to the eye. To the American student who is under the necessity of preparing for an examination in mathematical German it gives an excellent opportunity for self-instruction in the language through the study of material which is familiar enough to be readily intelligible, and at the same time novel enough to be worthy of careful attention on its own account.

DUNHAM JACKSON
University of Minnesota

PROCEEDINGS
of the
AMERICAN PHYSICAL SOCIETY
Minutes of the Schenectady Meeting
September 10, 11 and 12, 1931

The 172nd meeting of the American Physical Society was held in Schenectady, New York, on Thursday, Friday and Saturday, September 10, 11 and 12, 1931 upon invitation from Union College and the General Electric Company.

The scientific sessions were held in the Physics Building of Union College and in Rice Hall in the Research Laboratory of the General Electric Company. The presiding officers were the Vice-president, Paul D. Foote, P. I. Wold and Herbert E. Ives.

On Thursday morning at 10 o'clock the Society convened in Rice Hall where the program consisted of two invited papers commemorating the one hundredth anniversary of the notable experiments of Michael Faraday and Joseph Henry in the field of electro-magnetic induction. The paper on "Faraday's Diary" was written by Sir William Bragg, Director of the Royal Institution and read by Professor John Zeleny of Yale University. Professor W. F. Magie of Princeton University gave an address on the life and scientific work of Joseph Henry. This session was attended by 230 persons.

At noon on Thursday the members of the Society, 232 in number, were the guests of the General Electric Company at the Works Restaurant. At the same hour the ladies who came to the meeting, 76 in number, were guests at a luncheon at the beautiful Riverwood Inn on the Mohawk River.

On Thursday afternoon about 180 persons were taken through the General Electric Research Laboratory in groups of fifteen each making thirteen stops, where men in charge of the problems were present to explain with experimental demonstrations their particular research.

The Physical Society dinner was held at the Mohawk Golf Club on Thursday evening with 254 in attendance. The Vice-president, Paul D. Foote, presided calling for a few remarks from President Frank P. Day of Union College, President Karl T. Compton of the Massachusetts Institute of Technology, Dr. W. R. Whitney and Dr. Irving Langmuir of the General Electric Company, and Dr. Henry A. Barton, the newly appointed Director of the American Institute of Physics. The guests were further entertained by one of the employees of the General Electric Company who was a very clever magician.

On Friday morning at 9 o'clock the Society convened in two sections at the Physics Building of Union College for the reading of the twenty-five contributed papers. After these sessions discussion groups met to consider the following subjects:

(1) x-rays and crystal structure with Bergen Davis presiding.
(2) teaching of physics—P. I. Wold.
(3) electric discharge through gases—Irving Langmuir.
(4) acoustics—C. W. Hewlett.

After the close of the morning program the Society was invited to be the guests of Union College at luncheon in the rose garden on the Union College grounds. There were 302 present at this delightful occasion. After the luncheon 183 went to a picnic at Indian Ladder, the procession of about fifty automobiles being led by police escort all the way out and back.

Saturday morning was devoted to a symposium on magnetism. There were two invited papers, one by Professor S. L. Quimby of Columbia University on "New Experimental Methods in Ferro-Magnetism" and one by Dr. Francis Bitter of the Westinghouse Electric and Manufacturing Company on "Interpretation of Ferromagnetic Phenomena."

After this program discussion groups met again on
(1) molecular spectra, presided over by W. W. Watson.
(2) engineering physics—G. B. Pegram.
(3) electric discharge through gases—Irving Langmuir.

In the afternoon a carefully prepared program of short papers was presented for a discussion group on magnetism. The leader of this group was Lewi Tonks.

At the close of the Saturday morning session in Rice Hall the following motion presented to the Society by Professor John Zeleny was voted unanimously:

> *Resolved:* that the American Physical Society and all those attending this session express their heartiest thanks to the General Electric Company, Union College, the local committee, President Day, Professor Wold, Dr. Whitney and Dr. Jesse and all those connected with them for the facilities afforded us for our meeting and for the magnificent entertainment they have provided during this Schenectady meeting.

Meeting of the Council. At its meeting held on Thursday morning, September 10, 1931, two persons were elected to fellowship, thirty-two were transferred from membership to fellowship and twenty-nine were elected to membership. *Elected to Fellowship:* Erik G. Rudberg and Yoshikatsu Sugiura. *Transferred from Membership to Fellowship:* Carl A. F. Benedicks, P. M. S. Blackett, Arthur A. Bless, W. E. Curtis, N. A. de Bruyne, E. Gilbert Dymond, C. Drummond Ellis, K. George Eméleus, James Franck, August Hagenbach, Sunao Imanishi, Raynor C. Johnson, Robert W. King, H. A. Kramers, Henry Margenau, A. B. McLay, Yoshio Nishina, T. Peczalski, J. Alingh Prins, G. M. Shrum, Manne Siegbahn, Herbert W. Skinner, Masamichi So, Herta Sponer, Hildegard Stücklen, Tutomu Tanaka, C. C. Van Voorhis, Shou Chin Wang, William W. Watson, Max Wehrli, Trygve D. Yensen and Usaburo Yoshida. *Elected to Membership:* E. W. Anderson, Loring B. Andrews, David W. Armstrong, L. H. Bailey, Richard F. Baker, William S. Benedict, Elmer R. Binkley, Donald S. Bond, Carl C. Chambers, J.

Hollie Cross, A. H. Croup, Roger W. Curtis, Einosuke Fukushima, Leo G. Hall, Wendell F. Kinsey, J. E. Lennard-Jones, K. V. Pestrecov, Esme E. Rosaire, William W. Shirley, H. M. Smallwood, Scott W. Smith, William O. Smith, Arthur B. Stanely, Demetrius Tarris, D. D. Taylor, Walter Weizel, M. L. Wiedmann, Albert J. Williams Jr., and Robley C. Williams.

K. T. Compton reported for the American Institute of Physics that H. A. Barton had been elected Director of the Institute and that John T. Tate had been appointed adviser on publications. Dr. Barton was introduced to the Council and it was voted that he be invited to attend the meetings of the Council ex-officio as a non-voting member.

Editor John T. Tate reported the new journal "Physics" to be developing rapidly, with plenty of material for publication and about 900 subscriptions.

The regular scientific program of the Society consisted of twenty-five papers, numbers 8, 13 and 18 being read by title. The abstracts of these papers are given in the following pages. An Author Index will be found at the end.

W. L. SEVERINGHAUS, *Secretary*

1. The vectorial photoelectric effect in thin films of alkali metals. HERBERT E. IVES *Bell Telephone Laboratories.*—It is assumed that the photoelectric effect exhibited by thin films of alkali metals on specular platinum surfaces is proportional at any wave-length to the electric intensity just above the platinum. This electric intensity is found, using the optical constants of platinum, by computing the intensities of the wave patterns formed by the interference of the reflected and incident beams. These computations are made for various angles of incidence and for light polarized in and at right angles to the plane of incidence. The intensities thus found exhibit very large ratios of value for the two planes of polarization, in striking agreement with the characteristics of the vectorial photoelectric effect. The changes of amplitude of the perpendicular electric vector on entering the alkali metal film, as computed from the optical constants of the alkali metal, account for the experimentally found low values of the emission ratios at long, and their high values, at short wave-lengths.

2. The photoelectric effect from thin films of alkali metal on silver. HERBERT E. IVES, AND H. B. BRIGGS, *Bell Telephone Laboratories.*—The thin films of alkali metals which spontaneously deposit in vacuo on other metals have long been known to exhibit photoelectric effects which vary in amount and character, depending on the underlying material, but the exact nature of this dependence has been obscure. Silver, because of its region of exceedingly low reflecting power in the ultraviolet and the accompanying variation of optical constants is exceptionally well suited for studying the influence of the underlying metal. It is found that the region of low reflecting power profoundly affects the photoemission, but in a manner not to be explained simply by reduction of light reflected back through the alkali metal film. The results obtained are very satisfactorily explained upon computing, from the optical constants, the intensity of the standing waves formed by reflection just above the silver surface. The positions of the maxima and minima of photoemission, and their variations with angle of illumination and plane of polarization are accurately indicated.

3. Correlating the selective photoelectric effect with the selective transmission of electrons through crystalline surface structures. A. R. OLPIN, *Bell Telephone Laboratories.*—Evidence is produced to support the view that photoelectrically selective, two-component cathodic surfaces are crystalline in nature. Then, assuming that Fowler's equation for the energy of electrons selectively transmitted through a single potential valley, $W=(n^2h^2)/(8md^2)$, is equally valid for the energy of electrons selectively transmitted through the periodic sequence of valleys characteristic of the potential field within a crystal, and that all of the energy of photoelectrons is acquired from the incident light quanta, the wave-lengths of light to which such a surface should

respond selectively can be computed. Such computations have been made with d equal to the internuclear distance between electropositive ions in the lattice structure of alkali metal hydride, oxide and sulphide crystals. The hydride crystals belong to the sodium chloride type and the oxide and sulphide crystals are supposedly of the calcium fluoride type. The correlation between these computed values and the positions of the observed selective maxima is exceptionally good. Moreover, the fact that the alkali metal hydrides exhibit but one selective maximum and the oxides two or three maxima is in keeping with the geometry of their respective crystalline types.

4. Thermionic emission in caesium-oxide photocells at room temperatures. E. F. KINGSBURY, *Bell Telephone Laboratories.*—The measurements on these cells recently reported (Kingsbury and Stilwell, Physical Review **37,** 1549, June 1, 1931) have been extended to a number of cells of a wide variety of treatment during construction. A relation between the thermionic constants, log A and b_0, has been obtained which approximates in slope the relation obtained by Richardson and Young (Proc. Royal Society **A107,** 377, 1925) for potassium cells sensitized with oxygen. The caesium cells, however, give from 100 to 1000 more emission at corresponding temperatures. The variation in overall photo sensitivity to tungsten light seems to be independent of the thermionic constants. In general the photoresponse decreases with increasing temperature but the behavior is complex, some cells increasing with rise of temperature and some showing an erratic superposition of the two effects.

5. The emission of secondary electrons from tungsten. A. J. AHEARN, *Bell Telephone Laboratories.*—An apparatus is described for investigating critical potentials in the emission of secondary electrons from tungsten. Measurements on the velocity distribution in the primary beam show that secondary electrons from the electron gun are absent. Tube characteristics which might introduce spurious critical potentials in the secondary emission from tungsten appear to be absent. By heat treating the tungsten and cleaning up residual gases, maxima and critical slope changes were developed below 40 volts. From 40 to 500 volts, only 4 critical potentials were observed even with the sensitive methods of measuring and plotting the data, and all but one of these disappeared eventually after heat treatments of the tungsten target. The phenomena may be associated with the diffraction of electrons or the production and absorption of characteristic soft x-rays. Regardless of the mechanism operating at the critical potentials, their decrease or elimination beyond 40 volts points strongly to effects of surface contamination rather than to characteristics of tungsten.

6. Transmission of electrons through potential barrier of thoriated filament. W. B. NOTTINGHAM, *Bartol Research Foundation.*—Thermionic measurements on a thoriated filament showed the electron velocity distribution to be accurately Maxwellian at the temperature of the filament for values of applied potential negative of V_0. At V_0 thus determined, the work function was 3.2 to 3.5 volts. With small accelerating potentials, referred to V_0, the current increased rapidly and reached a fair saturation value at 1.5 to 2.0 volts. Electron velocity distributions from a *deactivated* or pure tungsten filament were Maxwellian at the temperature of the filament. Comparing curves for activated and deactivated filaments heated to give the same "saturation" emission, showed that the velocity distribution from the pure tungsten was accurately reproduced with the activated filament over the range of accelerating potential mentioned above. This result can be ascribed to the transmission of electrons *through* a potential barrier ($B-C=1.4$ volts), 4.5×10^{-8} cm wide at one volt under the top. The transmission coefficient $D(W)$ of the Nordheim-Fowler theory must be a function of the energy of the impinging electrons. Therefore the emerging electrons will certainly not have a Maxwellian distribution at the temperature of the filament. Experimentally the barrier transmits the faster electrons easily, as would be expected, with the result that those transmitted happen to have practically a Maxwellian distribution with a temperature $48\%\pm3$ higher than the filament.

7. On the theory of thermionic emission. N. H. FRANK, *Massachusetts Institute of Technology.*—A theory of thermionic emission between plane parallel electrodes including space charge effects is developed to include the modifications introduced by quantum mechanics. Two modifications appear; (a) the use of the Fermi-Dirac statistics instead of the classical

statistics, and (b) the introduction of a probability of emergence of electrons within the metal which is a continuous function of the electron energies. The effect of (a) alone is to change the expression for saturation current. Expressed in terms of saturation current, all results of classical theory remain unchanged. The introduction of (b) modifies all these results. For the case of accelerating anode potentials high enough to prevent the formation of a potential minimum, the charge density and potential distributions are but slightly altered. For high retarding anode potentials (no potential minimum), the current voltage characteristic is

$$i = i_s\, \epsilon^{-e\phi/kT} \cdot f$$

ϕ is anode potential, i_s saturation current. Classically $f = 1\lambda$ quantum-mechanically it is a slowly varying function of ϕ. The charge density and potential distributions for this case are essentially different than the classical expressions. The case of a potential minimum is handled as a combination of the above two cases. Just as in the classical case numerical or graphical integrations are necessary before numerical results can be obtained.

8. Determination of e/m by the refraction of x-rays. J. A. BEARDEN, *Johns Hopkins University.*—Since the usual dispersion theory has been so thoroughly established we may, by measuring the index of refraction of x-rays, use the theory as a means of determining e/m. Measurements of the index of refraction of the copper K series in a 90° quartz prism have been made by two methods. In the first method the incident beam struck the first face of the prism at a glancing angle larger than the critical angle of total reflection. In the second method the incident beam struck the second face at a very small angle. The alignment of the prism, slits, and plateholder was made as described by the writer in a previous paper (Phys. Rev. **37,** 1210 (1931)). Twenty-nine measurable exposures have been obtained under various conditions. The dispersion formula

$$\delta = 1 - \mu = \frac{e^2}{2\pi m} \sum_i \frac{N_i}{\nu^2 - \nu_i^2}$$

was used for determining e/m. The value of ν was obtained from the writer's grating wave-length measurements. e/m was thus found to be

$$e/m = 1.764 \times 10^7 \text{ e.m.u./g.}$$

This is in good agreement with the results obtained by Stauss (Phys. Rev. **36,** 1101 (1930)) but differs from either of the accepted values of e/m. Calculations of e/m have also been made using the complete dispersion formula which includes the absorption in the prism.

9. An x-ray study of the nature of solid solutions. ROBERT T. PHELPS AND WHEELER P. DAVEY, *Pennsylvania State College.*—(1). The solid solution of pure Al in pure Ag lowers the lattice parameter of the Ag by an amount which is proportional to the Al content of the solution. Saturation of Al in Ag is reached at 5.4 percent Al by weight. Further addition of Al gives aggregates of Ag_2Al of sufficient size to give x-ray diffraction patterns. (2). The experimental values for the densities of the solid solutions of Al in Ag are somewhat lower than those calculated on the basis of a direct substitution of Al atoms for Ag in the Ag lattice. This discrepancy is greater than the combined error in the two values. (3). Systematic examination of the various possible types of explanation for this discrepancy leaves us with only one tenable theory, namely that the Al in the solid solution is chemically combined with the adjacent Ag. If this explanation is used as a basis for a general theory of the nature of solid solutions, the picture is found to be consistent with the known facts for both solid solutions and liquid solutions. So far, it has not been found inconsistent with any known fact.

10. A 1,500,000 volt electrostatic generator. ROBERT J. VAN DE GRAAFF, *National Research Fellow, Princeton University.*—The application of extremely high potentials to discharge tubes affords a powerful means for the investigation of the atomic nucleus and other fundamental problems. The electrostatic generator here described was developed to supply suitable potentials for such investigations. In recent preliminary trials, spark-gap measurements showed a potential of approximately 1,500,000 volts, the only apparent limit being brush discharge from the whole surface of the 24-inch spherical electrodes. The generator has the basic advantage of supplying a direct steady potential, thus eliminating certain difficulties inherent in the applica-

tion of non-steady high potentials. The machine is simple, inexpensive, and portable. An ordinary lamp socket furnishes the only power needed. The apparatus is composed of two identical units, generating opposite potentials. The high potential electrode of each unit consists of a 24-inch hollow copper sphere mounted upon a 7 foot upright Pyrex rod. Each sphere is charged by a silk belt running between a pulley in its interior and a grounded motor driven pulley at the base of the rod. The ascending surface of the belt is charged near the lower pulley by a brush discharge, maintained by a 10,000 volt transformer kenotron set, and is subsequently discharged by points inside the sphere.

11. Negative hydrogen ions from H_2O by electrons of a critical velocity. DONALD W. MUELLER AND H. D. SMYTH, *Princeton University.*—Lozier and Bleakney have observed negative hydrogen ions appearing over a small range of electron velocities in apparatus containing water vapor. Their result has been qualitatively confirmed using a mass spectrograph. Hydrogen negative ion intensity falls off above and below 8 volts incident electron velocity. Oxygen and hydroxyl negative ions were also observed but increasing in amount above about twenty volts incident electron velocity.

12. On the absolute determination of gravity. A. C. LONGDEN, *Knox College, Galesburg, Ill.*—The importance of a new determination is discussed. In the work here described, a reversible pendulum is used in which roller bearings are substituted for knife-edges and quartz suspension rods or tubes are used instead of metal. Invar is disqualified on account of its magnetic qualities. The period of the pendulum is determined to within 1 or 2 parts in a million by a very direct method which involves no corrections and which can be performed in a few minutes, while the pendulum is swinging through a very small amplitude and while the *change* of amplitude is quite negligible. The author points out the errors of the "Coincidence Method" as it is generally used, and shows that it may either be improved, or abandoned as unnecessary. He also cites some of the results on record, which are accepted as highly exact, but which in reality include rather large errors. The method includes a number of refinements in comparing the length of the pendulum with that of a standardized invar rod.

13. Entropy of polyatomic molecules. D. S. VILLARS, *Research Laboratory, Standard Oil Co. (Ind.)*—By applying the data of Hund on ammonia and of Elert on methane to obtain the total number of completely antisymmetric eigenfunctions which can be formed from the different rotational states, one can get the *a priori* probabilities of the different non-combining symmetry varieties (nuclear doublet and quadruplet for ammonia and nuclear singlet, triplet and quintet for methane) and from them the entropies. The relative proportions at high temperature of the different varieties are one to one for ammonia and 2:9:5 for methane (resp.). The absolute entropy of the ammonia mixture is 51.5 cal. degree^{-1} at 298.1°K and of the methane mixture, 50.1 at the same temperature.

14. Some physical properties of compressed carbon monoxide. W. EDWARDS DEMING AND LOLA E. SHUPE, *Bureau of Chemistry and Soils, U. S. Department of Agriculture, Washington, D. C.*—Compressibility data obtained by Bartlett on carbon monoxide have been adjusted and extrapolated so that p, v, T data from -70°C to 400°C and from 25 to 1200 atm. are available. Using the graphical scheme for obtaining derivatives, previously described in similar calculations for nitrogen, the following physical properties have been computed, and are available in tables and curves at eleven temperatures and fourteen pressures, over the range noted above: specific volume, density, expansion coefficients, fugacity, C_p, $C_p - C_v$, C_v, μ. The C_v vs. t isobars for 300 to 1200 atm. show a minimum at about 100°. On the low temperature side of this minimum the curves are very steep; for 1200 atm. C_v drops from 4.4 R at -70° to 2.57 R at 100°. Above 100°, C_v is only a few hundredths cal./mole deg. higher than C_v^* (zero pressure) for pressures to 400 atm.; further increase in pressure raises C_v only a few tenths. Below 25°, C_v for $p = 25$ is slightly less than C_v^*; for $p = 100$, 150, 200, C_v falls considerably below C_v^* as t falls to -70°. The C_p vs. p isotherms show that above 500 atm. C_p does not change much with further increase in pressure. Below 0°, decrease in temperature is accompanied by considerable increase in C_p, when $p > 200$.

15. An optical study of heat transfer by convection from solid surfaces to air. R. B. KENNARD. *Bureau of Standards.*—A hot body is placed in one arm of a Jamin interferometer which is built about an open well so as to permit the free circulation of air about the body. The temperature distribution in the air is obtained without the introduction of any material thermometric apparatus. An equation relating the fringe shift to the air temperature is developed. Photographs are shown of the fringes near horizontal and vertical plane surfaces. The transition from laminar flow to turbulent flow is shown by a change in the direction of the fringes. The temperature gradient for laminar flow is constant for the temperature range used. If the temperature gradient were constant throughout and the same as for laminar flow, the "equivalent" film would be 5.5 mm thick and independent of the temperature of the hot plate. The interference fringes were photographed about a wire of 3/10 mm diameter, and about cylinders of 5 mm, 12.7 mm and 30 mm diameter. From these photographs the isothermals about these cylinders were plotted, and the relative heat emission along different radii estimated. The relation between the thickness of the layer of heated air and the diameter of the cylinder is noted.

16. Some evidence indicating the existence of Ba isotopes 136 and 137. R. C. GIBBS, AND P. G. KRUGER, *Cornell University.*—In 1925 Aston reported the chief isotope of Ba to be 138, with the possibility that isotopes 136 and 137 might exist in extremely small quantities. From such data one would expect the Ba lines to show no hyperfine structure, since elements with an even atomic weight in general have a nuclear spin of zero. The Ba II lines λ's 4554A and 4934A ($6s^2S_{1/2}-6p\ ^2P_{3/2,\ 1/2}$) show structure when photographed with a Fabry-Perot interferometer, the satellites combined having roughly one tenth the intensity of the parent line. This leads one to think that the satellites are probably due to an odd isotope (137) and that the parent line is due to the even isotopes (136 and 138). A mixture of 27 percent of isotope 136, 9 percent of isotope 137 and 64 percent of isotope 138 gives 137.37 for the average atomic weight, which agrees with the chemical atomic weight of Ba. This gives an even to odd ratio of isotopes of about 10:1, and so roughly checks with the intensity relation in the structure of the lines.

17. Quantitative intensity determinations in the spectra of normal and of singly ionized vanadium, V I and V II. GEORGE R. HARRISON, *Massachusetts Institute of Technology.*—The relative intensities of all lines of V I and V II stronger than 1/2 of 1 percent of the intensity of the principal lines and lying between λλ5200 and 2500A. have been determined under various conditions of excitation in the vacuum arc, using the first and second orders of a 35 ft. concave grating and standard methods of photographic photometry. The proportionate number of anomalous lines found is somewhat greater than in Ti I and II, and less than in Cr I and II, as is to be expected from the multiplet separations and the number of terms of similar J value which can perturb one another. The spectral analysis used is a fairly complete one kindly furnished in advance of publication by Dr. W. F. Meggers. The data obtained are being used to test the excitation conditions in the vacuum arc, the J-group sum rule of Johnson and the writer (Phys. Rev. **37,** 1702, 1931 and issue for Aug. 15, 1931), and the role played by quantum numbers and the magnetic and electrostatic term separations in determining the intensity perturbations produced in a given line. Attempts are now being made to extend these data to both longer and shorter wave-lengths.

18. Band spectrum intensities by graphical methods. ELMER HUTCHISSON, *University of Pittsburgh.*—In order to facilitate the comparison of experimentally determined band intensities with those predicted by theory, an easy and rapid method of determining the theoretical results is desirable. Making use of the author's previous calculations (Phys. Rev. **36,** 410 (1930); **37,** 45 (1931)), based upon the Franck-Condon principle, charts have been prepared which permit a graphical determination of the intensities of vibrational bands in electronic transitions. Transition probabilities associated with the lowest energy levels are given by means of contour lines on a chart in which the changes in the equilibrium distances between the atoms during the transitions are plotted as ordinates and the square roots of the ratios of the vibrational frequencies in the lower and upper states are plotted as abscissas. Besides the squares of the transition probabilities, the complete expression for the intensities in absorption involves the fourth powers of the frequencies of the bands and the populations of the initial states which

are also obtained graphically as a function of the temperature of the absorbing gas. The use of these charts allows a rapid estimation of the band intensities in any particular electronic transition. As an example of the use of these charts, the band intensities of the $^1\Sigma - ^1\Sigma$ transition of AgH are calculated. The computed values are found to be in fairly good agreement with the experimental results of Hulthèn and Zumstein (Phys. Rev. **28,** 13 (1928)).

19. The Kerr-effect in Rochelle salt. HANS MÜLLER, *Massachusetts Institute of Technology.*—An electric field parallel to the *a*-axes of Rochelle salt produces a large electro-optical effect which does not reverse with the direction of the field. This effect has been measured for temperatures between 0 and 35°C and fields up to 30 kv/cm. The effect exists in the entire temperature region but has a sharp maximum at about 23°C. The change of the difference between the indices of refraction $n_a - n_b$ resp. $n_a - n_c$ is not proportional to the square of the field strength but increases almost linearly up to 15 kv/cm. At higher fields the effect tends towards saturation. The effect is not due to temperature change due to conduction. It is much too large to be accounted for by electrostriction. The observations support the hypothesis that the anomalous dielectric and piezoelectric properties of Rochelle salt are due to the fact that the electric dipoles of the H_2O molecules of the water of crystalization behave similarly to the magnetic dipoles in the case of ferromagnetism.

20. The Hall effect in solid mercury. JAMES T. SERDUKE AND THOMAS F. FISHER, *Union College.* (*Introduced by P. I. Wold.*)—Various investigators have studied the Hall effect in Hg, especially in the liquid form. In the liquid form the results are uncertain and subject to doubt. In the solid form Fenninger in 1914 found the Hall constant to be not larger than 0.000011. The present investigators developed a method of obtaining a Hg strip 14 cm long, 2 cm wide and of various thickness down to 0.006 cm and have measured the Hall effect and resistivity in solid mercury at a temperature of about −60°C. The conclusions are that in this case the Hall effect is negative and the constant has a value of -0.00078 ± 10 percent. The Hall constant is independent of field strength, current density and thickness of specimen. No definitely measurable longitudinal effect, i.e. change in resistivity with magnetic field was found.

21. Exhibition of parallax panoramagrams made with a large diameter concave mirror. HERBERT E. IVES, *New York City.*—The general methods by which relief pictures may be made by a single exposure, using a large lens or mirror, have been described previously (J.O.S.A. **20,** 597(1930)). The pictures exhibited were made by means of a strip of spherical concave mirror of 48 inch diameter and 48 inch radius, built up out of three 16 inch sections. The light from the object after leaving the concave mirror is reflected to one side by means of a 45° half silvered mirror. An opaque line grating of 20 lines to the inch, with clear spaces 1/50 the width of the opaque is placed slightly in front of the sensitive plate, and a similar grating, slightly behind a positive print on glass converts this into a relief picture. Details of the "camera," which consists of a dark room with a large window, are given. The pictures are notable, as compared with pictures previously exhibited, made with a large lens, for the larger angle (60°) through which relief is observed.

22. The small shot effect in photoelectric currents. B. A. KINGSBURY, *Bell Telephone Laboratories.*—The small shot effect, as it occurs in a photoelectric current, has been used to secure an evaluation of the electron charge. A new and original method of amplifier calibration, which involved the use of a modulated light beam, simplified the measurements and the computation of the result. In the absence of space charge, the experimental value of the electron charge was 1.61×10^{-19} coulombs for a thermionic current, and about 25 percent greater for a photoelectric current. It was found that the small shot effect is enormously increased in photoelectric currents which are amplified by collision ionization. Statistical variations which might be expected to occur in a beam of radiant energy could not be detected, since, within the limits of experimental accuracy, the small shot effect in photoelectric currents was found to be independent of the frequency of the light producing electron emission.

23. Force relations in drawing copper wire. R. L. DOAN AND J. L. BETSILL, *Western Electric Company, Hawthorne Station.*—An empirical relationship has been derived between the draw-

ing force and percent reduction in drawing copper wire through successive chilled iron dies which takes into consideration the progressive hardening of the metal with cold work. This is: $\log F/\Delta = A - B \log X$. Where F is the drawing force, Δ the reduction in cross section and X the percent reduction at any particular die. A and B are factors which depend on the total reduction from the initial soft rod. The effect of varying the die angle has been investigated for 5°, 10°, 20°, 30° and 40° single angle dies. The drawing force was found to be a minimum and the tensile strength of the product wire a maximum for the 10° angle although more detailed experiments will be required to locate the optimum angle. The fall in tensile strength of the wire when drawn through large angle dies is associated with the development of internal ruptures which widen out and give rise to typical cup and cone fractures.

24. A three-dimensional vibrograph. J. E. SHRADER, *Drexel Institute, Philadelphia.*—A new vibrograph has been devised which indicates and records simultaneously in the same plane vibrations of a body in each of three directions mutually perpendicular. This vibrograph operates on the seismographic principle. A cubic mass of lead is suspended from a frame by a system of springs. The mass and its frame are enclosed in a case which is placed upon the vibrating body. Relative motions between the mass and its frame are shown by the deflection of beams of light from mirrors mounted on spindles attached to the suspended mass. Motion of rotation is communicated to the spindles by flexible strings. One end of each string is fastened to the frame and is then wrapped about the spindle and then passes to a light spiral spring which is attached to the opposite side of the frame. The record is made on double width moving-picture film. A timing record on the same film is made by the use of a small synchronous motor. The instrument shows amplitude of vibration, wave form, phase relations and frequency of three components of vibration simultaneously on the same plane.

25. The emission spectrum of metallic silver under electron bombardment and its relation to the absorption spectrum. F. L. MOHLER, *Bureau of Standards.*—In previous communications, Mohler and Boeckner have shown that the visible and near ultraviolet spectra emitted by metals bombared by low speed electrons are generally nearly equal energy continuous spectra of comparable intensity but silver is an exception. The intensity rises from 3200A to a value near 3600A, over 10 times the intensity at shorter wave-lengths. The shape of the intensity curve between 3200 and 3600A, when corrected for internal reflection, resembles a Fermi distribution of energy and an exact fit is obtained by assuming a reasonable value for the temperature of the metal. The result suggests that the emission process involves ionization of a discrete underlying level and the fall of one of the continuum of conduction electrons into the ionized level. The absorption spectrum of the underlying level should be a band extending to shorter wave-lengths with the shape of the long wave-length edge influenced by the Fermi distribution. The absorption rises from a low value near 3200 to a maximum near 2500A, and preliminary experiments indicate that the slope of this branch of the absorption curve does indeed change with temperature in a manner consistent with this interpretation.

AUTHOR INDEX TO ABSTRACTS OF SCHENECTADY MEETING

Ahearn, A. J.—No. 5

Bearden, J. A.—No. 8
Betsill, J. L.—see Doan
Briggs, H. B.—see Ives

Davey, Wheeler P.—see Phelps
Deming, W. Edwards and Lola E. Shupe—No. 14
Doan, R. L. and J. L. Betsill,—No. 23

Fisher, Thomas F.—see Serduke
Frank, N. H.—No. 7

Gibbs, R. C. and P. G. Kruger—No. 16

Harrison, George R.—No. 17
Hutchisson, Elmer—No. 18

Ives, Herbert E.—Nos. 1, 21
——— **and H. B. Briggs**—No. 2

Kennard, R. B.—No. 15
Kingsbury, B. A.—No. 22
Kingsbury, E. F.—No. 4
Kruger, P. G.—see Gibbs

Longden, A. C.—No. 12

Mohler, F. L.—No. 25
Mueller, Donald W. and H. D. Smyth—No. 11
Müller, Hans—No. 19

Nottingham, W. B.—No. 6

Olpin, A. R.—No. 3

Phelps, Robert T. and Wheeler P. Davey—No. 9

Serduke, James T. and Thomas F. Fisher—No. 20
Shrader, J. E.—No. 24
Smyth, H. D.—see Mueller
Shupe, Lola E.—see Deming

Van De Graaff, Robert J.—No. 10
Villars, D. S.—No. 13